Graduate School of
Systemic Neurosciences

LMU Munich

Role of EphA4 in Spinal Circuits Controlling Locomotion

Aarathi Balijepalli

Munich

Role of EphA4 in Spinal Circuits Controlling Locomotion

Dissertation of the Graduate School of Systemic Neurosciences

Ludwig Maximilians University, Munich

Aarathi Balijepalli

Munich, 2014

Supervisor	**Prof. Rüdiger Klein**
Second reviewer	**Dr. Ilona-Grunwald-Kadow**
Third reviewer	**Dr. Eloisa Herrera**
Date of oral defense:	**22nd September, 2014**

Table of Contents

1. Abstract

The understanding of the neural circuits of the spinal cord is central to the comprehension of sensory information received from the environment to allow an appropriate motor response. These motor behaviors are the result of activation of a complex series of neural circuits that control precise muscle movement. Designated neural networks in the ventral spinal cord, termed central pattern generators (CPGs), regulate important aspects of muscle movement such as coordination of left-right locomotion, generation of rhythm and contraction of flexor and extensor muscles. Although many studies have been performed to dissect these networks in the ventral spinal cord, little is known about the contribution of dorsal spinal cord neurons in CPG function. Furthermore, the requirement of the axon guidance molecule, EphA4, has been investigated thoroughly in ventral interneurons; however, its functions in the dorsal spinal cord are poorly understood.

The results presented in this thesis show, for the first time, the requirement of EphA4 in the dorsal spinal cord in maintaining left-right coordination of locomotion. Ablating EphA4 from the dorsal spinal cord alone produces a partial hopping phenotype. However, no shift in gait is observed in these mice when they are subjected to increasing speed during treadmill locomotion. Thus, EphA4 expressing dorsal interneurons participate in left-right coordination of locomotion, but do not integrate into or influence circuits that assimilate information on speed-dependent changes of gait. Interestingly, EphA4 is required for cortical control of adaptive locomotion as evidenced from experiments requiring the mice to modify their step to cross hurdles. Additionally, these experiments reveal cell autonomous and non-cell autonomous functions of EphA4.

Moreover, EphA4 ablation leads to morphological defects in the dorsal funiculus (DF), i.e. EphA4 mutants display a shallow DF compared to control littermates in the adult spinal cord. Indeed, ablating EphA4 in the dorsal cord alone is sufficient to cause this phenotype. Furthermore, the EphA4 mutants display a shallow DF during the development of the spinal cord itself, thereby suggesting that the phenotype is intrinsic to the spinal cord and not due to aberrant misprojections of the CST, as previously thought. EphA4 mutants also display a medial shift of dorsal interneurons that strongly express the zinc finger transcription factor, Zic2, to the midline. These results convincingly demonstrate that the medial shift of neurons to the midline hinders the ventral extension of the DF. Moreover, the axonal projections of EphA4 positive neurons, which usually project along an ascending ipsilateral tract into the DF, display aberrant midline misprojections in dorsal EphA4 mutants. Likewise, secondary spinal cord defects, such as, aberrant midline crossings of nociceptive sensory projections are also observed in the EphA4 mutants.

Collectively, these results delineate novel roles of EphA4 in preserving important circuits of the dorsal spinal cord that are required for the maintenance of left-right coordination of locomotion and the proper positioning and axon guidance of dorsal interneurons.

2. Introduction

The central nervous system (CNS), comprising the brain and the spinal cord, is an incredible and fascinating system. It is made up of many billion neurons, which form during embryonic and postnatal development, that are interconnected in complex circuits and play instrumental roles in controlling the countless complex behaviors that many animals display – from receiving sensory stimuli from the environment and responding with an appropriate motor response to cognitive behaviors such as learning and memory. More than a century ago, the requirement for a thorough comprehension of the developing and changing brain (processes that are vital and integral to CNS function) for understanding these complex behaviors was realized. Pioneering anatomical studies have shed light on the structure and organization of the nervous system leading to the subsequent investigation of its development. Major advances in technology have allowed scientists to extend this investigation to the molecular and genetic level. In fact, we now know that the development of the nervous system is the result of an event that occurs very early during embryogenesis – the expression of particular genes in a spatial and temporal manner in certain cells that transforms them into neural progenitors. The differentiation of these neural progenitors is influenced by both internal and external factors. Internal factors include the gene expression profile that is hardwired into neural progenitors and epigenetic processes. These factors govern cellular identity, the formation and extension of axonal processes to their final targets and the establishment of electrically viable synaptic connections. External factors consist of sensory stimuli, nutrient intake and other environmental influences which allow the nervous system to continuously adapt to nature and respond appropriately. In other words, the internal and external factors sculpt the functional architecture of the brain thus allowing it to process information and produce behaviors.

Since the spinal cord is central to the study undertaken in this thesis, the subsequent sections aim to provide information on the neuronal development, patterning, differentiation, axon guidance and sensory and motor functions in this system.

2.1. Development of the spinal cord

The development of the spinal cord begins after the formation of the three main cell layers during embryogenesis – the endoderm, which is the innermost cell layer, the mesoderm, the middle cell layer and the ectoderm which is the outermost cell layer [1]. Pioneering studies conducted by Hans Spemann and Hilde Mangold in 1924, in Xenopus embryos, led to the fundamental discovery of a specialized region, called the 'organizer,' in the axial mesoderm that provides the inductive signals for neural differentiation in the overlying ectodermal cells [2]. Further experiments conducted to reveal the identity of the inductive signals of the 'organizer' region, shed light on the precise signaling pathways involved in neural differentiation. Three independent studies, conducted in 1989, made the important discovery that ectodermal cells, by default, differentiate into neural progenitors [3-5]. Hence, the generation of neural tissue must be influenced by adjacent cells and indeed they provide signals which result in the inhibition of a pathway that constitutively represses the induction of neural differentiation in ectodermal cells [6].

Ectodermal cells that differentiate into neural cells are collectively termed as the neural plate. Via a process termed as neurulation, the neural plate folds upon itself, along the anteroposterior axis and gives rise to the neural tube. As development proceeds, the cells of the neural tube proliferate rapidly and occupy predetermined positions; however, the degree of cell proliferation and the final identity they acquire is dependent on the presence of various proteins

that exist in the environment. For example, the FGF family of proteins patterns the neural tube along the anteroposterior (AP) axis [7], whereas members of the BMP family of proteins and gradients of sonic hedgehog (Shh), pattern the neural tube along the dorsoventral axis [8]. Together, they give rise to the different brain structures at the rostral end and the spinal cord at the caudal end of the neural tube.

2.1.1. Anteroposterior (AP) patterning of the spinal cord

Patterning of the neural tube along the AP (also called rostrocaudal) axis begins with neural induction by signals from the underlying mesoderm. In fact, evidence has suggested that signals expressed by the organizer (noggin, follistatin and chordin) promote the expression of molecular markers that are typically found in the forebrain [9-11]. In the second step, signals thought to arise from the paraxial mesoderm ("transformation") are thought to give rise to more caudal structures, such as the midbrain, hindbrain and spinal cord [12-14]. It is now known that patterning along the AP, mediated by the concerted action of Wnt [15], retinoic acid (RA) [16] and FGF [17] signaling, is different along the length of the neural tube, thus enabling the generation of diverse neuronal subtypes [Figure 2.01].

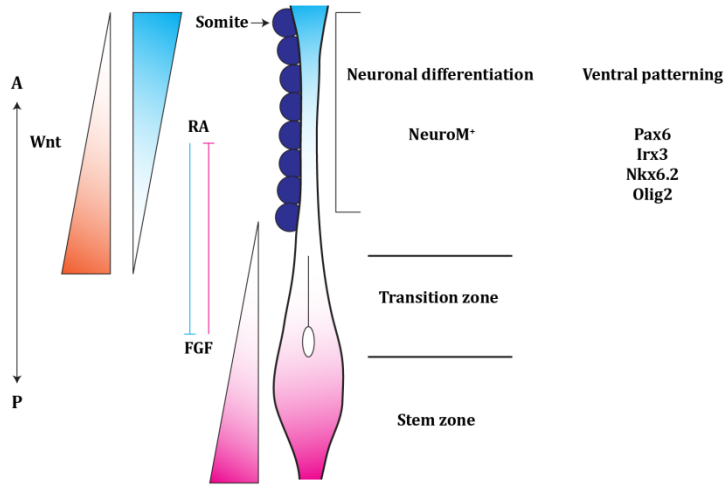

Figure 2.01: AP patterning of the developing neural tube. FGF is expressed in the caudal part of the developing neural tube: the stem zone. It is expressed in a gradient with high levels of FGF in the posterior region and low levels of FGF in the anterior region. FGF is required to maintain cells in the proliferative state. RA is derived from the adjacent somites also along a decreasing gradient along the anteroposterior axis. Exposure to RA allows expression of various transcription factors that lead to neuronal differentiation and ventral patterning in the spinal cord. FGF and RA function by mutually inhibiting each other along the anteroposterior axis. Wnt proteins are also expressed in an anteroposterior gradient, with high expression of Wnt proteins in the posterior neural tube. Adapted from [18]. A: anterior, P: posterior.

2.1.2. Dorsoventral (DV) patterning of the spinal cord

Patterning of the neural tube along the AP axis engages many molecular mechanisms leading to the generation of distinct cell populations in specific regions of the spinal cord. Conversely, similar molecular mechanisms are employed during DV patterning of the entire spinal cord. The adult spinal cord serves two important functions: a) it relays sensory information from the periphery to higher brain centers and b) it computes and communicates motor information to the limbs. Along the DV axis, the spinal cord is well separated; sensory neurons reside in the dorsal half of the spinal cord, whereas motor neurons occupy regions in the ventral half of the spinal cord. Patterning along the DV axis occurs as a result of signals derived from two regions of the developing neural tube:

1. The roof plate, a region which forms at the dorsal midline and generates gradients of BMP and Wnt proteins that are important in the development of the dorsal interneurons that participate in sensory information.
2. The floor plate, a region which forms at the ventral midline and is populated with specialized glial cells, produces gradients of Shh (sonic hedgehog), which are required for generating motor neurons and other ventral interneurons involved in motor function.

Together, signaling by Shh, BMPs and Wnts give rise to 11 distinct domains of neural progenitors; 6 dorsal domains; dP1-6, and 5 ventral domains; p3, pMN, p2-0 [Figure 2.02], by inducing the expression of transcription factors belonging to the homeodomain and basic-helix-loop-helix families of proteins.

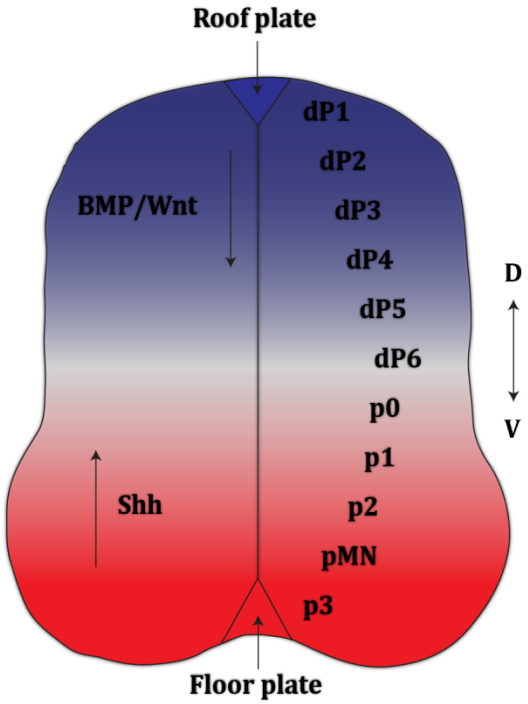

Figure 2.02: DV patterning of the neural tube by signals derived from the roof plate and floor plate. BMP/Wnt proteins are expressed in the roof plate cells along a dorsal-ventral gradient leading to the formation of 6 dorsal progenitor domains (dP1-6). Gradients of Shh are derived from the floor plate cells in a ventral-dorsal manner and are required for the generation of 5 ventral progenitor domains (p3, pMN and p2-0). D: dorsal, V: ventral.

2.1.2.1. BMP and Wnt signaling

The patterning of the dorsal spinal cord begins with the closure of the neural tube and the development of roof plate cells. Roof plate cells express several members of the BMP family (such as GDF7, BMP4 and BMP7) and Wnt family (Wnt1 and Wnt3a). They are required for the inhibition of the ventrally expressed Shh and the patterning of the dorsal progenitors. The

importance of the roof plate in patterning the dorsal interneurons was recognized from the spontaneously generated mutant mouse, *dreher*, where a mutation in the Lmx1a gene (a member of the LIM-homeodomain family) leads to an expansion of ventral progenitors at the expense of dorsal cells [19, 20].

Ablation of BMP proteins leads to a decrease in the dorsal most progenitor domains, pD1-3 (marked by the expression of Olig3), and dorsal interneurons that they differentiate into. BMP signaling does not affect the development of the other three ventral populations, that is, pD4-6 (marked by the expression of Lbx1), however, these regions expand at the expense of the dorsal most population [21].

2.1.2.2. Sonic hedgehog (Shh)

The notochord, derived from the mesoderm, is a fundamental structure required for defining the body axes [22]. It produces Shh that acts as a short-range signaling molecule and induces the formation of the floor plate cells, and as a long-range molecule (morphogen) that acts in a concentration dependent manner to induce the formation of motor neurons and ventral interneurons. The floor plate cells also acquire the ability to generate Shh that acts in a similar short and long-range manner.

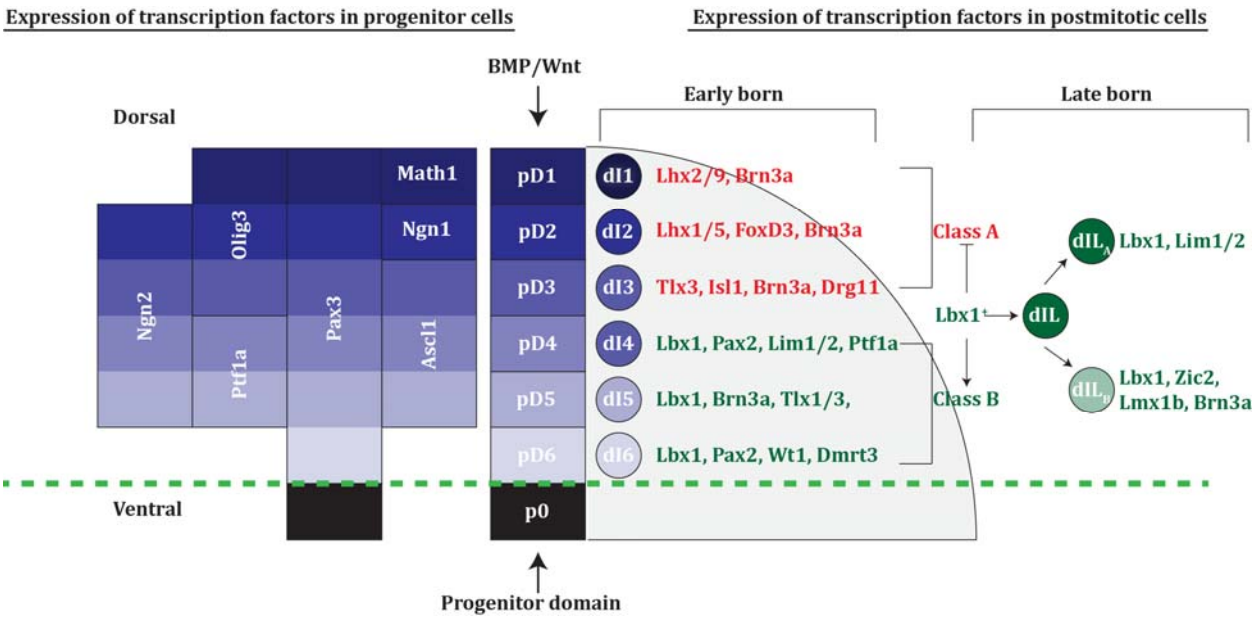

Figure 2.03: BMP/Wnt signaling is required for the generation of distinct dorsal interneurons [23, 24]. BMP and Wnt proteins, derived from the roof plate, act along a decreasing dorsal-ventral gradient and induce the expression of distinct transcription factors in progenitor cells (pD1-pD6). This leads to the generation of mature post-mitotic motor neurons and domains of dorsal interneurons which can be identified by specific transcription factors that they express. Post-mitotic neurons are generated during two rounds of neurogenesis in the dorsal spinal cord: six domains of early born neurons (dI1-6) are generated between E9-11, whereas two domains of late born neurons (dIL_A and dIL_B) are generated between E12-14.

2.2. Interneurons of the dorsal spinal cord

2.2.1. Early born dorsal interneurons

Signaling via roof plate derived proteins, such as Wnts and BMPs leads to the generation of six dorsal progenitor domains (p1-6), that differentiate further, to give rise to six domains of post-mitotic neurons (dI1-6), around embryonic day 9-11 in the mouse, which are the early-born neurons of the dorsal spinal cord. The dorsal most neurons (dI1-3), termed ‘class A’ neurons, arise from progenitors that are specified by roof plate signals [23, 25]. These progenitors are identified by the expression of the transcription factor, Olig3 [26]. The more ventral neurons

(dI4-6), termed 'class B' neurons, develop in the absence of roof plate signals and are marked by the expression of the transcription factor, Lbx1 [23, 24]. A second round of neurogenesis occurs around embryonic day 12-14, which gives rise to two additional populations of neurons; dIL_A and dIL_B. These neurons express Lbx1 and are generated in a salt and pepper manner [23, 24]. The dIL_A population is generated as a result of asymmetric cell division, whereas dIL_B neurons divide symmetrically or asymmetrically [27] [Figure 2.03].

dI1 interneurons are derived from the Math1 expressing progenitor domain (pD1). Post-mitotic interneurons, expressing the transcription factors Lhx2/9 and Brn3a, are excitatory in nature, as they express glutamatergic markers, and migrate and settle in the dorsal horn in the post-natal spinal cord. These interneurons can be further divided into two subtypes: $dI1_i$ interneurons (that express Lhx9) settle in the deep lateral horn and extend their axons ipsilaterally, and $dI1_c$ interneurons (that express Lhx2) settle in the medial lateral horn and extend their axons contralaterally. dI1 dorsal interneurons relay somatosensory information regarding the position of the limbs and the trunk to the cerebellum via the spinocerebellar and reticulospinal tracts [28, 29]. dI2 interneurons are derived from the pD2 progenitor domain that can be identified by the expression of Ngn1. The post-mitotic neurons express the LIM-homeodomain transcription factors, Lhx1 and Lhx5. These interneurons are excitatory, project their axons contralaterally and relay somatosensory information to the thalamus [30, 31]. Dorsal progenitors that express the transcription factors Ascl1 and Pax3 (pD3) differentiate to give rise to the dI3 population of dorsal interneurons. The post-mitotic neurons express the transcription factors Islet1 (Isl1) and Brn3a and are excitatory in nature. They migrate and settle in the deep dorsal laminae, project ipsilaterally to motor neurons and are required for relaying somatosensory information on regulation of cutaneous paw grasping [31, 32]. The expression of

transcription factors such as, Ptf1a, Pax3 and Ngn2, are required for the differentiation of the pD4 progenitors into dI4 interneurons. Post-mitotic markers for this population include Ptf1a, Lim1/2 and Lbx1. This population is inhibitory in nature, extend their axons ipsilaterally and settle in the superficial dorsal horn [24, 33]. dI5 interneurons arise from the pD5 progenitor population, which express the transcription factors Ascl1 and Pax3. The post-mitotic neurons can be identified by Lmx1b, which is expressed specifically in this population, and Brn3a. dI5 interneurons express glutamatergic markers such as Vglut2 making them excitatory in nature. They finally settle in the dorsal horn and are involved in relaying somatosensory information [31, 34]. The pD6 progenitor population expresses transcription factors such as Pax3 and gives rise to the inhibitory dI6 population. This population of dorsal interneurons has been studied extensively and marked by transcription factors such as Wt1, Dmrt3 and Lbx1. They migrate and settle in the ventral spinal cord and participate in motor functions [31, 35, 36]. The Dmrt3 expressing subpopulation has been shown to be required for coordinating motor neuron output and provides rhythmicity to motor movements. Furthermore, mutations in the gene encoding Dmrt3 has been reported to generate additional gaits in Icelandic horses; whereas, Dmrt3 knockout mice display significant increases in stride length compared to wildtype littermates [35] [Figure 2.03 and 2.04].

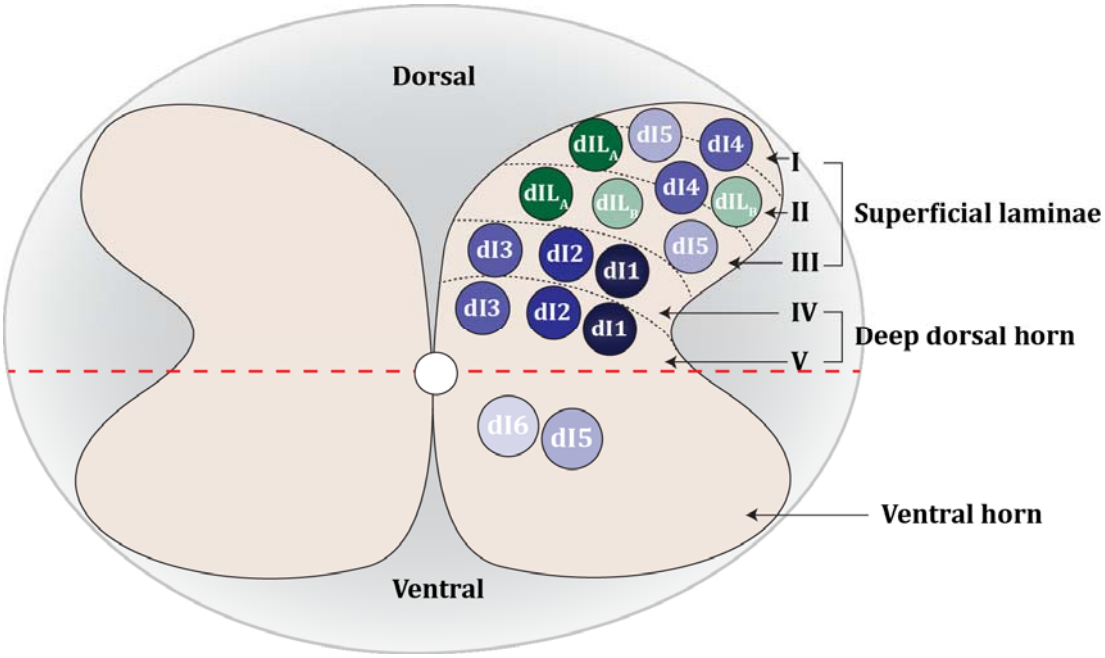

Figure 2.04: Interneurons of the dorsal spinal cord [31, 37]. Dorsal progenitors differentiate into mature post-mitotic neurons, after which, they migrate and occupy pre-determined positions in the superficial laminae (dI4, dI5, dIL$_A$ and dIL$_B$) and the deep dorsal horn (dI1-3). dI6 interneurons and a subpopulation of dI5 interneurons migrate and settle in the ventral spinal cord. Adapted from [37]

2.2.2. Late born dorsal interneurons

During the second round of neurogenesis (between E12-14), two additional subpopulations of dorsal interneurons are born (dIL$_A$ and dIL$_B$). These interneurons arise from progenitors that express Ascl1 and Ptf1a. Post-mitotically they express transcription factors such as Lim1/2 and Pax2 in the dIL$_A$ population and are inhibitory, and Lmx1b and Tlx3 in the excitatory dIL$_B$ population. These interneurons migrate and settle in the superficial laminae in the postnatal spinal cord where they receive sensory information from nociceptive afferents [27, 37] [Figure 2.03 and 2.04].

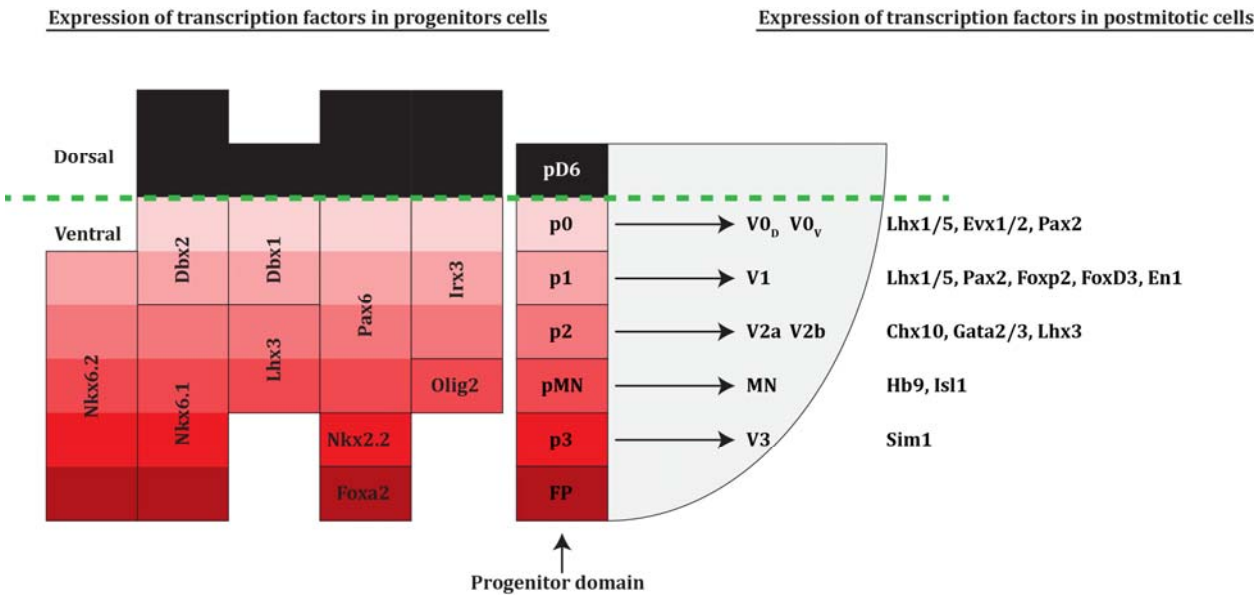

Figure 2.05: Shh signaling is required for the generation of distinct ventral interneurons [8, 31]. Shh, derived from the floor plate, acts along a decreasing ventral – dorsal gradient and induces the expression of distinct transcription factors in the progenitor cells. This leads to the generation of mature post-mitotic motor neurons and domains of ventral interneurons which can be identified by specific transcription factors that they express. FP: floor plate, MN: motor neuron.

2.3. Interneurons of the ventral spinal cord

In the developing mouse spinal cord, V0 interneurons are derived from the dorsal most progenitors of the ventral spinal cord (p0) around embryonic day 10-13. The progenitors can be identified by the expression of transcription factors such as Dbx1/2, whereas, post-mitotic V0 interneurons express Evx1 and Lhx1 [38]. During embryonic development, these interneurons migrate and occupy positions in the ventro-medial spinal cord. They can be further divided into a dorsal ($V0_D$) population that expresses Dbx1 and ventral population ($V0_V$) that expresses Evx1. $V0_D$ interneurons are excitatory in nature, whereas, $V0_V$ interneurons are inhibitory. Both populations form commissural axonal projections and are implicated in contributing to locomotory behaviors. Additionally, another population of V0 interneurons has been identified

recently ($V0_{C/G}$) that expresses the transcription factor Pitx2. These interneurons are either cholinergic ($V0_C$) or glutamatergic ($V0_G$) in nature and project ipsilaterally to motor neurons [39, 40]. V1 interneurons are derived from Pax6, Nkx6.2 and Dbx2 expressing neural progenitors (p1). Post-mitotically, they express the transcription factor Engrailed-1 (En-1) and are located in the ventral horn. V1 interneurons are inhibitory in nature and form ipsilateral projections to motor neurons and can be further divided into two subtypes: the Renshaw cells (RC) and Ia inhibitory interneurons which provide reciprocal inhibition to motor neurons [41-43].

V2 interneurons are derived from progenitors that express the transcription factor Lhx3 (p2). This population of mostly ipsilaterally projecting interneurons can be further divided into V2a and V2b subtypes. Post-mitotic V2a interneurons, marked by the expression of the transcription factor Chx10, are excitatory in nature, whereas, V2b interneurons, which can be identified by the expression of Gata2/3, are inhibitory. They participate in locomotor function and are required for maintaining left-right coordination of locomotion. Furthermore, these neurons also integrate information on speed-dependent changes of gait during ground/ treadmill locomotion [40, 44, 45]. V3 interneurons are derived from the Nkx2.2 expressing progenitor domain (p3). Post-mitotic neurons can be identified by the expression of the transcription factor Sim1. In the post natal spinal cord, they are located in ventro-medial and dorso-medial regions. These neurons are excitatory in nature and mostly extend their axons contralaterally and are thought to function by providing balance to neurons responsible for generating rhythm [Figure 2.05 and 2.06] [40, 46].

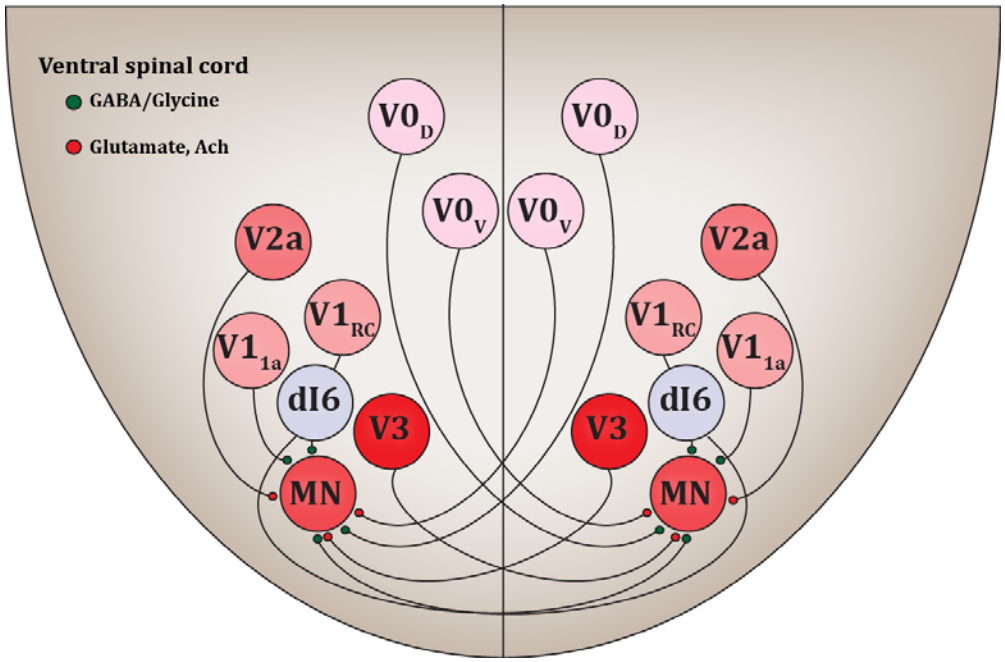

Figure 2.06: Interneurons of the ventral spinal cord [8, 31]. Ventral progenitors exit the cell cycle and differentiate into mature post-mitotic neurons, after which, they migrate and occupy pre-determined positions in the ventral spinal cord. Interneurons participate in motor functions, such as rhythm generation, flexor and extensor activity and coordinate left-right locomotion by mostly impinging on motor neurons (MN). Adapted from [31]

2.4. Motor system

Limbed animals display different forms of locomotion such as swimming and walking. Neural networks that reside in the ventral spinal cord, collectively termed central pattern generators (CPGs), generate these locomotory behaviors. They control important features of these behaviors such as 1) coordination of left-right locomotion 2) alternation of flexors and extensors and 3) the capacity to generate rhythm. These movements are repetitive and cyclical and are not controlled by input from the brain. However, CPG activity is initiated in pathways originating from higher brain centers such as the mesencephalic locomotor region (MLR) and the lateral hypothalamus and descend via the reticulospinal tracts that terminate in the spinal cord [47].

Most of our understanding of CPG circuits comes from *in vitro* studies performed in the hindlimb locomotor circuits of the lumbar spinal cord initially in lamprey, Xenopus and cats and more recently in rodents [[48, 49] and references within]. These studies have utilized the isolated spinal cord preparation, developed in the 1980s, to study rhythmic activity in hindlimb motor neurons by recording from either the ventral roots or from hindlimb muscles [50, 51]. The isolated spinal cord preparation has proven to be an invaluable tool to study CPG circuits for the following reasons: a) it produces a stable locomotor pattern for many hours *in* vitro, b) activity in the ventral roots can be evoked and manipulated with a number of neurotransmitters such as dopamine, 5-HT, NMDA [52, 53] to delineate motor patterns generated by the spinal cord (also called fictive locomotion) and c) the locomotor patterns generated by inducing fictive locomotion correlate with studies that investigate the walking pattern in intact adult animals [52]. This, along with the genetic studies conducted on identifying interneuron populations involved in CPG function allow the precise dissection of motor movements generated in the spinal cord.

2.4.1. Left-right coordination of locomotion

Commissural interneurons (CINs) in the ventral spinal cord are involved in controlling left-right coordination of locomotion. The axonal projections of these neurons cross the midline and influence the CPG circuitry in the contralateral spinal cord. CINs mediate left-right alternation via a dual inhibitory pathway, where inhibitory CINs (iCINs) that express the neurotransmitter GABA/glycine, project to contralateral motor neurons and inhibit their activity directly. Simultaneously, excitatory CINs (eCINs) that express glutamate, project to inhibitory interneurons including V1-Renshaw cells (RC) [54] and thus inhibit motor neuron activity

indirectly [55, 56]. Additionally, via a single excitatory pathway, eCINs were also found to project directly to contralateral motor neurons and promote synchrony [57].

V0 and V3 interneurons are commissural interneurons that participate in left-right coordination of locomotion. V0 interneurons are subdivided into excitatory $V0_V$ and inhibitory $V0_D$ subpopulations. Ablation of the V0 population, using diphtheria toxin A (DTA), leads to a rabbit-like hopping phenotype in these mice during fictive locomotion. This population nicely fits the dual inhibitory pathway, as V0 interneurons have been shown to project to motor neurons. The absence of both direct inhibitory input to motor neurons and probably indirect inhibitory input to RC and other inhibitory interneurons that project to motor neurons, causes eCINs to activate motor neurons in both halves of the spinal cord explaining the hopping gait [55, 58]. V3 interneurons were shown to participate in left-right coordination of locomotion by blocking neurotransmitter function. The authors found irregularities in the amplitude and frequency in fictive locomotion experiments, along with imbalance in motor activity. Furthermore, they demonstrated the projection of V3 neurons to RC interneurons, V1Ia inhibitory interneurons and motor neurons, suggesting roles in both dual inhibitory pathway and single excitatory pathway [46, 59].

V2a interneurons have been suggested to drive activity in CINs. Ablation of the excitatory V2a population leads to irregularities in amplitude and frequency in isolated spinal cord preparations. However, the locomotor patterns were normal at low frequencies and were disrupted only at high frequencies. Furthermore, V2a interneurons have been shown to project to the $V0_V$ population implicating that they specifically drive activity of neurons involved in the direct dual inhibitory pathway and other groups of neurons are involved in driving activity in V3 and $V0_D$ [59-62].

2.4.2. Flexor-extensor (F/E) alternation

Flexor and extensor muscles are required for alternating limb movements. Flexor and extensor circuits in the spinal cord are thought to function by reciprocal inhibition of motor neurons. Mostly ipsilaterally projecting interneurons drive flexor and extensor activity as F/E activity patterns are preserved in the hemisected spinal cord. Additionally, these interneurons are inhibitory as blocking their neurotransmission leads to synchronous locomotor patterns. Renshaw cells (RC) and V1Ia interneurons have been implicated in F/E activity. They are inhibitory classes of interneurons that project ipsilaterally to motor neurons and are rhythmically active during locomotion [49]. RCs have been demonstrated to participate in controlling the firing rate of motor neurons, whereas V1Ias are thought to be involved in motor neuron inhibition. Ablating RCs and V1Ia interneurons however, leads to slowing of locomotor activity, but does not abolish F/E completely [43]. Thus, other ipsilaterally projecting interneurons have been thought to be involved in controlling F/E activity.

Recently, the Goulding group has demonstrated the role of the V1 (including V1Ia interneurons) and V2b populations in F/E alternation. Both these populations of interneurons are inhibitory in nature and project ipsilaterally to motor neurons. The authors found that ablating these populations specifically leads to marked deficits in locomotor activity and limb reflexes, as ablating other inhibitory interneurons did not show defects in F/E activity. Thus, they conclude that CINs do not drive F/E activity directly; however, it may be possible that eCINs such as V3 interneurons drive the activity of V1 and V2b interneurons that are required for F/E activity [41].

2.4.3. Rhythm generation

In the spinal cord, rhythm is generated indirectly by ipsilaterally projecting interneurons that drive pattern generation, which in turn drive activity in motor neurons. These rhythm generating neurons possess the following properties [63]:

a. They are excitatory in nature – experiments conducted in the rodent and cat spinal cord have demonstrated that iIINs and iCINs are not required for providing rhythmic input to motor neurons, as the rhythmic drive was not affected when inhibitory neurotransmission was blocked [49]
b. They are situation in the ventromedial spinal cord
c. They receive appropriate input from descending projections that affect motor activity
d. They are rhythmically active during drug-induced fictive locomotion
e. Since rhythm generating neurons drive pattern generation, the onset of activity in these neurons must precede that of pattern generating neurons

Hb9 (basic-helix-loop-helix domain containing class 9) positive cells have been well studied to assess their role in rhythm generation as they meet most of the criteria listed above. These neurons are excitatory in nature and are located in the ventromedial region of the spinal cord. They have also been shown to be rhythmically active during drug-induced fictive locomotion and possess intrinsic oscillatory properties and, hence, have been designated as 'pacemaker' cells in the past [49, 64, 65]. However, contradictory results were obtained from experiments conducted by the Harris-Warrick group, using calcium imaging and electrophysiological recordings. They found a lag in the onset of the calcium peak from Hb9 positive neurons compared to ipsilateral ventral root bursting, suggesting that activity in Hb9 neurons does not precede activity in pattern generating neurons. Furthermore, activity in the Hb9

neurons was not persistent after displaying initial activity; however, activity in motor neurons was persistent. These results led the authors to argue against a role for Hb9 neurons as the sole pacemaker or rhythm generating neurons. Instead they propose that Hb9 neurons may function in tandem with other interneurons of the ventral spinal cord in generating and setting the rhythm of locomotion [66].

Recently, a previously undescribed population of eIINs, that express the transcription factor Shox2, has been shown to participate in rhythm generation. These interneurons are a subset of the Chx10 positive V2a interneurons and display a great extent of overlap. However, ~25% of Shox2 interneurons do not express Chx10. These neurons are rhythmically active during locomotion and optogenetic silencing produces a marked decrease in locomotor frequency, with normal F/E and left-right coordination of locomotion. Therefore, the authors suggest that these neurons participate in rhythm generation. Furthermore, using anatomical techniques, they demonstrate that these interneurons project to motor neurons in addition to recurrent interconnections [67].

2.5. Voluntary control of stepping movements

Voluntary movements, such as catching, reaching or playing tennis, are neither repetitive nor stereotypic. Such movements demand modification of limb trajectories on a moment-to-moment basis and require input from the motor cortex in the brain. The spinal cord receives supraspinal input via the corticospinal tract (CST), one of the longest longitudinally projecting tracts. The CST arises from pyramidal neurons in layer V of the motor cortex and remains ipsilateral [68]. Signaling via the axon guidance molecules Robo/Slit is essential in confining the CST axons to the ipsilateral side [69]. At the brainstem/cervical junction, the CST axons

decussate and project contralaterally as they enter the spinal cord via the dorsal funiculus (DF). The CST axons are prevented from re-crossing the midline via repulsive Eph4/ephrinB3 signaling [70].

Studies performed in cats subjected to adaptive tasks such as stepping over obstacles during treadmill walking display increased activity in electrical recordings from the motor cortex only when crossing the obstacle [71]. Similarly, experiments performed in rodents by electrically stimulating the motor cortex showed increased EMG activity in forelimb muscles [72]. Furthermore, ablating the entire motor cortex does not affect normal stepping behaviors in mice, however, modification of limb trajectory is significantly reduced in these mice compared to mice with intact motor cortex [73]. Thus, the interplay between CPG neurons and CST input is necessary for fine-tuned or adaptive locomotion.

2.6. Eph/ephrin signaling

Axon guidance molecules guide developing neurons in finding their correct synaptic partners thus establishing neural circuits. Molecules expressed in a highly dynamic structure at the leading edge of the axon, termed the growth cone, allow the axon to traverse through a labyrinth of environmental cues to find their targets. Varieties of molecules serve as guidance cues to developing axons: receptor tyrosine kinases (RTKs), cell adhesion molecules, morphogens and extracellular matrix proteins. These molecules function as either long-range or short-range attractive or repulsive cues in guiding axons.

Eph receptors and their ligands, ephrins (Eph receptor interacting protein), constitute the largest family of the RTKs [74, 75]. The Eph receptors are classified into the A and B type based on sequence similarities and ligand binding affinities. Similarly, ephrin ligands are also

subdivided into class A and B. To date, nine EphAs (EphA1-9 and EphA10) and five EphBs and eight ephrins (five ephrinAs and three ephrinBs) have been documented in mammals [75]. A-type Eph receptors typically bind ephrinAs and B-type Eph receptors bind ephrinBs with the exception of EphA4 which can bind ephrinBs and EphB2 which can bind ephrinA5 [76, 77].

Eph receptors are transmembrane proteins that consist of extracellular and intracellular regions. The extracellular region is made up of a ligand-binding domain (LBD), a cysteine-rich domain, followed by two fibronectin type III domains. The intracellular part of the receptor consists of a juxtamembrane region, a kinase domain, a SAM (sterile alpha motif) binding domain and a PDZ binding domain. EphrinAs are GPI (glycophosphatidylinositol) anchored proteins that have an extracellular receptor binding domain, whereas ephrinBs are transmembrane proteins that consist of an extracellular receptor binding domain and an intracellular PDZ-binding domain [75] [Figure 2.07].

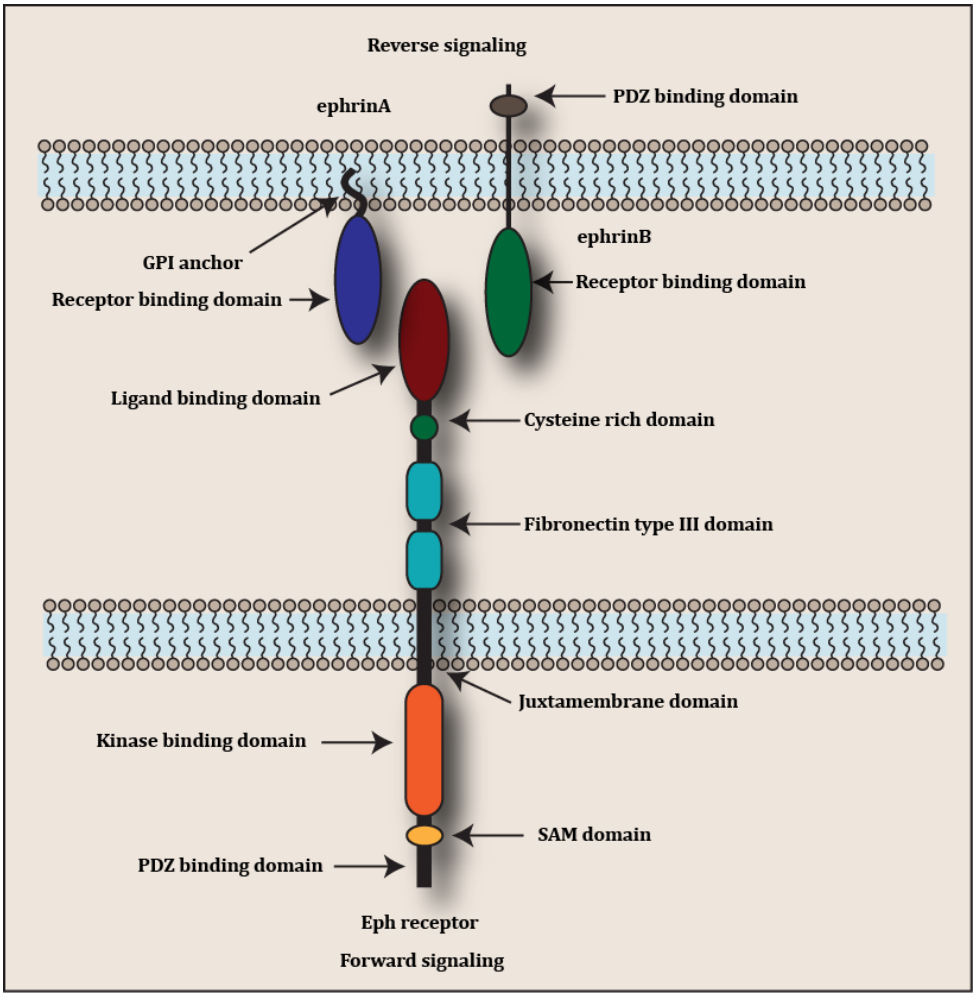

Figure 2.07: Schematic representing the structure of Eph receptors and ephrin ligands. The extracellular domain of Eph receptors consist of a ligand binding domain, cysteine rich domain and two fibronectin type III domains. The intracellular region is made up of the juxtamembrane region, kinase binding domain, SAM domain and PDZ binding domain. EphrinAs are GPI anchored proteins, whereas ephrinBs are transmembrane proteins with a PDZ binding domain.

Three features of the Eph/ephrin system make signaling via these receptors unique: Eph receptors are membrane bound proteins and are activated only by membrane bound ligands [78]; signaling occurs in a bidirectional manner, that is, downstream of both the receptor (forward) and

the ligand (reverse) [74, 75]; higher order clustering of Eph receptors is necessary for the downstream signaling [79].

2.6.1. Eph/ephrin forward signaling

Forward signaling via both classes of Eph receptors share similar mechanisms. For example, downstream signaling pathways are activated with the binding of the ligand that induces the formation of higher order clusters via transphosphorylation of tyrosine residues (most importantly of two tyrosine residues in the juxtamembrane region) on more than one Eph receptor [70, 80]. This allows the activation of signaling cascades that ultimately lead to versatile responses by the cell, such as cell proliferation, endocytosis of the Eph receptor (which may lead to axonal repulsion) and changes in cytoskeletal structures in the growth cone.

For example, the Rho family of GTPases is involved in remodeling of the cytoskeleton via Rho, Rac and Cdc42. The concerted action of Rho GTPases, controls different aspects of cellular outcomes, for example, activated EphA receptors directly initiate Rho activity which promotes growth cone collapse and retraction of the axon [81]. On the other hand, Rac and Cdc42, promote the formation of F-actin and leads to extension of lamellipodia and filopodia respectively [82].

Rho GTPases function by constantly switching between an active GTP-bound state and an inactive GDP-bound state. The balance between these two forms is maintained by:

1. Guanine nucleotide exchange factors (GEFs) that promote the release of the GDP and binding of GTP. Ephexin, one of the most well characterized GEFs, binds to the kinase domain of activated EphA receptors and regulates the activity of Rho GTPases [83]. The Vav family proteins (specifically Vav2 and Vav3) have been shown to be recruited upon ephrinA

activation of the EphA2 receptor. Vav proteins function by activating Rac1 and promoting endocytosis of the ligand-receptor complex in neurons [84, 85] [Figure 2.08].

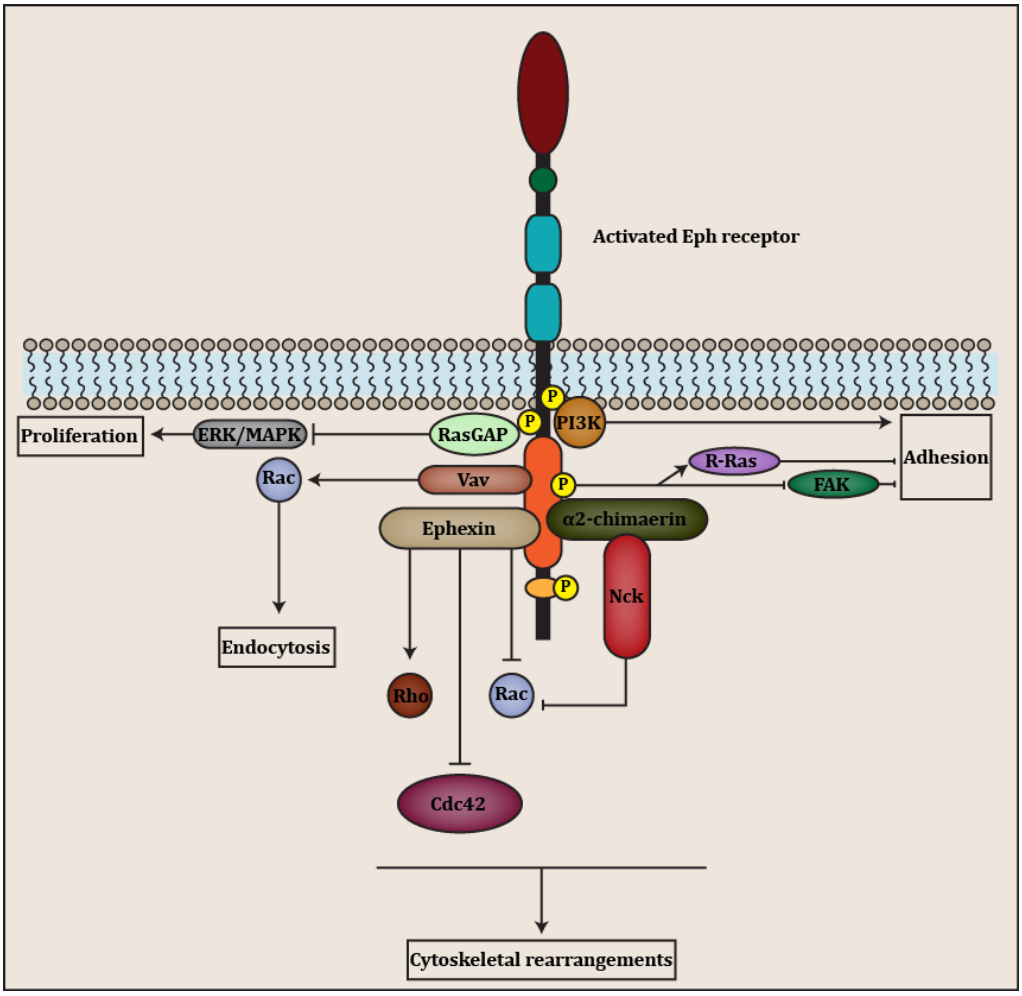

Figure 2.08: Eph-dependent forward signaling. Binding of ephrin ligand induces clustering of the Eph receptor (activated Eph receptor) which leads to phosphorylation of two important tyrosine residues in the juxtamembrane region. Activation of various signaling cascades by recruitment of appropriate protein complexes leads to different cellular outcomes [75].

2. GTPase activating factors (GAPs) are required for inactivating the Rho GTPases and thus allowing them to return to their inactive form. The chimaerin family of proteins has been well established as Rac-GAP proteins. In rodents, two forms of chimaerins exist, α-chimaerin

and β-chimaerin. They further give rise to two isoforms each, α1/α2 and β1/β2. Of these isoforms, only α2-chimaerin and β2-chimaerin contain SH2 domains, in addition to the RacGAP domain and diacylglycerol-binding domain. In the nervous system, the function of α2-chimaerin has been well studied. It binds to the activated EphA4 receptor which leads to the recruitment of adaptor proteins, such as Nck (Grb4), which contains one SH2 domain and three SH3 domains, thus forming a stable complex that is required for the modulation of Rac activity during axonal growth cone collapse [86, 87] [Figure 2.08].

Other protein families, such as the Ras family of GTPases are also regulated by activated Eph receptors. For example, phosphorylation of the juxtamembrane region of the Eph receptor recruits RasGAP, which further activates downstream signaling via ERK (extracellular signal regulated kinase) and MAPK (mitogen activated protein kinase), necessary for cell proliferation and migration. Similarly, the combined activity of PI3K (phosphoinositide 3 kinase), R-Ras and FAK promote cell adhesion [82] [Figure 2.08].

2.6.2. Eph/ephrin reverse signaling

Reverse signaling via ephrin ligands share diverse mechanisms owing to differences in their structure. EphrinAs are tethered to the membrane via a GPI (glycophosphatidylinositol) anchor and thus lack an intracellular domain. GPI-anchored proteins, including ephrinAs are often localized to specialized regions in the cell membrane, termed lipid rafts that are rich in cholesterol and sphingolipids. Binding to the Eph receptor promotes clustering of ephrinAs within lipid rafts thus allowing the recruitment of Src proteins and further downstream signaling [Figure 2.09 A]. EphrinAs are also known to interact with co-receptors such as p75 which leads to phosphorylation of Fyn and inducing downstream signaling pathways which ultimately leads

to growth cone collapse in retinal cells [88]. Furthermore, during development, ephrinAs have been shown to interact with the TrkB receptor which regulates synapse formation and branching of axons in retinal ganglion cells (RGCs) [89] [Figure 2.09 B].

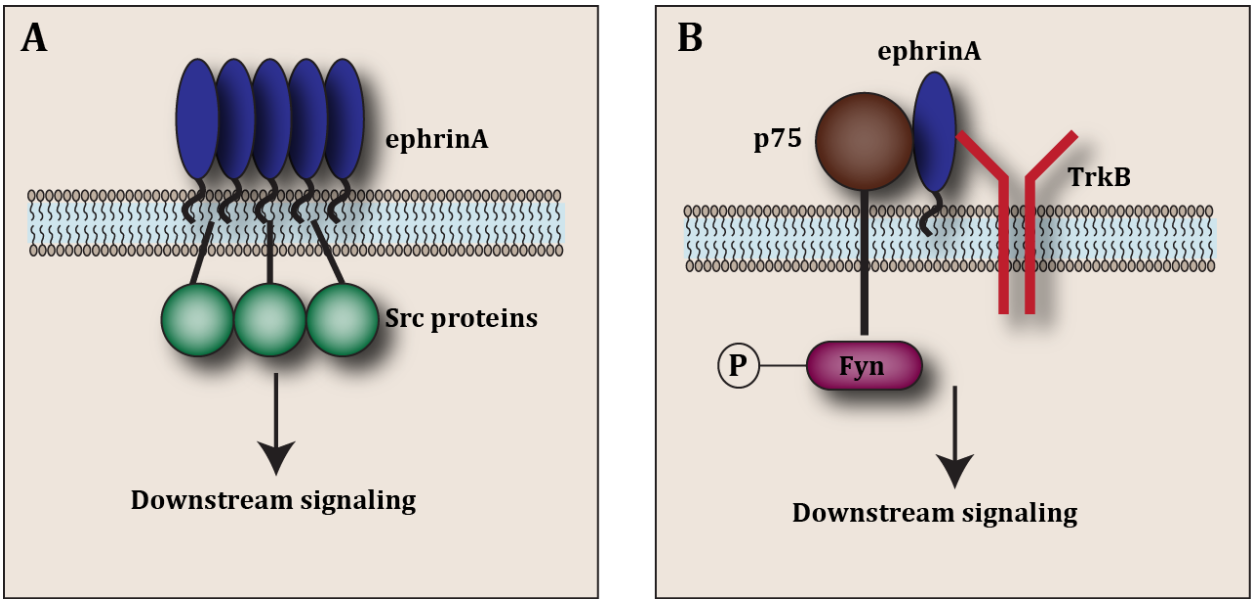

Figure 2.09: EphrinA-dependent reverse signaling. Binding of Eph receptor induces clustering of ephrinAs which leads to recruitment of Src proteins and further downstream signaling [A]. ephrinAs also interact with coreceptors such as p75 and TrkB which induces the phosphorylation of downstream signaling proteins such as Fyn [B].

EphrinBs employ different methods to induce downstream signaling as they are transmembrane proteins. Binding of the Eph receptor induces clustering of ephrinBs which leads to the phosphorylation of specific tyrosine residues and the subsequent recruitment SH2 (Src homology 2) – containing proteins such as Grb4 [90-92]. Signaling via this pathway induces cytoskeletal rearrangements which are important processes required for spine maturation [91, 93]. Furthermore, ephrinB-dependent signaling occurs via the PDZ domain which acts as a docking site for proteins such as GRIP and PDZ-RGS3 that inhibit the chemoattractive functions the G-protein coupled receptor, CXCR4 [94, 95] [Figure 2.10].

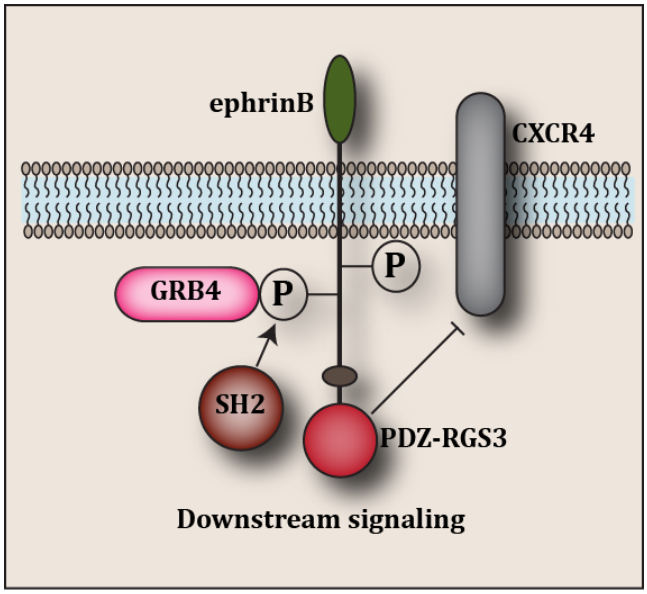

Figure 2.10: EphrinB-dependent reverse signaling. Binding of Eph receptors induces the phosphorylation of important tyrosine residues in the cytoplasmic domain of ephrinBs by the Src protein, SH2. This allows the docking of Grb4, an adaptor protein leading to further downstream signaling. ephrinBs also induce the recruitment of the PDZ domain binding protein, PDZ-RGS3 which leads to inhibition of the G-protein coupled receptor, CXCR4.

2.6.3. EphA4/ephrinB3 dependent axon guidance

Since the functions of EphA4 and ephrinB3 are of particular interest to this project, their roles in guiding CST axons and axonal projections in the spinal cord are discussed here.

2.6.3.1. EphA4 and ephrinB3 in CST axons

The corticospinal tract (CST) arises in layer V of the motor cortex. It traverses a long distance through the brain and when it reaches the medulla, the axons of the CST decussate across the midline and project contralaterally [96]. The CST axons enter the spinal cord via a structure termed the dorsal funiculus (DF) and its axons are confined to the contralateral side throughout the length of the spinal cord. CST axons express EphA4 whereas the spinal cord midline expresses ephrinB3. The CST axons are prevented from re-crossing the midline due to

the interaction of EphA4 with ephrinB3, which triggers repulsive axon guidance leading to the collapse of the growth cone and retraction of the axons away from the midline. Null mutations of either EphA4 or ephrinB3 render CST axons insensitive to repulsion by the spinal cord midline leading to extensive midline misprojections of CST axons, as observed in anterograde tracing experiments using biotin dextran amine in these mice [70, 97]. The confinement of the CST axons to the contralateral spinal cord is mediated by EphA4-dependent forward signaling. Evidence for this comes from experiments that used mutated alleles of the ephrinB3 gene or EphA4. The first mutated allele of ephrinB3, ephrinB3^{neo}, is essentially a loss-of-function hypomorphic allele that leads to abolished forward and reverse signaling. These mice display extensive midline misprojections of the CST axons in anterograde tracing experiments. The second allele, ephrinB3^{lacz}, is a truncated version of ephrinB3 in which β-gal replaces the cytoplasmic domain of the protein and mice expressing this allele do not display midline misprojections of the CST axons. On the contrary, signaling deficient EphA4 mutants (EphA4 kinase dead) display extensive midline misprojections implicating the need for the EphA4 kinase domain in guiding CST axons [98]. Thus, CST axon guidance is mediated by EphA4-dependent forward signaling and ephrinB3-mediated reverse signaling is dispensable for the guidance of these axons [99, 100].

Furthermore, other studies have tested the consequence of inhibiting the activity of downstream effectors of EphA4 such as α2-chimaerin and Nck. Anterograde tracings, using biotin dextran amine, to trace CST axons in α2-chimaerin knockout mice display bilateral innervation of the spinal cord in comparison to unilateral innervation observed in control mice [101]. Similar results were obtained using retrograde pseudorabies viral tracings of CST axons in these mice reiterating the involvement of the EphA4 forward signaling via its downstream

effector, α2-chimaerin in CST axon guidance [73]. Likewise, Nck conditional mutants also display aberrant midline misprojections of CST axons [87] [Figure 2.11].

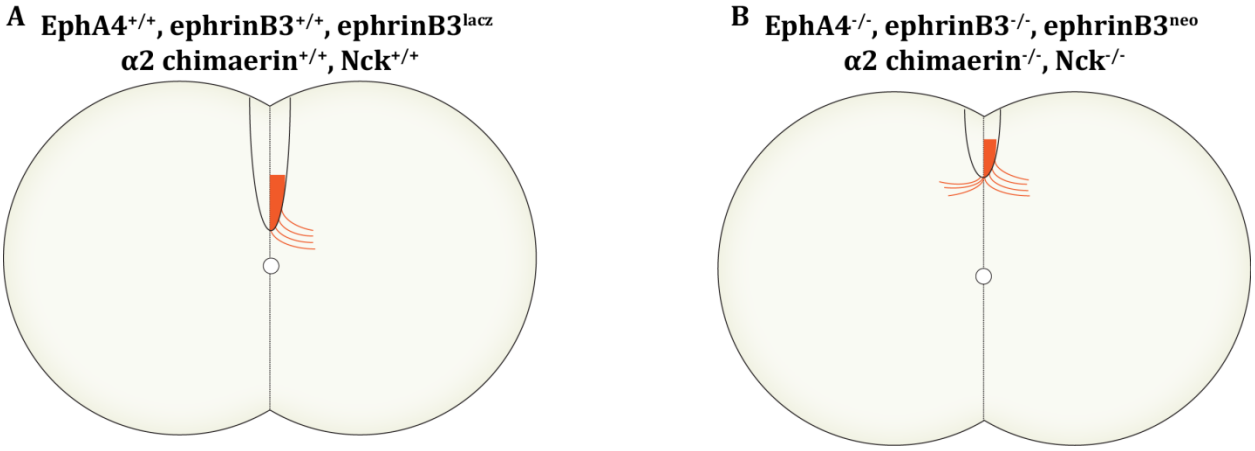

Figure 2.11: Summary of CST axon phenotypes in wildtype and mutant mice. Anterograde tracing of CST axons, using biotin dextran amine, displays unilateral CST projections in wildtype spinal cords [A]. Conversely, anterograde tracing of CST axons in various EphA4 knockout and ephrinB3 knockout mice displays bilateral projections in the spinal cord. Furthermore, ablation of downstream effectors of EphA4, such as α2-chimaerin and Nck also display bilateral CST innervation of the spinal cord [B].

These mice also display defects in the structure of the DF; EphA4 and ephrinB3 knockout mice have a shallow DF compared to their wildtype littermates [70]. Additionally, it is known that CST axons project to spinal interneurons and provide supraspinal input that is necessary for fine-tuned locomotion. Unilateral electrical stimulation of the motor cortex in ephrinB3$^{-/-}$ and α2-chimaerin$^{-/-}$ mice evokes strong bilateral forelimb responses as compared to unilateral responses seen in control mice [73, 99]. Furthermore, α2-chimaerin$^{-/-}$ mice display defects in adaptive/ voluntary locomotor tasks such as crossing obstacles in a treadmill stepping paradigm. Control mice cross the obstacles by alternating their limbs whereas; knockout mice display significant bilateral limb movements when crossing the obstacles thus implicating EphA4-dependent

forward signaling via its downstream effector, α2-chimaerin in adaptive control of locomotion [73].

2.6.3.2. EphA4 and ephrinB3 in spinal cord interneurons

The most striking defect in EphA4 and ephrinB3 knockout mice is their altered gait. Wildtype mice usually produce alternating limb movements during locomotion; however, ablating EphA4 and/or ephrinB3 leads to bilateral limb movements or a hopping gait in these mice. This phenotype is mediated by EphA4-dependent forward signaling as ephrinB3^{lacZ} mice (where β-gal replaces the cytoplasmic tail of ephrinB3) do not display any defect in locomotory behaviors, whereas EphA4 kinase dead mutants recapitulate the hopping gait observed in EphA4 full knockouts [98]. Furthermore ablating EphA4 downstream effectors such as α2-chimaerin and the adaptor protein Nck, phenocopies the EphA4 knockout mice, that is, they display a robust hopping gait, thus adding further evidence to the requirement of EphA4-mediated forward signaling in maintaining alternating limb movements [87, 101]. Furthermore, RhoA, a known downstream target of α2-chimaerin, has also been shown to be required in maintaining locomotory circuits of the spinal cord. Indeed, ablating RhoA specifically in neuronal cells, produces locomotor defects similar to those observed in EphA4 and ephrinB3 knockout mice [102].

EphA4 positive neurons have been shown to be an ipsilaterally projecting excitatory component of the mammalian CGP. Indeed, these neurons have been shown to express the vesicular glutamate transporter, VGlut2 [103]. They remain ipsilateral owing to their interaction with ephrinB3 expressed at the midline which repels EphA4 positive neurons and thus confines them to one side of the spinal cord. In the absence of EphA4 or ephrinB3, these neurons no

longer respect the midline and display aberrant misprojections. As mentioned in the earlier sections, left-right coordination of locomotion is controlled by commissural interneurons that are both excitatory and inhibitory. Thus, in the EphA4 knockout mice, the aberrant misprojections of normally ipsilateral projections provide additional excitatory drive to contralateral CPGs leading to the hopping phenotype observed in these mice. Evidence for this comes from experiments that utilize the isolated spinal cord technique (fictive locomotion). In these experiments, spinal cords from wildtype and knockout mice were bathed with glycine/GABA uptake blockers such as sarcosine and nipecotic acid thus leading to strengthening of inhibition. Recordings from wildtype cords revealed continued alternating locomotor patterns; however, knockout cords displayed a switch from synchrony to alternation with the strengthening of inhibitory drive. Furthermore, selectively ablating EphA4 in VGlut2 expressing cells produces a similar synchronous locomotor pattern thus demonstrating that increased excitatory drive to contralateral CPGs is responsible for the hopping phenotype observed in these mice [103, 104]. Another study conducted by the Kiehn group has shown that EphA4, specifically expressed in the ventral spinal cord is required to maintain CPG function, whereas, dorsally expressed EphA4 is dispensable [105]. This study is in contradiction with our results and is discussed extensively in section 5.1

2.7. Project aims

The aims of the project undertaken in this thesis were as follows:

1. The roles of EphA4 and ephrinB3 in locomotor function have been well studied in the ventral spinal cord. It is largely accepted that the ventral spinal cord is involved in processing motor information whereas the dorsal spinal cord processes sensory information. However, owing to an increase in our understanding of the development and functions of spinal cord

interneurons, we now know that certain dorsal interneuron cell types participate in motor functions. Given the widespread expression of EphA4 in the entire spinal cord, we asked if EphA4, expressed specifically in dorsal interneurons, is required in motor functions. To assess this, we performed behavioral assays with specific dorsal spinal cord mutants and tested their role in CGP functions using the treadmill walking paradigm.

2. EphA4 is required for guiding CST axons when they enter the spinal cord and EphA4 knockout mice display aberrant midline crossings. We therefore asked if EphA4 is required for cortical control of adaptive locomotion. For this, we performed behavioral assays using specific forebrain EphA4 mutant mice and subjected them to the adaptive locomotion paradigm.
3. EphA4 is also known to be required for the correct formation of the DF as ablating EphA4 leads to a shallow DF. In order to understand how EphA4, expressed in the spinal cord, affects DF formation, we used EphA4 mutant mice and performed immunohistochemical and immunofluorescence assays.

3. Materials and Methods

3.1. Materials

3.1.1. Chemicals and reagents

Chemicals were purchased from Millipore, Sigma, Merck, Roche, Biomol and Roth. Enzymes and buffers were purchased from New England Biolabs (NEB). All water used to prepare buffers and solutions were filtered using Milli-Q-Water System (Millipore).

3.1.2. Buffers and solutions

3.1.2.1. 10X Phosphate buffered saline (PBS) – for 1 liter; pH 7.3

80g NaCl

2g KCl

11.5g $NaH_2PO_4.7H_2O$

2g KH_2PO4

3.1.2.2. 4% Paraformaldehyde (PFA) – for 100ml; pH 7.4

4g Paraformaldehyde

10µl 5M NaOH

10ml 10X PBS

Milli-Q-H2O to 100ml

Half the amount of water indicated above was heated to 65˚C after which 4g of paraformaldehyde was added and left to stir for 10 minutes. 100µl of 5M NaOH was added to the

solution. Once the solution turned clear, 10ml PBS (10X) was added to the solution and allowed to cool. HCl was added to adjust the pH to 7.4. The volume was adjusted to 100ml.

3.1.3. Genotyping oligonucleotides

All oligonucleotides were purchased from Metabion or Eurofins MWG Operon

EphA4WT-F	5'–CAATCCGCTGGATCTAAGTGCCTGTTAGC–3'
EphA4WT-R	5'–ACCGTTCGAAATCTAGCCCAGT–3'
EphA4KO-F	5'–GACTCTAGAGGATCCACTAGTGTCGA–3'
EphA4KO-R	5'–TTTTCTCCCTCTTTAAGCAAGGATCAAGC–3'
EphrinB3161-F	5' - GGGATATGGAAGCTTTGAGAC - 3'
EphrinB3308-R	5'- GGTATCACCACCCACAACCAGC - 3'
EphrinB3Neo	5' - GAGATCAGCAGCCTCTGTTCC - 3'
Cre1	5'–GCCTGCATTACCGGTCGATGCAACGA–3'
Cre2	5'–GTGGCAGATGGCGCGGCAACACCATT–3'
LacZ-F	5'–CCAGCTGGCGTAATAGCGAA–3'
LacZ-R	5'–CGCCCGTTGCACCACAGATG–3'
PLAP-F	5' –AACCCAGACTTCTGGAACCG–3'
PLAP-R	5' –CTGCACCAGATTCTTCCCGT–3'
Lox-F	5' –GCACACTTAGCAATTCAGTGTGGG–3'
Lox-R	5'–CAGTTAATTAGTGGTGGGTTCCTG–3'
Tomato-F	5'–AAGGGAGCTGCAGTGGAGTA–3'
Tomato-R	5' –CCGAAAATCTGTGGGAAGTC–3'

Table 3.01: List of oligonucleotides for genotyping

3.1.4. Antibodies

3.1.4.1. Primary antibodies

Antibody	Species	Source	Dilution	Application
α-βgal	Chicken	Abcam	1:2000	IF
α-Lbx1	Guinea Pig	C. Birchmeier	1:10000	IF
α-Pax2	Rabbit	Invitrogen	1:200	IF
α-Brn3a	Mouse	Millipore	1:1000	IF
α-Zic2	Rabbit	E.Herrera	1:1000	IF
α-CGRP	Rabbit	Calbiochem	1:2000	IF
α-Parvalbumin	Mouse	Swant	1:1000	IF
α-TrkA	Goat	R&D	1:500	IF
α-TrkC	Goat	R&D	1:500	IF
α-Ctip2	Rat	Abcam	1:1000	IF
α-EphA4 (S20)	Rabbit	Beck and Dickson	1:300	WB
α-Tubulin	Mouse	Sigma	1:20000	WB

Table 3.02: List of primary antibodies

3.1.4.2. Secondary antibodies

Antibody	Species	Source	Dilution	Application
Rabbit–α–Cy2	Donkey	Jackson Immunoresearch	1:400	IF
Rabbit–α–Cy3	Donkey	Jackson Immunoresearch	1:400	IF
Mouse–α–Cy2	Donkey	Jackson Immunoresearch	1:400	IF
Mouse–α–Cy3	Donkey	Jackson Immunoresearch	1:400	IF
Guinea pig–α–Cy2	Donkey	Jackson Immunoresearch	1:400	IF
Guinea pig–α–Cy3	Donkey	Jackson Immunoresearch	1:400	IF
Chicken–α–Cy2	Donkey	Jackson Immunoresearch	1:400	IF
Chicken–α–Cy3	Donkey	Jackson Immunoresearch	1:400	IF
Rat–α–Cy5	Donkey	Jackson Immunoresearch	1:400	IF
Goat–α–Cy2	Donkey	Jackson Immunoresearch	1:400	IF
Rabbit–α–HRP	Donkey	GE Healthcare	1:5000	WB
Mouse–α–HRP	Donkey	GE Healthcare	1:5000	WB

Table 3.03: List of secondary antibodies

3.1.5. Agarose gel electrophoresis

3.1.5.1. 50X Tris-acetate-EDTA Buffer (TAE) – for 1 liter; pH 8.5

242g Tris base

5.1ml Glacial acetic acid

37.2g $Na_2EDTA.2H_2O$

H2O up to 1 liter

3.1.5.2. Gel loading buffer

25ml Glycerol

1ml 50X TAE

0.1g Orange G

24ml H2O

3.1.6. Polyacrylamide gel electrophoresis

3.1.6.1. Lysis Buffer

50mM Tris pH 7.5

150mM NaCl

50mM EDTA

1% Triton

Milli-Q-Water

The solution was stored at 4˚C till it was used. Before using, 1 tablet of Protease Inhibitor (Roche) was added to 50ml of lysis buffer and 1ml of PhosphoSTOP (Roche) was added to 10ml of lysis buffer.

3.1.6.2. SDS-PAGE resolving gel (7.5%)

4.85ml H2O

2.6ml 1.5M Tris pH 8.8; 0.4% SDS

2.5ml 30% (w/v) Acrylamide; 0.8% (w/v) Bis-Acrylamide

50µl 10% APS

5µl TEMED

3.1.6.3. SDS-PAGE stacking gel (4%)

3.05ml H_2O

1.3ml 0.5M Tris pH 6.8; 0.4% SDS

0.65ml 30% (w/v) Acrylamide; 0.8% (w/v) Bis-Acrylamide

50µl 10% APS

5µl TEMED

3.1.6.4. 6X Sample Buffer

12% SDS

300mM Tris-HCl pH 6.8

600mM DTT

0.6% BPB

60% Glycerol

Milli-Q-H_2O

This buffer was stored at -20˚C.

3.1.6.5. 5X Electrophoresis Buffer

154.5 g Tris base

721g Glycine

50g SDS

The volume was adjusted to 10 liters with Milli-Q-water and stored at room temperature.

3.1.6.6. 1X Transfer Buffer

3.03 g Tris base

14.4 g Glycine

200 ml Methanol

The volume was adjusted to 650 ml with Milli-Q-water to mix and dissolve the ingredients after which the final volume was adjusted to 1 liter. The buffer was stored at room temperature.

3.1.6.7. PBS-Tween (PBS–T)

1X PBS

0.1% Tween®20

This buffer was stored at room temperature.

3.1.6.8. Blocking Buffer (10ml)

0.5g 5% Skim milk

10ml PBS – T

3.1.7. X-gal staining

3.1.7.1. 0.5M Na-phosphate Buffer Stock; pH 7.3

71g Na_2HPO_4

72g NaH_2PO_4

The volume was adjusted to 1000ml with Milli-Q-water. The buffer was stored at room temperature.

3.1.7.2. Fixative

0.4ml 25% Glutaraldehyde

2.5ml EGTA pH 7.3

0.1ml 1M $MgCl_2$

47ml 0.1M Na-phosphate buffer pH 7.3

The buffer was stored at 4˚C.

3.1.7.3. Wash Buffer

2ml 1M $MgCl_2$

0.1g DOC

0.2ml NP – 40

The volume was adjusted to 1000ml using 0.1M Na-phosphate buffer pH 7.3. The buffer was stored at room temperature.

3.1.7.4. X-gal Staining Solution

0.106g $C_6N_6FeK_4$ (Sigma)

0.082 $C_6N_6FeK_3$ (Sigma)

0.5ml of 100mg/ml X-gal (dissolved in N-N-dimethylformamide) was added to fresh, pre-heated buffer at 37˚C. The volume was adjusted to 50ml using wash buffer. The solution was protected from light and stored at 4˚C.

3.1.7.5. 100% BABB

1 part Benzyl alcohol

2 parts Benzyl benzoate

The solution was protected from light and stored at room temperature.

3.1.7.6. 50% BABB

50% BABB

50% Methanol

This solution was protected from light and stored at room temperature.

3.1.8. Alkaline phosphatase staining

3.1.8.1. NTMT Solution (200ml)

4ml 5M NaCl

20ml 1M Tris-HCl pH 9.5

10ml 1M $MgCl_2$

200µl Tween® 20

This solution was prepared fresh before each use.

3.1.8.2. Developing Solution (10ml)

11µl 5-bromo-4chloro-3-indolyl-phosphate (BCIP)

14µl Nitro blue tetrazolium (NBT)

10ml NTMT

This solution was prepared fresh before each use.

3.1.9. Nissl Staining

3.1.9.1. Nissl stain

0.1% Cresyl violet

0.3% Acetic acid

This solution was stored at room temperature.

3.1.10. Embedding solutions for vibratome and cryostat sectioning

3.1.10.1. 0.1M Acetate Buffer; pH 6.5

99ml 1M Sodium acetate

960µl 1M Acetic acid

The volume was adjusted to 1 liter using Milli-Q-water and stored at room temperature.

3.1.10.2. Embedding Solution

Solution a

90g Ovalbumin (Sigma)

200ml 0.1M Acetate buffer

Ovalbumin was dissolved in acetate buffer by stirring overnight at room temperature. The solution was filtered through gauze to remove undissolved ovalbumin and air bubbles.

Solution b

15g Gelatin

100ml 0.1M Acetate buffer

Gelatin was dissolved in warm acetate buffer. The solution was cooled down to room temperature.

Solutions 'a' and 'b' were mixed, aliquoted and stored at -20˚C.

3.1.10.3. 15% Sucrose (50ml)

7.5g Sucrose

1X PBS upto 50ml

The solution was stored at 4˚C.

3.1.10.4. 30% Sucrose (50ml)

15g Sucrose

1X PBS upto 50ml

The solution was stored at 4˚C.

3.1.11. Mouse lines

EphA4 full knockout mice were generated in our laboratory [106] and maintained in a mixed 129 x C57Bl6/J genetic background.

EphrinB3$^{-/-}$ mice [70] were provided by Regeneron. Inc and were maintained in a mixed 129 x C57Bl6/J genetic background.

EphA4^{PLAP} mice [107] were obtained from Marc Tessier-Lavigne, Rockefeller University, and maintained in a mixed 129 x C57Bl6/J genetic background. They were used to label the cell bodies with β-gal and axonal projections with human placental alkaline phosphatase (PLAP).

EphA4^{lx} mice [108] were obtained from Binhai Zheng, UCSD, and maintained in a mixed 129 x C57Bl6/J genetic background. They were used in combination with the below mentioned Cre lines to generate specific conditional EphA4 mutants.

PGK–Cre mice were generated by the laboratory of Yvan Lallemand [109] and maintained in a mixed 129 x C57Bl6/J genetic background. They were used as deleter lines to phenocopy the full knockouts.

Emx1–Cre mice (B6.129S2-*Emx1$^{tm1(cre)Krj}$*/J) [110] were maintained in a mixed 129 x C57Bl6/J genetic background. They were crossed to EphA4^{lx} mice to generate EphA4 forebrain knockouts.

HoxB1–Cre mice (B6.129S-*Hoxb1$^{tm1(cre)Og}$*/J) [111] were maintained in a mixed 129 x C57Bl6/J genetic background. They were crossed to EphA4^{lx} mice to generate EphA4 spinal cord specific knockouts.

Pax7–Cre mice [112] were maintained in a mixed 129 x C57Bl6/J genetic background. They were crossed to EphA4^{lx} mice to generate dorsal spinal cord EphA4 mutants (dI1-6).

Lbx1–Cre mice [113] were obtained from Carmen Birchmeier, MDC Berlin, and maintained in a mixed 129 x C57Bl6/J genetic background. They were crossed to EphA4^{lx} mice to generate dorsal spinal cord EphA4 knockouts (dI4-6).

Wnt1–Cre mice [114] were maintained in a mixed 129 x C57Bl6/J genetic background. They were crossed to EphA4^{lx} mice to generate dorsal spinal cord EphA4 knockouts (dI1-2).

Ptf1a–Cre mice [115] were maintained in a mixed 129 x C57Bl6/J genetic background. They were crossed to EphA4^{lx} mice to generate dorsal spinal cord EphA4 knockouts (dI4).

Rosa26R mice [116] were maintained in a mixed 129 x C57Bl6/J genetic background. They were used as a reporter line.

R26-CAG-td Tomato (Ai9) mice (B6.Cg-Gt*(ROSA)26Sor*$^{tm9(CAG\text{-}tDTomato)Hze}$/J) [117] were maintained in a mixed 129 x C57Bl6/J genetic background. They were used as a reporter line.

3.2. Methods

3.2.1. Genotyping

3.2.1.1. Tail DNA preparation and genotyping using PCR

To genotype the mice and the embryos, DNA was extracted from the tail and the hindlimbs respectively. The tissue was boiled in 100µl 50mM NaOH for 15 minutes three times and vortexed between each boiling step. The NaOH was neutralized with 10µ 1.5mM Tris-HCl, pH 8.8 and then centrifuged to allow the remaining debris to settle down. The samples were then stored at 4˚C if they were not used immediately. 1-2µl of the DNA was used as a template for the polymerase chain reaction (PCR). The PCR mix was prepared in a volume of 50µl as follows:

2.5mM dNTPs

50mM specific primers

1x Taq polymerase buffer

0.5µl Taq polymerase (NEB)

Milli-Q-water to 50µl

The PCR programs used are summarized in the table below:

Program	Primers	Denaturing	Denaturing	Annealing	Extension	No cycles
Cre	Cre 1+2	94°C for 2’	94°C for 1’	67°C for 1’	72°C for 2’	40
EphA4 WT	EphA4 WT F+R	95°C for 2’	95°C for 30s	60°C for 1’20’’	72°C for 1’15’’	30
EphA4 KO	EphA4 KO F+R	95°C for 3’	94°C for 1’	65°C for 1’	72°C for 1’	38
EphrinB3	EphrinB3 F+R+Neo	94°C for 2’	94°C for 45s	58°C for 45s	72°C for 1’	34
Lox	Lox F+R	94°C for 4’	94°C for 30s	62°C for 45s	72°C for 1’	39
LacZ	LacZ F+R	95°C for 5’	95°C for 30s	58°C for 30s	72°C for 30s	36
PLAP	PLAP F+R	95°C for 2’	95°C for 30s	55°C for 45s	72°C for 1’	29
Tomato	Tomato F+R	94°C for 3’	94°C for 20s	61°C for 30s	72°C for 30s	35

Table 3.04: List of PCR primers and programs for used to amplify the alleles

3.2.1.2. Agarose gel electrophoresis

PCR products were loaded on either 1 or 2% agarose gels. The gels were prepared by dissolving agarose in 1X TAE buffer by boiling. Once the solution was sufficiently cooled, 3µl of ethidium bromide was added per 100ml of 1X TAE buffer. The solution was then poured into a gel chamber and appropriate sized combs were placed in the chamber following which the gel was allowed to solidify. The solidified gel was placed in an electrophoresis chamber containing 1X TAE buffer and the combs were then removed. The PCR products were mixed with 5µl of 10X gel loading buffer and were loaded in the wells and separated for ~30 minutes at ~200V. The DNA was then visualized under UV light using a gel documentation system (BioRad).

3.2.2. Biochemistry

3.2.2.1.Protein extraction and estimation

Dissected brains and spinal cords were incubated in ice-cold lysis buffer containing protease and phosphatase inhibitors for 20 minutes on ice. The tissues were then homogenized using a homogenizer for 1 minute at maximum speed and incubated on ice for 5 minutes. The lysates were transferred to eppendorf tubes and centrifuged for 15 minutes at 13000rpm. The supernatant was transferred to fresh Eppendorf tubes and used for protein estimation. Protein concentration was measured using the DC Protein Assay (BioRad).

3.2.2.2. Immunoblotting

Proteins were separated by SDS-PAGE on a 7.5% gel, running at 120V for 90 minutes. They were then transferred onto nitrocellulose membranes (Whatman) by semi-dry blotting at 80mA for 2 hours. The membranes were then blocked in blocking solution for 1 hour at room

temperature following which they were incubated in blocking solution containing primary antibody overnight at 4˚C while rocking on a shaker. The next day, the membranes were washed 3 times with PBS-T for 5 minutes each and then incubated with secondary antibody for 1 hour at room temperature. The membranes were subsequently washed 3 times with PBS-T for 5 minutes each and then incubated with 1ml of ECL (Amersham) and exposed to X-ray films (Amersham). Subsequent detection of another protein was performed using primary antibodies in blocking solution containing 0.03% Na-azide.

3.2.3. Histology and imaging

3.2.3.1. Cardiac perfusions

Adult mice were anaesthetized by an intraperitoneal (I.P.) injection of chloralhydrate (5% chloralhydrate; 0.9% NaCl). The skin and the rib cage were cut open and the diaphragm was removed and the heart was exposed. A needle, connected to a peristaltic pump, was inserted in to the left ventricle and an incision was made in the liver. 20ml of ice cold PBS was circulated to replace the blood, following which, 20ml of ice cold 4% PFA was circulated to fix the tissues. Upon fixation, the brain and the spinal cord were dissected and post-fixed in 4% PFA overnight at 4˚C.

3.2.3.2. Vibratome sectioning

2 ml of embedding solution was added to a small plastic mould and was allowed to solidify by the addition of 100µl of 25% glutaraldehyde solution. The perfused and post–fixed brains and spinal cords were washed extensively with PBS, dried gently using a paper towel and placed on top of this layer. Additionally, 3.5ml of embedding solution with 175µl of 25%

glutaraldehyde was added on top of the tissue and allowed to solidify. The mould was allowed to solidify at room temperature for 5 minutes and the 80µm transverse sections were cut with the vibratome.

3.2.3.3. Dissection of embryos and spinal cords

The morning after setting up the breeding, vaginal plugs were checked and counted as day 0.5 of pregnancy. On the appropriate day, the mice were sacrificed by cervical dislocation. The skin was cut open and the uterus was dissected into ice cold PBS. The embryos were separated from the uterus and the spinal cords were dissected after eviscerating all other organs. The spinal cords were fixed for 2 hours with 4% PFA at room temperature after which they were washed extensively in PBS and incubated with ice cold 15% sucrose solution at 4˚C till they sank. The spinal were then transferred to 30% sucrose solution at 4˚C till they sank following which they were embedded in OCT compound (Tissue Tek) in small plastic moulds, allowed to solidify on dry ice and then stored at -80˚C.

3.2.3.4. Cryostat sectioning

25µm thick sections were cut using a Leica Cryotome. The sections were collected on coated glass slides (Menzel–Gläser) and allowed to dry for at least 2 hours at room temperature before they were stored at -20˚C.

3.2.3.5. Immunofluorescence

Cryo-protected sections were allowed to air dry for 30 minutes at room temperature. The sections were permeabilized using a solution of 0.5% Triton-X100 in PBS for 30 minutes at

room temperature following which they were blocked using a solution of 0.3% Triton-X100 in PBS along with 5% donkey serum and 5% bovine serum albumin for 2 hours at room temperature. The sections were then incubated in primary antibody [Table 3.02], diluted in blocking solution, overnight at 4˚C. The next day, the sections were washed 3 times in 0.1% Triton-X100 in PBS for 30 minutes each after which they were incubated in secondary antibody [Table 3.03] diluted in blocking solution. Washes were performed as mentioned before. Nuclear staining was achieved by using To-Pro-3 (Molecular Probes) at a dilution of 1:3000 in PBS for 10 minutes. The sections were washed 3 times with PBS for 5 minutes each after which they were mounted using fluorescence mounting medium (DAKO) and allowed to air dry overnight. Images were acquired using an Olympus FV1000 confocal microscope.

3.2.3.6. X-gal staining

Whole embryos or spinal cord cryo-protected sections were rinsed briefly in 0.1M Na-phosphate buffer and were fixed with fixative solution for 15-30 minutes at room temperature. The samples were then washed thoroughly with wash buffer three times for 15 minutes at room temperature. The samples were then transferred to pre-warmed (37˚C) staining solution for a minimum of 2 hours or overnight at 37˚C in a light protected manner. When the desired staining intensity was obtained, the samples were washed extensively with wash buffer and post fixed with 4% PFA overnight at 4˚C. The embryos were processed further by washing with PBS the next day following which they were dehydrated in a series of methanol grades (1:1 methanol: PBS) and 100% methanol for 10 minutes each. The embryos were then transferred to 50% and 100% BABB solution until they sank. Spinal cord sections were washed with PBS after post fixation and mounted with Mowiol and the slides were allowed to air dry. Brightfield images of

the embryos were taken using the Leica MZFIII stereomicroscope and sections were imaged using the Zeiss Axioplan2 epifluorescence microscope.

3.2.3.7. PLAP staining

Placental alkaline phosphatase (PLAP) activity was detected using the alkaline phosphatase (AP) assay. Cryo-protected sections allowed to air dry for 30 minutes after which they were incubated in PBST for 2 hours at 65˚C to block endogenous AP activity. The sections were then post fixed with 4% PFA for 1 hour at room temperature and subsequently washed in PBST several times. The sections were then incubated for 20 minutes in NTMT solution at room temperature. Finally, the staining was developed by incubating the sections in developing solution (NTMT solution containing BCIP and NBT) overnight at room temperature. The sections were then washed with PBS several times and air dried following which they were mounted using Mowiol and brightfield images were taken using the Zeiss Axioplan2 epifluorescence microscope.

3.2.3.8. Nissl staining:

Cryo-protected sections were air dried for 30 minutes. They were then incubated with 1:1 chloroform: ethanol for 2 hours to remove fat molecules. Subsequently, they were rehydrated using a decreasing gradient of ethanol (100%, 95%, and 70%) for 5 minutes each and then stained in pre-warmed (37˚C) staining solution for 2–5 minutes. The sections were then rinsed in water many times and followed by dehydration using an increasing gradient of ethanol (70%, 95%, and 100%) for 5 minutes each. The sections were then cleared using HistoClear for 5 minutes; air dried and mounted using DPX.

3.2.4. Behavior

3.2.4.1. Catwalk assay

Adult mice were trained to walk in one direction on a gangway for 5-6 trials. The next day, the forepaws of the mice were painted with blue paint and the hindpaws with red paint and the mice were made to walk on a sheet of paper placed on the same gangway thus allowing us to capture the footprint of the mouse for subsequent gait analysis.

3.2.4.2. Normal walking paradigm

Adult mice were trained to walk in one direction on a clear treadmill belt (ExerGait – Columbus Instruments) for 6 days in 2 trials which lasted 20 minutes each. They were trained at 2 speeds – a slow speed of 9cm/s and fast speed of 15 cm/s. On the 7th day of the experiment, the paw placement of the mice was recording from underneath using a high speed camera at 100 frames per second. For each animal, 3 trials (2000 frames of video) at each speed were used for the analysis. The gait of the mice were captured at speeds of 6cm/s, 9cm/s, 13cm/s, 17cm/s, 21cm/s and 25cm/s. TreadScan^{TM} 3.0 (Clever Sys.) was used to identify the phase coupling values along with information on swing, stance phases of each limb along with stride time and length for each limb. This information was exported as Excel files for subsequent analysis.

3.2.4.3. Adaptive locomotion

In addition to the unobstructed stepping paradigm described above, two obstacles, 0.5cm and 1cm in height were mounted on the treadmill belt. Adult mice were trained to step over these hurdles for 6 days in 2 trials which lasted 20 minutes each. They were trained at 2 speeds – a slow speed of 9cm/s and fast speed of 15 cm/s. On the 7th day of the experiment, the paw

placement of the mice was recording using two high speed cameras: one from underneath and one from the side at 100 frames per second. For each animal, 3 trials (2000 frames of video) at each speed were used for the analysis. The gait of the mice were captured at speeds of 6cm/s, 9cm/s, 13cm/s and 17cm/s. Depending on the speed, they encountered the hurdles once every 5 seconds. The analysis was performed manually by scoring for the number of hops and alternations while crossing the hurdles.

4. Results

4.1. Characterization of Cre lines

In order to probe the involvement of EphA4 expressed in the brain and spinal cord, we used a number of Cre lines to specifically knockout EphA4 in distinct subpopulations of these regions [Figure 4.01 A and B]. To confirm the expression pattern of specific Cre lines, we first crossed all the lines to Rosa26R mice (Rosa26R-LacZ$^{lx/lx}$), a reporter line that conditionally expresses the β-galactosidase (β-gal) gene. The expression of the Cre was visualized in whole mount E10.5 embryos or cryo-protected spinal cord and brain sections at the stages indicated in the figures, using the X-gal staining method. X-gal or BCIG (5-bromo-4-chloro-3-indolyl-β-galactopyranoside) is a substrate of β-gal and produces an intense blue color upon its hydrolysis.

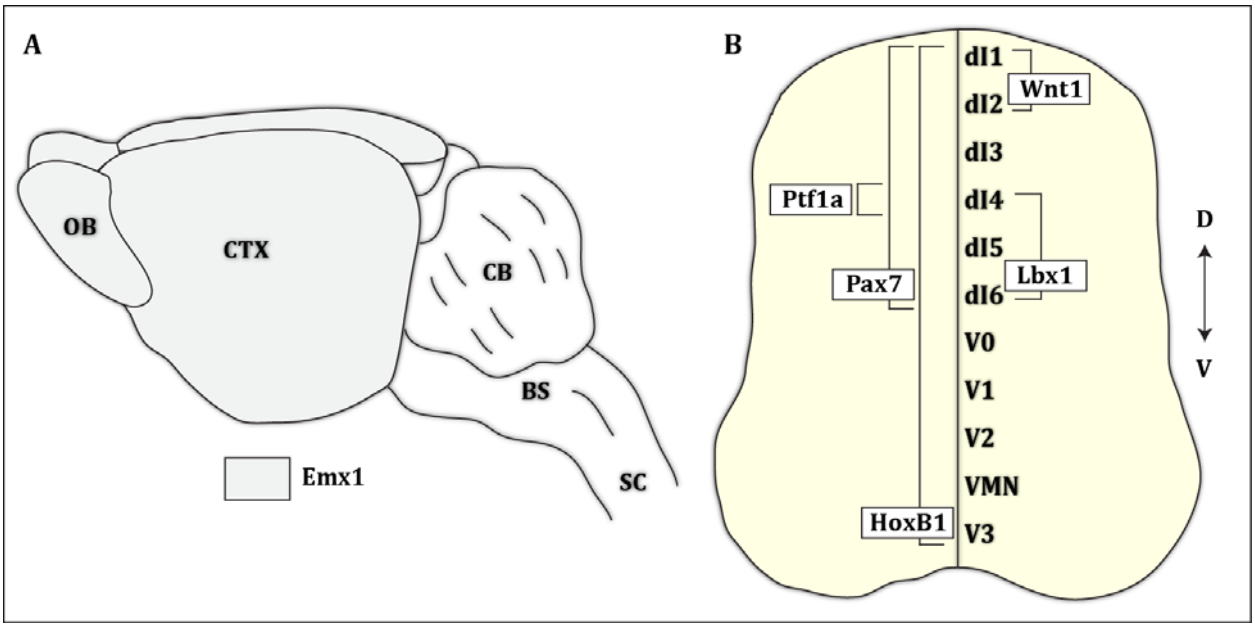

Figure 4.01: Summary of Cre lines. [A] Schematic representation of expression of Emx1 in the forebrain. [B] Expression of various transcription factors in the spinal cord: HoxB1 is expressed in the entire spinal cord; Pax7 in dI1-6; Lbx1 in dI4-6; Wnt1 in dI1-2 and Ptf1a in dI4. OB: olfactory bulb; CTX: cortex; CB: cerebellum; BS: brainstem; SC: spinal cord.

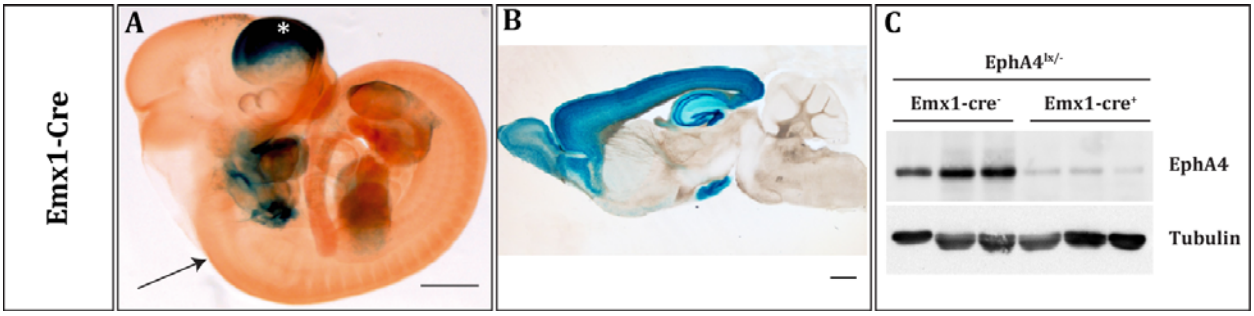

Figure 4.02: Expression of Emx1-Cre line. Emx1-Cre mice were crossed to the reporter line Rosa26R. [A] The expression of the Cre was visualized by whole mount X-gal staining in E10.5 embryos and [B] in the adult. The expression of the Cre was restricted to the forebrain early in development and no expression was detected in the spinal cord. [C]. Western blot analysis to show specific loss of EphA4 from adult motor cortex in the presence of the Cre but not in control littermates. Scale bars are 1000µm in [A]and 500µm in [B]. Data were generated by Dr. S. Paixão.

Emx1 is a transcription factor that belongs to the homeobox family of proteins and is expressed specifically in the forebrain [110]. We used this line to ablate EphA4 specifically in the cortex, thus maintaining the expression of EphA4 in the spinal cord intact. The expression of the Cre was active early during development (E10.5) where we detected a strong recombination of the Cre specifically in the forebrain [asterix in Figure 4.02 A] and no X-gal staining was detected in the spinal cord [arrow in Figure 4.02 A]. Furthermore, the expression was maintained even in the adult forebrain [Figure 4.02 B]. Additionally, when we crossed the Emx1-Cre mice to EphA4$^{lx/-}$ mice and performed western blot analysis from the adult motor cortex, we found a loss of EphA4 protein in the knockouts compared to control littermates [Figure 4.02 C].

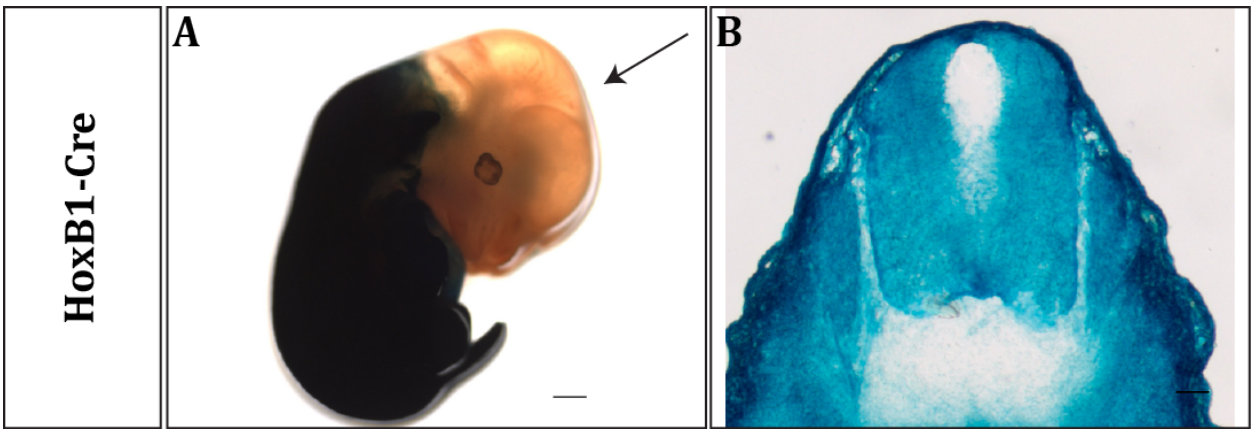

Figure 4.03: Expression of HoxB1-Cre line. HoxB1-Cre mice were crossed to the reporter line Rosa26R. The expression of the Cre was visualized by whole mount X-gal staining in E10.5 embryos [A] and E12.5 spinal cord sections [B]. The expression of the Cre was restricted to the entire spinal cord early in development and no expression was detected in the brain. Scale bar is 500µm in [A] and 100µm [B].

Next, we studied the expression pattern of HoxB1-Cre. HoxB1 is a protein that belongs to the homeodomain family of transcription factors [111] and is expressed in the entire spinal cord [111]. The expression of the Cre was seen early during development (E10.5), specifically in the hindbrain (rhombomere 3 and 4 [111]), but not in more rostral regions of the brain [arrow in Figure 4.03 A]. Furthermore, HoxB1-Cre expression was seen in the entire spinal cord [Figure 4.03 B], as expected.

Pax7 is a transcription factor that belongs to the paired box containing family of proteins and plays an important role during the development of the neural crest [118]. In the spinal cord, Pax7 is expressed in the dorsal progenitor cells [119] and was therefore used to knockout EphA4 specifically in the dorsal spinal cord. To check the expression of Pax7-Cre, we used whole mount E10.5 embryos and found Pax7-Cre (X-gal) expression in the spinal cord [arrow in Figure 4.04 A] as expected. In E12.5 spinal cord sections, robust expression of the Cre (X-gal) was seen only in the dorsal half of the spinal cord, with few cells recombined in the ventral spinal cord

[Figure 4.04 B]. The same pattern of expression was seen in the adult spinal cord [Figure 4.04 C]. Furthermore, we checked the expression of the Cre in the adult motor cortex and found very few cells that showed expression of the Cre (X-gal) [Figure 4.04 D; magnified in D']. Additionally, we wanted to ensure that there was no loss of EphA4 protein due to the recombination of the Cre in the motor cortex. Therefore, we crossed Pax7-Cre mice to EphA4$^{lx/-}$ and performed western blot analysis from different brain regions from adult control and knockout mice. No reduction of EphA4 protein was detected in the motor cortex [Figure 4.04 F] and hippocampus [Figure 4.04 G]. However, Pax7-Cre recombined extensively in the cerebellum [Figure 4.04 E] and we detected a drastic reduction in EphA4 protein levels in the knockouts compared to control littermates [Figure 4.04 H].

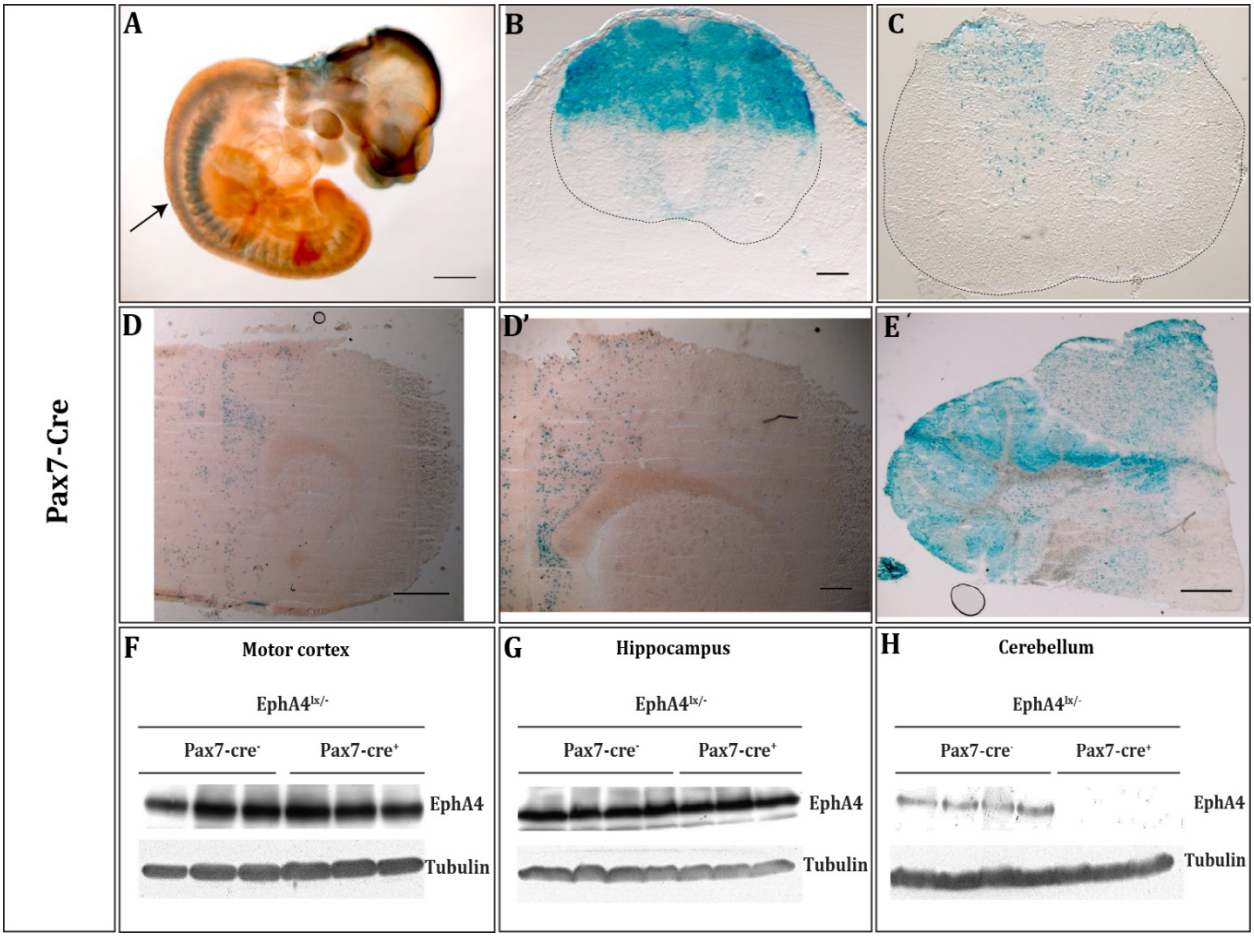

Figure 4.04: Expression of Pax7-Cre line. Pax7-Cre mice were crossed to the reporter line Rosa26R. The expression of the Cre was visualized by whole mount X-gal staining in E10.5 embryos [A], E12.5 spinal cord sections [B], adult spinal cord sections [C], adult brain sections at the level of the motor cortex [D, D'] and cerebellum [E]. Western blot analysis to show specific loss of EphA4 in the presence of the Cre but not in control littermates from adult motor cortex [F], hippocampus [G] and cerebellum [H]. Scale bar in [A] is 500µm, [B] is 100µm, [D] is 500µm, [D'] is 250µm and [E] is 500µm.

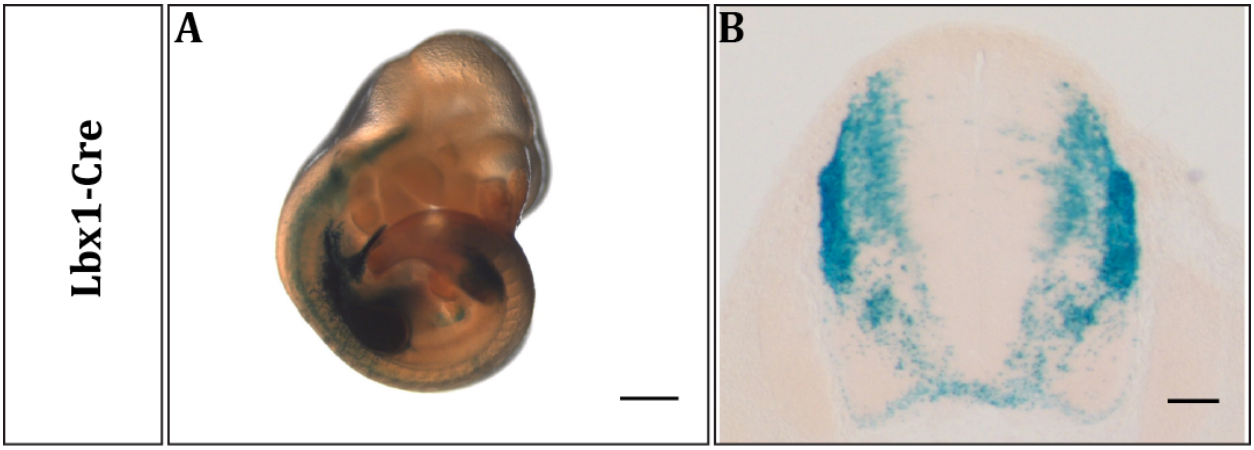

Figure 4.05: Expression of Lbx1-Cre line. Lbx1-Cre mice were crossed to the reporter line Rosa26R. The expression of the Cre was visualized by whole mount X-gal staining in E10.5 embryos [A] and E12.5 spinal cord sections [B]. Scale bar in [A] is 500µm and [B] is 100µm.

Lbx1, a homeodomain transcription factor [120], is expressed specifically in a subset of dorsal spinal cord cells (dI4-6) [113, 121]. In agreement with literature [113], the expression of the Lbx1-Cre was detected as early as E10.5 [Figure 4.05 A] and was restricted to a subset of dorsal spinal cord interneurons (dI4-6) [Figure 4.05 B].

Wnt1 is a protein that belongs to the wingless-type MMTV integration site family [122] and participates in developmental processes such as patterning and growth [123]. In the spinal cord, Wnt1 is expressed in the dorsal spinal cord (dI1-2) and is required to pattern the spinal cord

along its dorsal-ventral axis [124]. Surprisingly, we found extensive expression of the Cre in an extended area of the spinal cord upon examination of E12.5 sections [Figure 4.06] and therefore, further investigation of this mouse line is required.

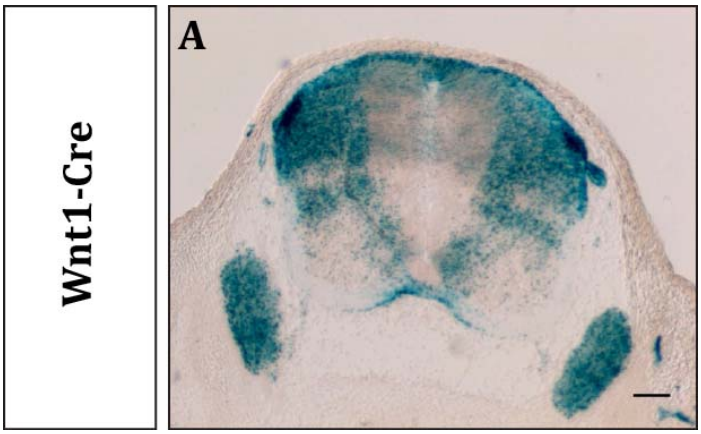

Figure 4.06: Expression of Wnt1-Cre line. Wnt1-Cre mice were crossed to the reporter line Rosa26R. The expression of the Cre was visualized by X-gal staining of E12.5 spinal cord sections. Scale bar is 100μm.

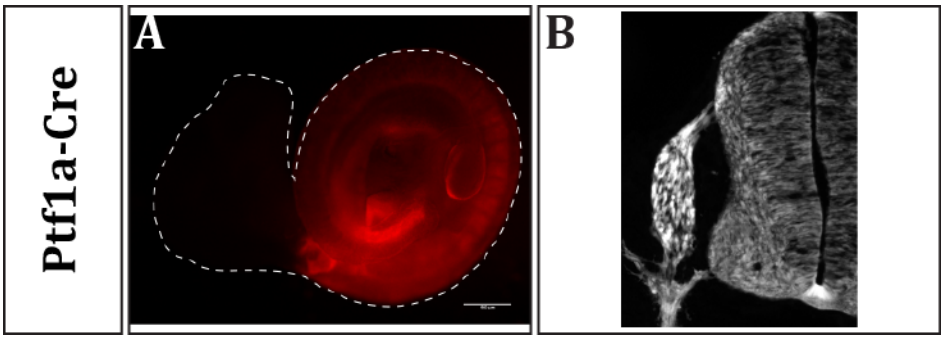

Figure 4.07: Expression of Ptf1a-Cre line. Ptf1a-Cre mice were crossed to the Ai9-tomato reporter line. The expression of the Cre was visualized in E10.5 whole mount embryos [A] and in E11.5 spinal cord sections [B]. Scale bars are 100μm in [A]. Data were generated by Dr. S. Paixão.

Ptf1a, is a transcription factor that encodes a basic helix-loop-helix domain [115] that is expressed in dI4 of the developing spinal cord and subsequently gives rise to GABAergic neurons of the dorsal horn [33]. Upon examination of E10.5 whole mounts and E11.5 spinal cord

sections from Ptf1a-Cre mice crossed to the reporter line, Ai9-tomato, we again found extensive ectopic expression of the Cre [Figure 4.07 A and B].

4.2. EphA4 mutants display defects in left-right coordination and adaptive control of locomotion

4.2.1. Removing EphA4 from dorsal spinal cord neurons partially affects left-right coordination of locomotion

Numerous studies have shed light on the requirement of EphA4 in controlling left-right coordination of locomotion, a stereotyped and repetitive action that is capable of functioning in the absence of supraspinal input [44, 102-104]. However, these studies have focused their attention on the role of EphA4 in the ventral spinal cord. Recent evidence has established that neurons born dorsally during development migrate to the ventral cord and integrate into locomotory circuits [24, 58]. Indeed, these dorsal neurons were shown to be active (via c-fos expression) during locomotion [125]. We therefore asked whether EphA4 originating in dorsal neurons was involved in left-right coordination of locomotion.

To test this, we performed gait analysis using the catwalk assay. The forepaws of the mice were painted in blue and the hindpaws in red following which they were trained to walk on a sheet of paper in a gangway. The captured footprints of the mice were analyzed (only hindpaws) by measuring the distance covered by a single hindpaw during a stride [B in Figure 4.08 H] and compared to distance covered by the other hindpaw during a stride [A in Figure 4.08 H]. The ratio of B/A was calculated and the data was categorized into 3 bins; ‘normal’ if the ratio was ~0.5, ‘intermediate’ if the ratio was ~0.25 or ~0.75 and ‘hop’ if the ratio was ~0 or ~1

[Figure 4.08 H]. The gait of the mouse was represented as a percentage of the ratio of B/A in each bin to the total number of steps covered by the mouse.

The gait in the control mice (EphA4$^{lx/-}$) was mostly asynchronous, that is, the mice produced alternating limb movements [Figure 4.08 A]. When we quantified the gait of these mice, we found that 80% of the steps fell into the normal bin, with very few steps in the intermediate bin and even fewer steps in the hop bin [Figure 4.08 I]. Conversely, when we analyzed the PGK-Cre mice (EphA4$^{lx/-;}$ PGK-Cre^{+}), we found no steps in the normal bin, very few steps in the intermediate bin and more than 95% of the steps in the hop bin [Figure 4.08I]. We utilized the PGK-Cre mice instead of the EphA4 null mice since the former is a deleter line that phenocopies the EphA4 null mice [109], thus allowing us to maintain uniform genetic conditions as with all other conditional mutants that we assessed. Upon analysis of the forebrain specific EphA4 conditional mutants (EphA4$^{lx/-}$; Emx1-Cre^{+}) we found the gait of the mice to be alternating [Figure 4.08 B]. Likewise, on quantifying the data, most of the steps fell into the normal bin with very few steps in the intermediate and hop bins [Figure 4.08 I].

Next, we investigated dorsal spinal cord EphA4 conditional mutants using Pax7-Cre (EphA4$^{lx/-}$; Pax7-Cre^{+}), Lbx1-Cre (EphA4$^{lx/-}$; Lbx1-Cre^{+}), Wnt1-Cre (EphA4$^{lx/-}$; Wnt1-Cre^{+}) and Ptf1a-Cre (EphA4$^{lx/-}$; Ptf11a-Cre^{+}) mice. We found that when EphA4 was ablated using Pax7-Cre and Lbx1-Cre, the mice displayed a partial hopping phenotype; they showed asynchronous hindlimb movements (alternation) along with synchronous movements (hopping) coupled together with intermediate steps that were neither synchronous nor asynchronous movements [Figure 4.08 D &E]. Indeed when we quantified this data, we found approximately equal distribution of the steps into the three bins [Figure 4.08 I].

Furthermore, when we ablated EphA4 in more restricted cell populations using Wnt1-Cre and Ptf1a-Cre, we found that the mice displayed a greater percentage of asynchronous limb movements compared to intermediate and synchronous movements [Figure 4.08 F, G and I]. However, owing the ectopic expression pattern of these two Cre lines [Figure 4.06 and 4.07], these results require further investigation.

Collectively, these results demonstrate the requirement of EphA4, expressed specifically in the spinal cord for maintaining left-right coordination of locomotion. Furthermore, ablating EphA4 in the dorsal spinal cord alone, leads to a partial hopping phenotype, suggesting that dorsal interneurons expressing EphA4 contributed to left-right coordination of locomotion. Since we saw the same phenotype when we used Pax7-Cre (dI1-6) and the more restricted Lbx1-Cre (dI4-6) to ablate dorsally expressed EphA4, we can conclude that dorsal contribution of EphA4 to left-right locomotion arises within this subpopulation of dorsal interneurons.

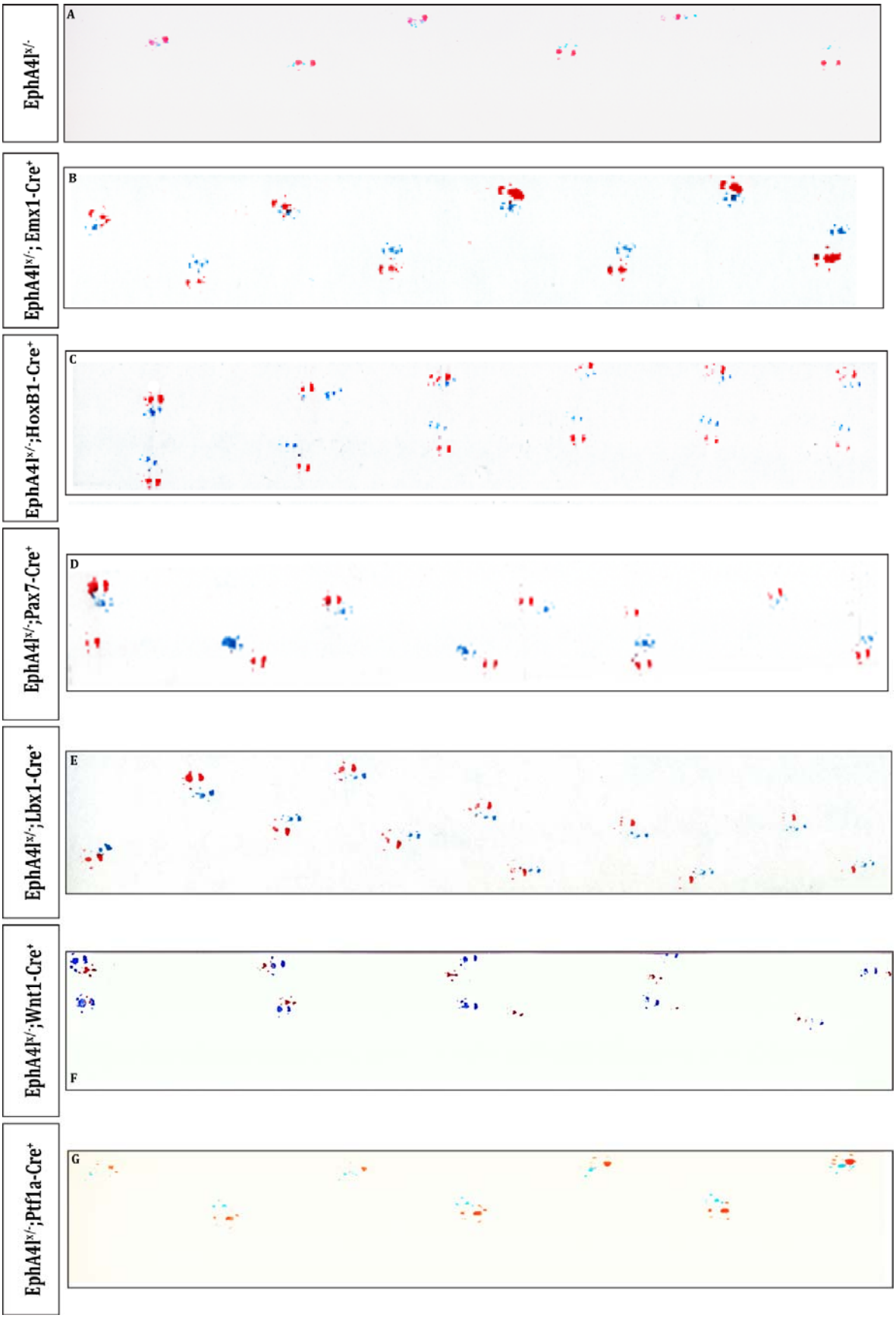
EphA4f/-
A
EphA4f/-; Emx1-Cre+
B
EphA4f/-;HoxB1-Cre+
C
EphA4f/-;Pax7-Cre+
D
EphA4f/-;Lbx1-Cre+
E
EphA4f/-;Wnt1-Cre+
F
EphA4f/-;Ptf1a-Cre+
G

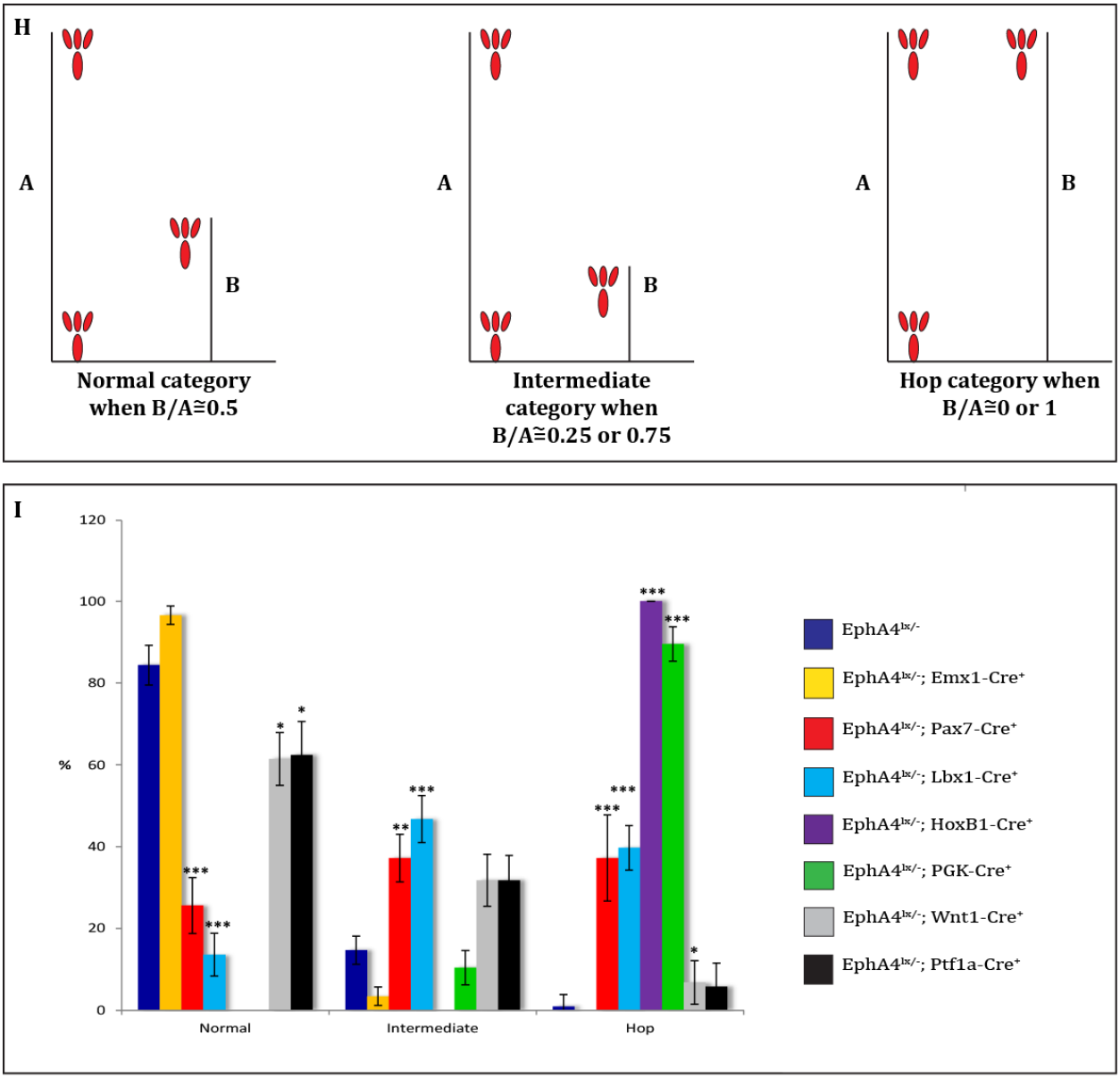

Figure 4.08: Gait analysis of EphA4 mutants. The forepaws and hindpaws of the mice from the indicated genotypes were painted in blue and red respectively. The mice were trained to walk on a sheet of paper on a gangway and thus the footprint was captured [A-G]. Only the gait of the hindpaws was analyzed by measuring the distance between each stride of individual hindpaws (B) and (A) and calculating the ratio of the distances (B/A). The data was classified into three bins as in [H]. Bar graph depicting the percentage of the ratio (B/A) (in each bin) to the total number of steps [I]. Error bars, S.E.M. EphA4$^{lx/-}$ (n=21); EphA4$^{lx/-}$; Emx1-Cre^{+} (n=4); EphA4$^{lx/-}$; Pax7-Cre^{+} (n=8); EphA4$^{lx/-}$; Lbx1-Cre^{+} (n=4); EphA4$^{lx/-}$; HoxB1-Cre^{+} (n=3); EphA4$^{lx/-}$; PGK-Cre^{+} (n=4); EphA4$^{lx/-}$; Wnt1-Cre^{+}

(n=5); EphA4$^{lx/-}$; Ptf1a-Cre^{+} (n=4). Error bars represent SEM. * p<0.05, ** p<0.01, *** p<0.001. Data in panels [A-E] was generated by Dr. S. Paixão.

4.2.2. Dorsally expressed EphA4 does not influence circuits that change gait with increase in speed of locomotion

A number of studies have established the capability of mammals to generate a diverse set of gaits depending on the speed of locomotion [126-128]. Pioneering experiments conducted using the treadmill locomotion paradigm in cats displayed a shift in the gait from trotting to galloping with an increase in the speed of the treadmill [129]. Furthermore, the neural circuits in the ventral spinal cord that participate in integrating information on speed of locomotion and gait are now beginning to be understood. Recent research has shown that disrupting these circuits causes a shift from the normal trotting gait to galloping gait with increase in speed of the treadmill in mice [45]. Since we observed a partial hopping phenotype using the dorsal EphA4 conditional mutants, we asked if these neurons influence the ventral circuitry that integrates information on speed and gait during locomotion.

To address this question, we subjected the EphA4 mutants to the treadmill locomotion paradigm. The gait of the mice was recorded with a high speed camera, (located beneath the treadmill belt) and the speed of the treadmill belt was gradually increased (between 6cm/s and 25cm/s). The captured gaits were analyzed using the TreadScan software which provided homologous phase coupling values, a measure of the time at which both feet on the same girdle begin their strides (a complete step which comprises of a stance phase, where the foot is in contact with the treadmill belt, and a swing phase, where the foot is in the air). The phase coupling is scored on a scale from 0 to 0.5, where 0 is perfect hopping and 0.5 is perfect alternation of the limbs.

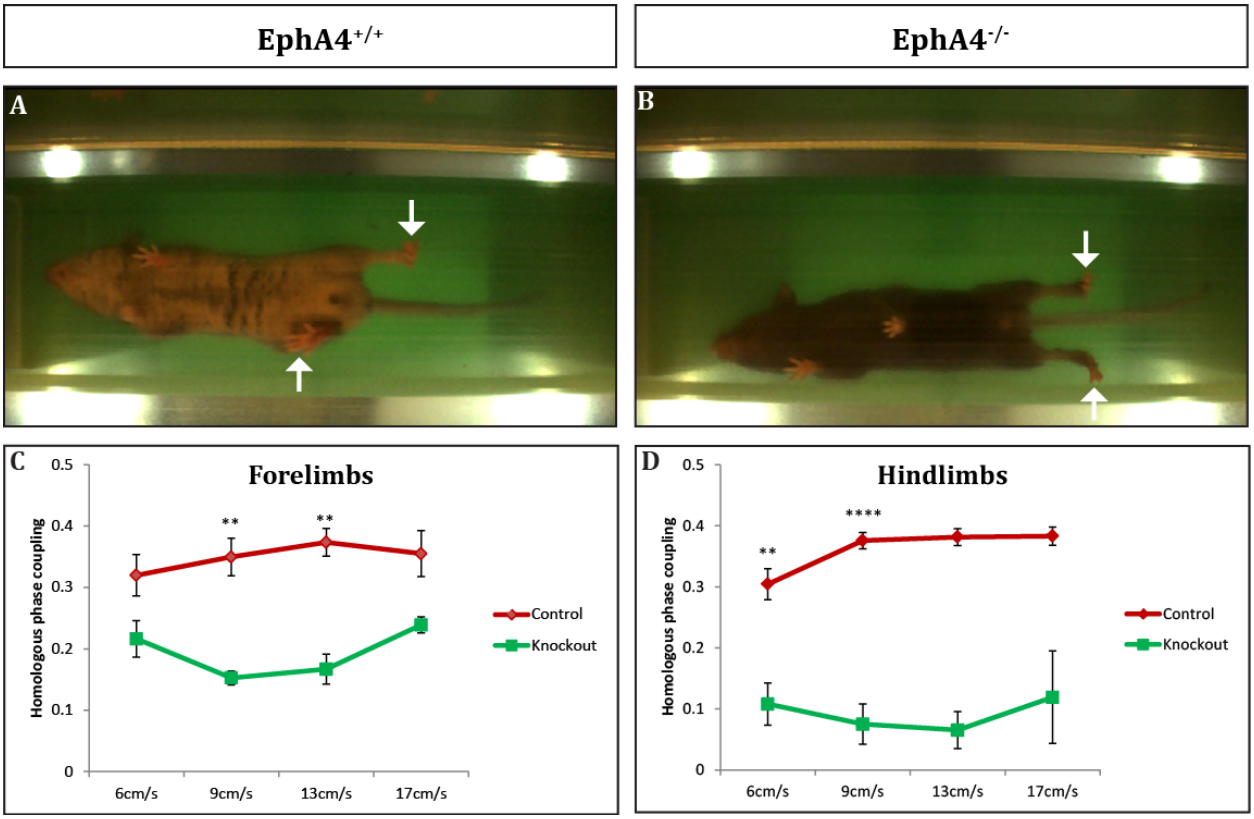

Figure 4.09: EphA4 ablation results in robust synchronous movements of the limbs but does not shift gait with increase in speed of locomotion. Representative images of EphA4$^{+/+}$ [A] and EphA4$^{-/-}$ [B]. The white arrows indicate limb movement on the same girdle. Homologous phase coupling values for the forelimbs [C] and hindlimbs [D] from the indicated genotypes (red line indicates EphA4$^{+/+}$ and green line indicates EphA4$^{-/-}$) at 6cm/s. 9cm/s, 13cm/s and 17cm/s from the indicated genotypes. n=2-5 mice per group. Error bars represent SEM. **p<0.01, ***p<0.001 with t-test between genotype; p>0.05 with 2-way ANOVA to test interaction between genotype and speed.

Since it is already known that the EphA4$^{-/-}$ mice hop, we first analyzed their response to increases in speed of locomotion in comparison to their wildtype littermates [Figure 4.09 A and B]. We found that for both forelimbs and hindlimbs, the wildtype mice displayed homologous phase coupling values between 0.3 and 0.4 at all speeds tested, thereby confirming that the limbs alternate during locomotion [red lines in Figure 4.09 C and D]. However, when we analyzed the forelimbs of EphA4$^{-/-}$ mice, we found a significant difference of homologous phase coupling

values (between 0.1 and 0.2) in comparison to the wildtype littermates at 9cm/s and 13cm/s [Figure 4.09 C]. Homologous phase coupling values for the hindlimbs of the EphA4$^{-/-}$ mice showed a robust and significant difference (between 0 and 0.1) compared to wildtype littermates at 6cm/s and 9cm/s [Figure 4.09 D]. However, we did not find any interaction between increase in speed locomotion and shift of gait between EphA4$^{+/+}$ and EphA4$^{-/-}$ mice indicating that speed does not influence the degree of hopping.

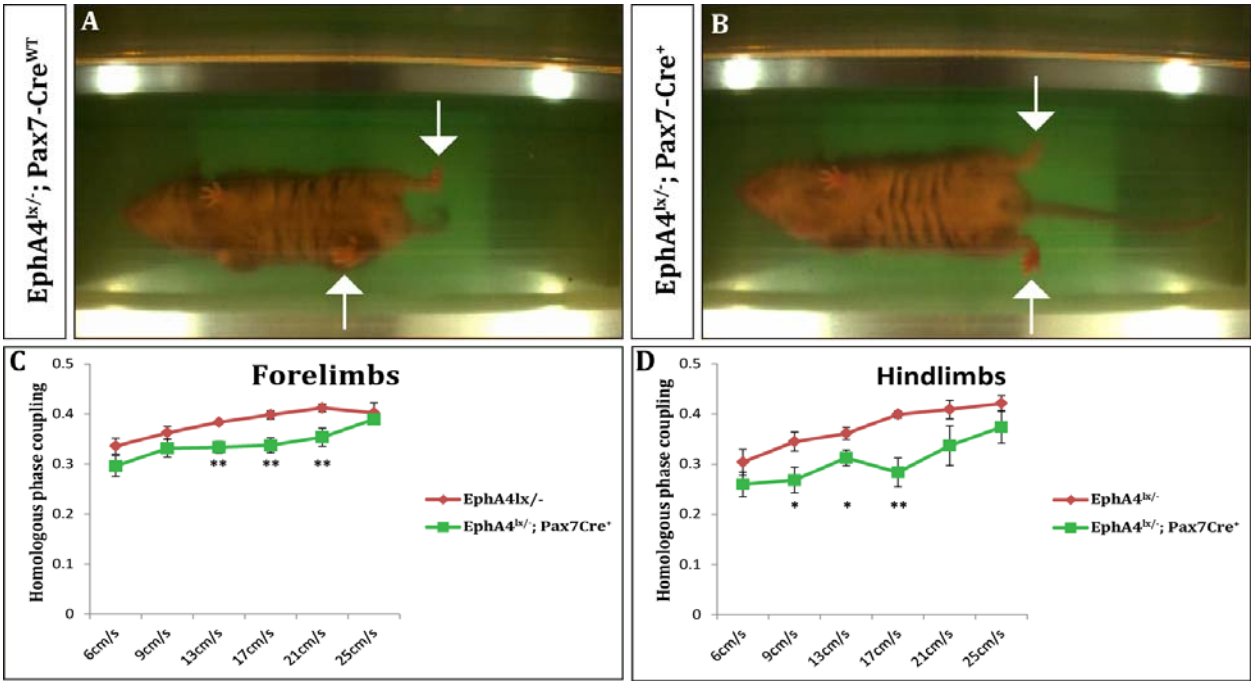

Figure 4.10: EphA4 ablation in the dorsal spinal cord using Pax7-Cre results in partial synchronous movements of the forelimbs and hindlimbs but does not shift gait with increase in speed of locomotion. Representative images of EphA4$^{lx/-}$; Pax7-Cre^{WT} [A] and EphA4$^{lx/-}$; Pax7-Cre^{+} [B]. The white arrows indicate limb movement on the same girdle. Homologous phase coupling values for the forelimbs [C] and hindlimbs [D] from the indicated genotypes (red line indicates EphA4$^{lx/-}$; Pax7-Cre^{WT} and green line indicates EphA4$^{lx/-}$; Pax7-Cre^{+}) at 6cm/s (n=8WT and 9KO) 9cm/s (n=9WT and 11KO), 13cm/s (n=9WT and 11KO), 17cm/s (n=8WT and 10KO), 21cm/s (n=8WT and 4KO) and 25cm/s (n=4WT and 3KO) from the indicated genotypes. Error bars represent SEM.

**p<0.01, ***p<0.001 with t-test between genotype; p>0.05 with 2-way ANOVA to test interaction between genotype and speed.

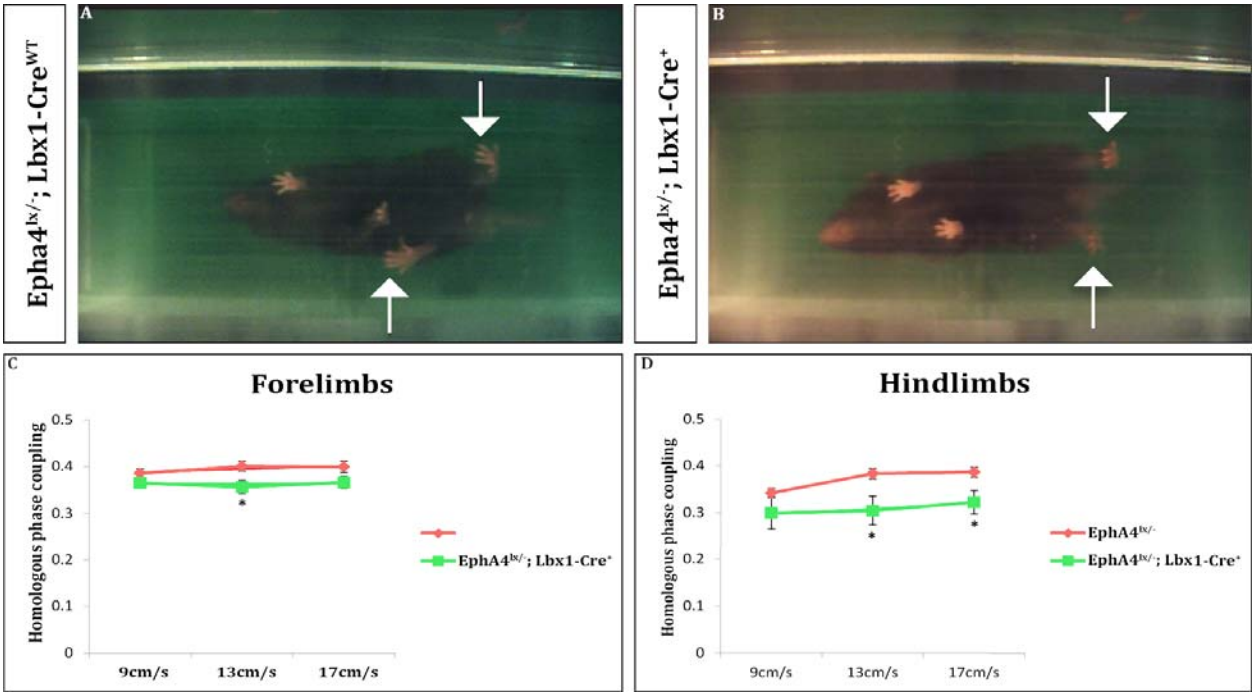

Figure 4.11: EphA4 ablation in dI4-6 using Lbx1-Cre results in partial synchronous movements of the forelimbs and hindlimbs but does not shift gait with increase in speed of locomotion. Example images of EphA4$^{lx/-}$; Lbx1-Cre^{WT} [A] and EphA4$^{lx/-}$; Lbx1-Cre^{+} [B]. The white arrows indicate limb movement on the same girdle. Homologous phase coupling values for the forelimbs [C] and hindlimbs [D] from the indicated genotypes (red line indicates EphA4$^{lx/-}$; Lbx1-Cre^{WT} and green line indicates EphA4$^{lx/-}$; Lbx1-Cre^{+}) at 9cm/s (n=12WT and 12KO), 13cm/s (n=12WT and 11KO) and 17cm/s (n=12WT and 9KO) from the indicated genotypes. Error bars represent SEM. *p<0.05 with t-test between genotype; p>0.05 with 2-way ANOVA to test interaction between genotype and speed.

Since we observed a partial hopping phenotype in dorsal spinal cord specific mutants, we investigated the influence of increase in speed of locomotion on gait in these mice. When we ablated EphA4 using the Pax7-Cre and Lbx1-Cre mice and performed the treadmill locomotion

paradigm [Figure 4.10 A and B and Figure 4.11 A and B], we found small, yet significant, differences in the homologous phase coupling values between control (red line in Figure 4.10 C and D and Figure 4.11 C and D) and knockout (green line in Figure 4.10 C and D and Figure 4.11 C and D) mice at certain speeds in both forelimbs (Pax7-Cre: WT=0.38±0.0032S.E and KO=0.30±0.016S.E at 13cm/s, p =0.00175; WT=0.39±0.0081S.E and KO=0.28±0.002S.E at 17cm/s, p = 0.0039; WT=0.41±0.008S.E and KO=0.35±0.017S.E at 21cm/s, p=0.0058. Lbx1-Cre: WT=0.40±0.01S.E and KO=0.35±0.014, p=0.019) and hindlimbs (Pax7-Cre: WT=0.34±0.019S.E and KO=0.26±0.025S.E at 9cm/s, p=0.032; WT= 0.36±0.012S.E and KO=0.31±0.015 at 13cm/s, p=0.032; WT=0.39±0.006S.E and KO=0.28±0.028S.E at 17cm/s, p=0.0027. Lbx1-Cre: WT=0.38±0.011S.E and KO=0.30±0.0306S.E at 13cm/s, p=0.020; WT=0.38±0.0109S.E and KO=0.32±0.025S.E at 17cm/s, p= 0.019). However, there was no interaction between increase in speed of locomotion and genotype demonstrating an absence of speed dependent shift in the gait of the mice.

	Speed	EphA4$^{lx/-}$; Pax7-Cre^{+}	EphA4$^{lx/-}$; Lbx1-Cre^{+}	T-test (p)
Forelimbs	9cm/s	0.331567 (SEM ± 0.01757)	0.364306 (SEM±0.005567)	n.s. (0.079552)
	13cm/s	0.33387 (SEM ± 0.011921)	0.355653 (SEM±0.014243)	n.s. (0.25466)
	17cm/s	0.337678 (SEM ± 0.014758)	0.365709 (SEM±0.012424)	n.s (0.169356)
Hindlimbs	9cm/s	0.268326 (SEM ± 0.025358)	0.2989478 (SEM ± 0.0341987)	n.s. (0.486402)

	13cm/s	0.312627 (SEM ± 0.015731)	0.3044 (SEM ± 0.0306191)	n.s. (0.813534)
	17cm/s	0.283809 (SEM ± 0.028511)	0.3223979 (SEM ± 0.0253594)	n.s (0.330459)

Table 4.01: Summary of forelimb and hindlimb homologous phase coupling values after EphA4 ablation using Pax7-Cre and Lbx1-Cre. No differences in forelimb homologous phase coupling values were observed between the two dorsal Cre lines at 9cm/s, 13cm/ and 17cm/s. SEM is standard error of mean, n.s. not significant; p value > 0.05.

Furthermore, we compared the two dorsal EphA4 mutants to access differences in the extent of the hopping. We found that both mutants display similar homologous phase coupling values at 9cm/s, 13cm/s and 17cm/s for both, forelimbs and hindlimbs, and hence are not different from each other [Table 4.1]. Therefore, the dorsal contribution of EphA4 must arise from the more restricted dI4-6 subpopulation (Lbx1-Cre), however, this result must be confirmed by performing control experiments, that is, by ablating EphA4 in the dI1-3 subpopulation. When we ablated EphA4 using Wnt1-Cre (dI1-2), we saw a partial hopping phenotype in the catwalk assay [Figure 4.08 F and I]. However, owing to the faulty expression of the Cre itself [Figure 4.06], these experiments cannot be validated and must be repeated with a more suitable Cre line.

4.2.3. EphA4 is required for skilled motor tasks that involve the motor cortex

The spinal cord controls left-right coordination of locomotion in the absence of supraspinal input, however, voluntary movements are controlled by inputs from the motor cortex in the brain. Such inputs allow the modification of limb movements in response to challenges encountered in the environment of the animal (adaptive locomotion) [73]. EphA4 is expressed in

the motor cortex and is required for the guidance of the cortico-spinal tract (CST) axons (one of the many descending tracts from the brain to the spinal cord) [104]. Hence, we asked, if EphA4, expressed in the CST axons, is involved in controlling adaptive locomotion.

To address this question, we ablated EphA4 specifically in the forebrain using Emx1-Cre mice. We then subjected the mice to the adaptive locomotion paradigm where we assessed the gait while the mice crossed two hurdles, 0.5cm and 1cm in height, during treadmill locomotion at different speeds [Figure 4.12 A, B, C and D]. The gait was recorded with two high speed cameras: one camera was placed beneath the treadmill belt, thus allowing us to visualize all four paws and making it suitable for analysis with the TreadScan software; the other camera was placed perpendicular to the treadmill belt such that we could observe the stepping movements of the mice in a side view. For the adaptive locomotion paradigm, we analyzed the gait of the mice using the data generated in the side view rather than from the bottom view as it allowed us to assess clearly each limb crossing the hurdle. We manually scored the gait of the mouse while crossing the hurdles (for both forelimbs and hindlimbs) by assigning the step as:

- Alternation, if one paw crossed the hurdle before the other paw lifted off the treadmill belt
- Hopping, if both paws lifted off the treadmill belt before either one crossed the hurdle

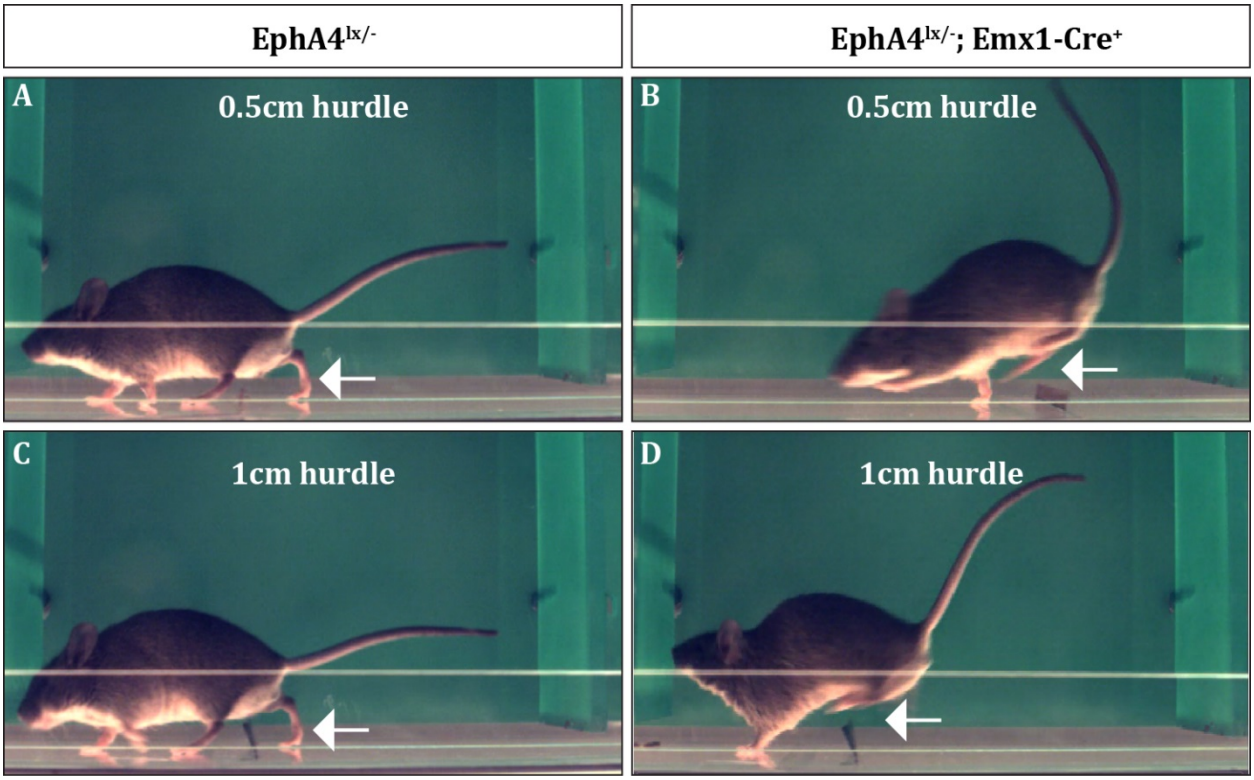
EphA4lx/-
EphA4lx/-; Emx1-Cre+
A
0.5cm hurdle
B
0.5cm hurdle
C
1cm hurdle
D
1cm hurdle

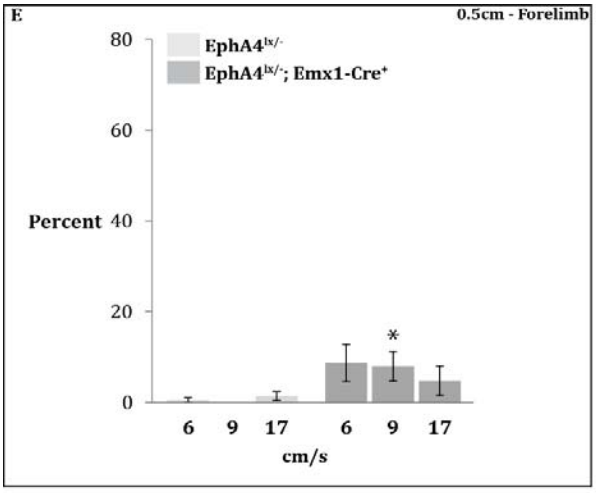
E
0.5cm - Forelimb
EphA4lx/-
EphA4lx/-; Emx1-Cre+
Percent
80
60
40
20
0
6
9
17
6
9
17
cm/s
*

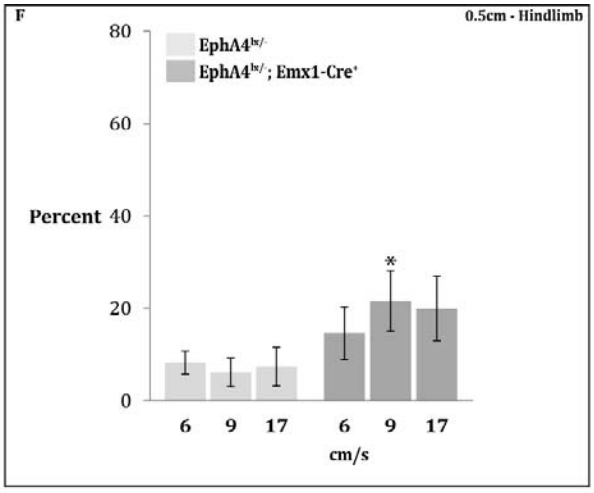
F
0.5cm - Hindlimb
EphA4lx/-
EphA4lx/-; Emx1-Cre+
Percent
80
60
40
20
0
6
9
17
6
9
17
cm/s
*

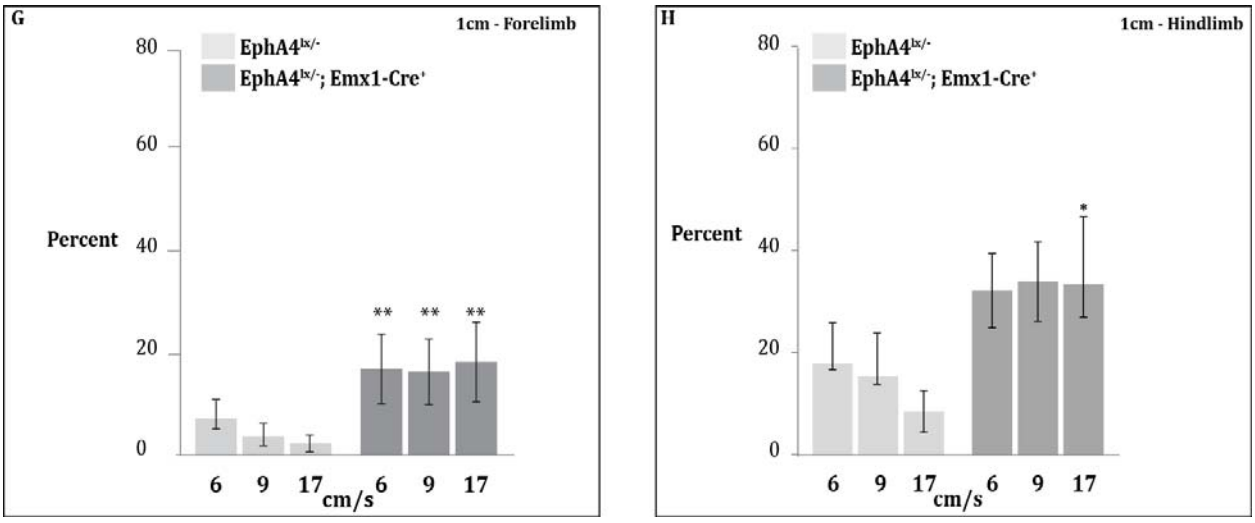

Figure 4.12: Adaptive locomotion is affected in forebrain specific EphA4 mutants. Example images of EphA4$^{lx/-}$; Emx1-Cre^{WT} [A] and EphA4$^{lx/-}$; Emx1-Cre^{+} [B] crossing a hurdle of 0.5cm height. Example images of EphA4$^{lx/-}$; Emx1-Cre^{WT} [C] and EphA4$^{lx/-}$; Emx1-Cre^{+} [D] crossing a hurdle of 1cm height. The white arrows indicate limb movement on the same girdle. Percent of hops over the 0.5cm hurdle by forelimbs [E] and hindlimbs [F] and 1cm hurdle by forelimbs [G] and hindlimbs [H] at 6cm/s (n=20WT and 22KO), 9cm/s (n=19WT and 20KO), 13cm/s (n=19WT and 20KO) and 17cm/s (n=17WT and 9KO). Error bars represent SEM. *p<0.05, **p<0.01 with t-test between genotypes. Data were generated with Dr. S. Paixão.

The number of hops were quantified and represented as a percentage of the total number of steps. EphA4$^{lx/-}$; Emx1-Cre^{+} mice differed significantly from EphA4$^{lx/-}$; Emx1-Cre^{WT} littermates while crossing the 0.5cm hurdle only at 9cm/s (WT=0%±0%S.E and KO=7.93%±3.25%S.E, p=0.026) with both forelimbs and hindlimbs (WT=6.16%±3.09%S.E and KO=21.56%±6.59%S.E, p=0.049) [Figure 4.12 E and F]. Interestingly, EphA4$^{lx/-}$; Emx1-Cre^{+} mice displayed a two-fold increase in percentage of hopping compared to their wildtype littermates, when crossing the 1cm hurdle [Figure 4.12 G], at all speeds. However, they differed significantly only at 17cm/s (WT=8.92%±4.08%S.E and KO=35.04%±9.81%S.E, p=0.027)

[Figure 4.12 H]. Furthermore, no speed dependent shift in gait was observed in these mice with both hurdles.

In the catwalk assay mentioned previously [Figure 4.08 B and I], EphA4$^{lx/-}$; Emx1-Cre^{+} mice did not display a hopping phenotype compared to their wildtype littermates. To ensure that the hopping phenotype we observed is entirely due to EphA4-dependant cortical control of adaptive locomotion, we subjected the mice to the treadmill locomotion paradigm and analyzed the gait at different speeds using the TreadScan software [Figure 4.13 A and B]. Homologous phase coupling values from both forelimbs and hindlimbs revealed no differences between EphA4$^{lx/-}$; Emx1-Cre^{WT} (red line in Figure 4.13 C and D) and EphA4$^{lx/-}$; Emx1-Cre^{+} (green line in Figure 4.13 C and D) thus demonstrating that cortical control of adaptive locomotion does not influence left-right coordination of locomotion (that is usually controlled by the CPGs of the spinal cord).

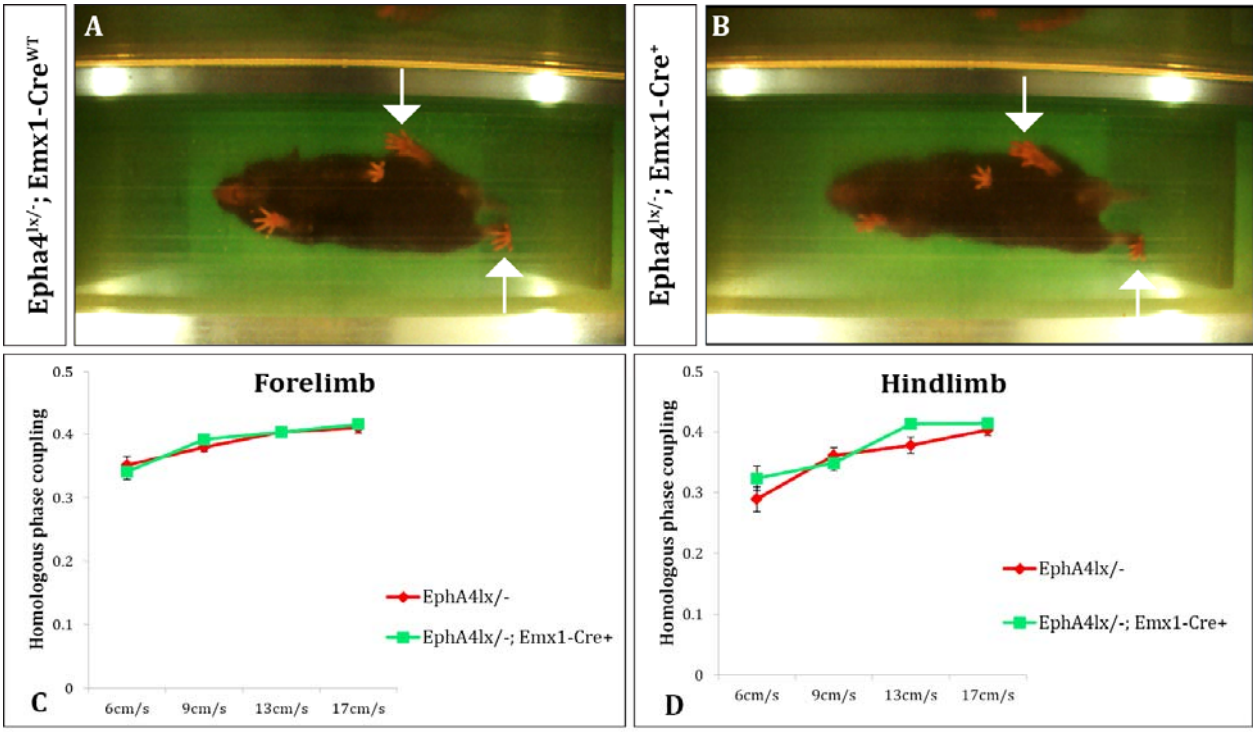

Figure 4.13: EphA4 ablation in the forebrain using Emx1-Cre results in preservation of asynchronous movements of the forelimbs and hindlimbs and does not shift gait with increase in speed of locomotion. Example images EphA4lx$^{/-}$; Emx1-Cre^{WT} [A] and EphA4$^{lx/-}$; Emx1-Cre^{+} [B]. The white arrows indicate limb movement on the same girdle. Homologous phase coupling values for the forelimbs [C] and hindlimbs [D] from the indicated genotypes (red line indicates EphA4$^{+/+}$ and green line indicates EphA4$^{-/-}$) at 6cm/s. 9cm/s, 13cm/s and 17cm/s from the indicated genotypes. n=17-23 mice per group. Error bars represent SEM. $p>0.05$ with t-test between genotype; $p>0.05$ with 2-way ANOVA to test interaction between genotype and speed.

When we used the adaptive locomotion paradigm in dorsal spinal cord mutants (EphA4$^{lx/-}$; Pax7-Cre^{WT} and EphA4$^{lx/-}$; Pax7-Cre^{+} mice) to assess their stepping behavior over the 0.5cm and 1cm hurdles [Figure 4.14 A, B, C and D], we found a significant increase in the percentage of hopping of EphA4$^{lx/-}$; Pax7-Cre^{+} mice over both hurdles compared to their control littermates at certain speeds in both the forelimbs (0.5cm hurdle: WT=2.88%±1.85%S.E and KO=30.03%±8.18%S.E at 9cm/s, p=0.015; WT = 1.09% ± 1.09% S.E and KO=19.28%±7.05%S.E at 13cm/s, p=0.033. 1cm hurdle: WT=1.19%±1.19%S.E and KO=42.76%±7.99%S.E at 13cm/s, p=0.0003) and hindlimbs (0.5cm hurdle: WT=8.37%±3.41%S.E and KO=29.90%±7.97%S.E at 13cm/s, p=0.034. 1cm hurdle: WT=14.92%±5.96%S.E and KO=49.18%±7.51%S.E at 13cm/s, p=0.0039; WT=7.5%±7.5%S.E and KO=55.33%±16.17%S.E at 17cm/s, p=0.027) [Figure 4.14 E]. This result is interesting since we observe a defect in adaptive locomotion in dorsal EphA4 mutants, where EphA4 in the CST axons is left intact. It may be possible that EphA4 is required in a cell-autonomous manner (defect in adaptive locomotion using Emx1-Cre) and in a non-cell autonomous manner (defect in adaptive locomotion using Pax7-Cre) to orchestrate precise voluntary behaviors (see discussion, section 5.2 for further consideration).

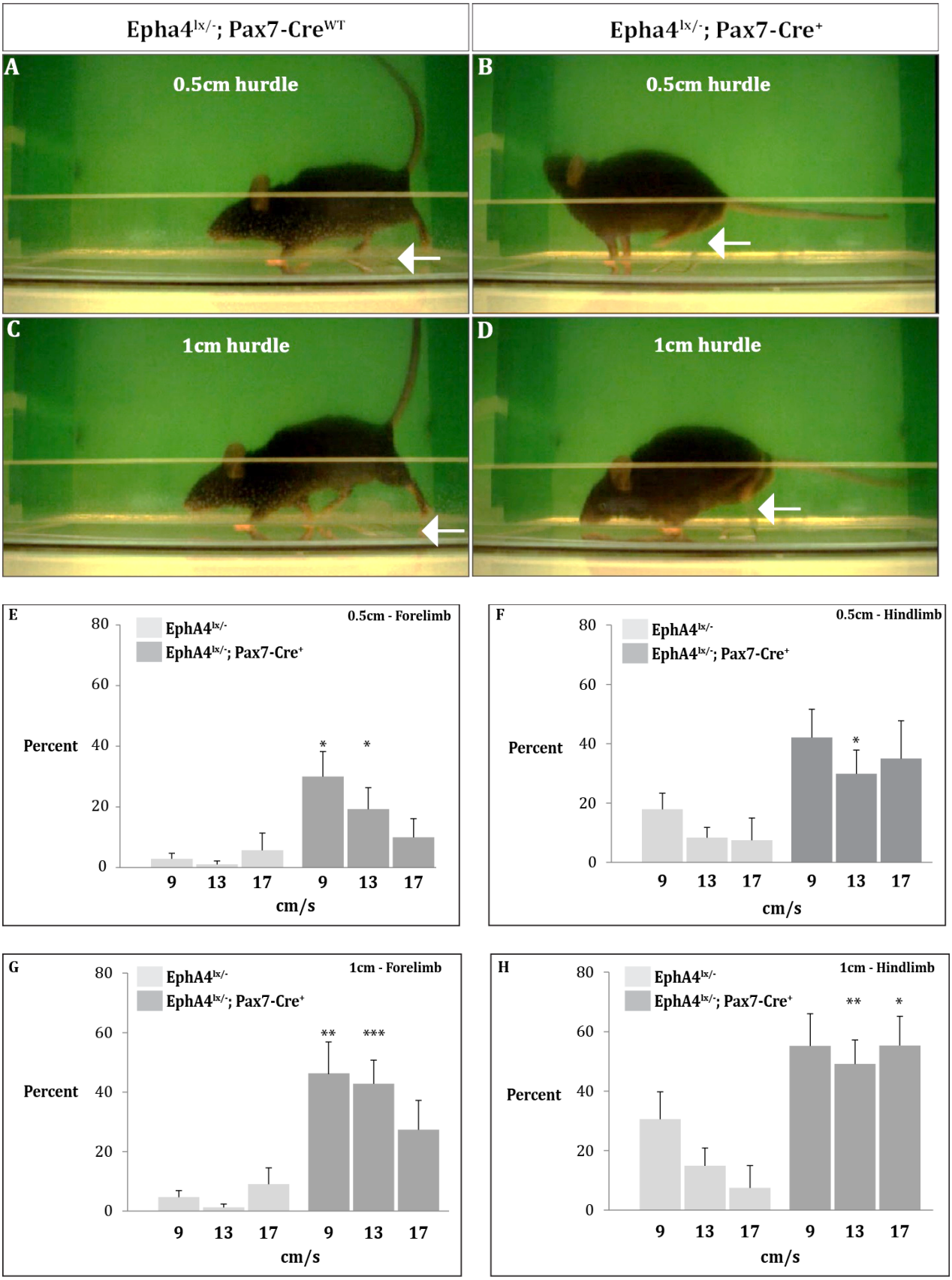
Epha4lx/-; Pax7-CreWT
Epha4lx/-; Pax7-Cre+
A
0.5cm hurdle
B
0.5cm hurdle
C
1cm hurdle
D
1cm hurdle
E
0.5cm - Forelimb
EphA4lx/-
EphA4lx/-; Pax7-Cre+
Percent
cm/s
F
0.5cm - Hindlimb
G
1cm - Forelimb
H
1cm - Hindlimb

Figure 4.14: Adaptive locomotion is affected in dorsal spinal cord EphA4 mutants. Example images of EphA4lx$^{/-}$; Pax7-Cre^{WT} [A] and EphA4$^{lx/-}$; Pax7-Cre^{+} [B] crossing a hurdle of 0.5cm height. Example images of EphA4lx$^{/-}$; Pax7-Cre^{WT} [C] and EphA4$^{lx/-}$; Pax7-Cre^{+} [D] crossing a hurdle of 1cm height. The white arrows indicate limb movement on the same girdle. Percent of hops by forelimbs and hindlimbs while crossing both hurdles at 9cm/s (n=7WT and 10KO), 13cm/s (n=7WT and 8KO) and 17cm/s (n=5WT and 5KO) [E]. Error bars represent SEM *p<0.05, **p<0.01, ***p<0.001 with t-test between genotypes.

Taken together, these results provide compelling evidence for the role of dorsally expressed EphA4 in CPG function since ablating EphA4 in dorsal spinal cord neurons leads to a partial hopping phenotype as observed in catwalk assays. However, dorsally expressed EphA4 does not participate in speed dependent changes in gait of the mice since the partial hopping phenotype is observed in all speeds tested. Furthermore, EphA4 is also required for the cortical control of adaptive or voluntary behaviors as forebrain ablation of EphA4 leads to increased hopping when the mice are challenged with obstacles. Moreover, dorsal EphA4 mutants also display defects in adaptive behaviors suggesting their indirect involvement in voluntary locomotion.

4.3. EphA4 is required for correct development of the dorsal spinal cord

4.3.1. Ablation of EphA4 in the dorsal spinal cord causes a shallow dorsal funiculus

Upon performing histological studies on fixed transverse sections of the lumbar spinal cord, we found that in control animals, the ventral tip of the dorsal funiculus (DF) extended until the central canal [Figure 4.15 A] and thus had a normal shape. Conversely, in EphA4$^{lx/-}$; PGK-

Cre^{+} mice we confirmed that the white matter of the DF was largely reduced and thus displayed a shallow DF morphology [104] [Figure 4.15 H].

When we removed EphA4 from the forebrain alone, using Emx1-Cre (Emx1-Cre; $EphA4^{lx/PLAP}$), we found that the DF morphology was similar to the control mice [Figure 4.15 B]. We quantified the size of the DF (depicted as a ratio of the distance to the ventral tip of the DF to the distance to the central canal [Figure 4.15 J]) and found no differences between control and forebrain specific (Emx1-Cre; $EphA4^{lx/PLAP}$) mutants [Figure 4.15 I]. Using the spinal cord specific HoxB1-Cre (HoxB1-Cre; $EphA4^{lx/PLAP}$), we deleted EphA4 from the entire spinal cord alone leaving EphA4 intact in the brain. We found that the DF morphology was similar to that displayed by the PGK-Cre mice [Figure 4.15 G and I], thus proving that the described phenotype arises from the spinal cord.

Furthermore, we assessed the contribution of dorsally expressed EphA4 to the DF phenotype by removing EphA4 in the dorsal cord using Pax7-Cre (Pax7-Cre; $EphA4^{lx/PLAP}$). We found a reduction in the size of the DF that was similar to that observed in the PGK-Cre and, the spinal cord specific HoxB1-Cre mutants [Figure 4.15 C and I]. Additionally, we also ablated EphA4 in specific subpopulations of the dorsal spinal cord to assess their contribution to the DF phenotype. We used Lbx1-Cre to knockout EphA4 from dI4-6 (Lbx1-Cre; $EphA4^{lx/PLAP}$) and found a reduction in the size of the DF similar to the other spinal cord mutants [Figure 4.15 D and I]. When we used Wnt1-Cre to knockout EphA4 from dI1-2 (Wnt1-Cre; $EphA4^{lx/PLAP}$), we found a shallow DF morphology and the reduction in size of the DF was comparable to other spinal cord mutants [Figure 4.15 E and I]. However, since we found ectopic expression of the Cre itself [Figure 4.06], we were unable to validate these results and hence could not conclude the contribution of EphA4 to the DF phenotype in these subpopulations of the dorsal spinal cord.

We also used Ptf1a-Cre to specifically remove EphA4 from dI4 (Ptf1a-Cre; EphA4$^{lx/PLAP}$). We found no defect in the DF morphology and the size of the DF was comparable to wildtype mice [Figure 4.15 F and I]. This result was rather surprising owing to the ectopic expression of the Cre all over the spinal cord [Figure 4.07]. Hence, it would be worthwhile to investigate the expression of the Cre prior to concluding the contribution of EphA4 to the DF morphology in this subpopulation of the dorsal spinal cord.

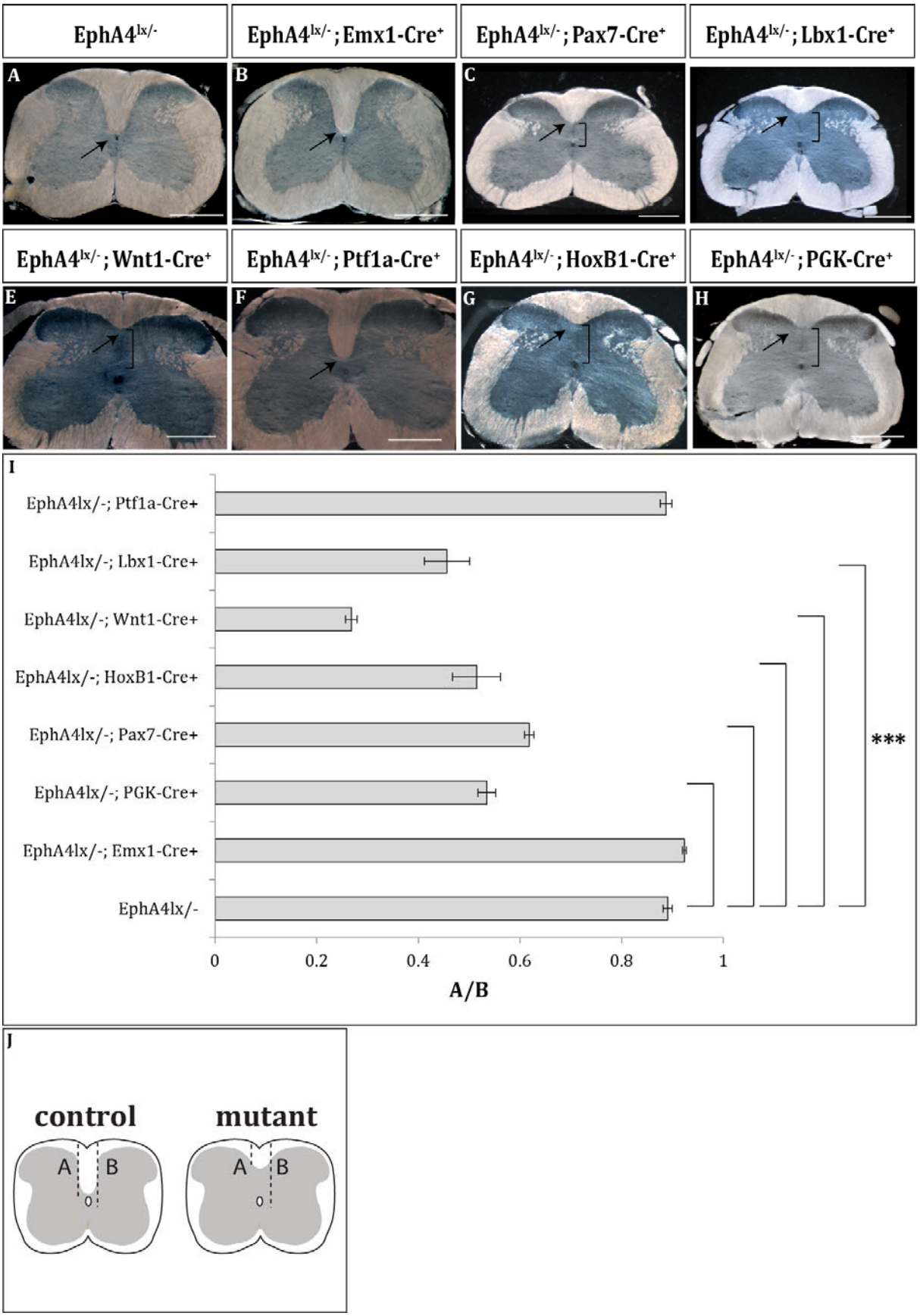
EphA4lx/-
EphA4lx/-; Emx1-Cre+
EphA4lx/-; Pax7-Cre+
EphA4lx/-; Lbx1-Cre+
A
B
C
EphA4lx/-; Wnt1-Cre+
EphA4lx/-; Ptf1a-Cre+
EphA4lx/-; HoxB1-Cre+
EphA4lx/-; PGK-Cre+
E
F
G
H
I
EphA4lx/-; Ptf1a-Cre+
EphA4lx/-; Lbx1-Cre+
EphA4lx/-; Wnt1-Cre+
EphA4lx/-; HoxB1-Cre+
EphA4lx/-; Pax7-Cre+
EphA4lx/-; PGK-Cre+
EphA4lx/-; Emx1-Cre+
EphA4lx/-
***
0
0.2
0.4
0.6
0.8
1
A/B
J
control
mutant
A
B
0
A
B
0

Figure 4.15: The dorsal funiculus morphology is affected in EphA4 spinal cord mutants. (A-H). Dark field images of transverse spinal cord sections from adult mice at the lumbar level of the genotypes indicated in each panel. The control, EphA4$^{lx/-}$ [A] and the forebrain specific EphA4 mutant, Emx1-Cre; EphA4$^{lx/-}$ [B] and Ptf1a-Cre; EphA4$^{lx/-}$ [F] displayed a similar morphology where the ventral tip of the dorsal funiculus extends until the central canal (arrows). Spinal cord specific EphA4 mutants, Pax7-Cre; EphA4l$^{x/-}$ [C], Lbx1-Cre; EphA4$^{lx/-}$ [D] and HoxB1-Cre; EphA4$^{lx/-}$ [G], Wnt-Cre; EphA4$^{lx/-}$ [E] displayed a reduced or shallow DF (brackets) similar to PGK-Cre; EphA4$^{lx/-}$ [G] mutants. Bar graph depicting the size of the DF that was quantified in spinal cords sections from all genotypes [I] Error bars represents SEM. Scheme summarizing the phenotypes [J]. ***p<0.001 with t-test Scale bars: 500µm. Data in panels [A-D] were generated by Dr. S. Paixão.

4.3.2. EphA4 is expressed in neurons that surround the dorsal funiculus in the embryonic spinal cord

How does EphA4 contribute to the DF phenotype? Previously, EphA4 has been shown to be required for the guidance of the descending CST tract. Furthermore, CST tracing experiments in EphA4 null mice revealed aberrant midline misprojections and implicated it to be the cause of the shallow DF phenotype observed in these mice [104]. Since the CST axons arrive in the spinal cord during the first postnatal week of development [104], we first investigated the contribution of EphA4 in the embryonic spinal cord, prior to the arrival of CST axons. For this, we made use of the EphA4$^{\beta geo\text{-}PLAP}$ gene-trap allele, where β-gal is expressed in the cell bodies and human placental alkaline phosphatase (PLAP) is expressed in the axons of EphA4 positive cells [107].

To visualize the EphA4 (β-gal) positive cells, we performed X-gal staining using the EphA4^{PLAP} mice (from now EphA4$^{PLAP/+}$). We observed robust expression of EphA4 (X-gal), by embryonic day 13.5 (E13.5) all over the spinal cord. Upon closer observation, we found that the dorsal spinal cord contained a population of darkly stained EphA4 (X-gal) cells that were well separated from the midline [indicated with an arrow in Figure 4.16 A]. One day later in

development, that is, by E14.5, the DF began to form by extending ventrally [indicated with the stippled line in Figure 4.16 B]. The EphA4 (β-gal) cells were observed to line the ventral tip of the DF [indicated by an arrow in Figure 4.16 B], while continuing to be bisected by the midline, throughout development [Figure 4.16 C and C'].

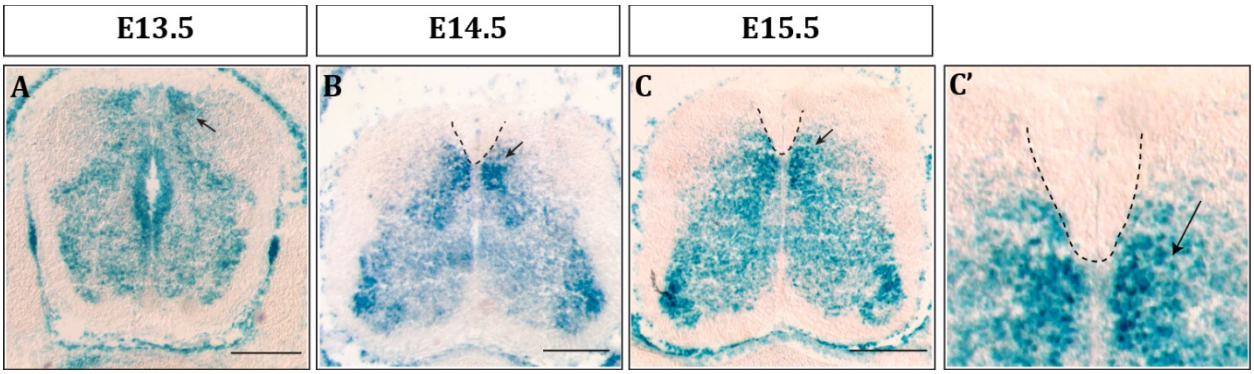

Figure 4.16: EphA4 expression in the developing spinal cord. β-galactosidase (β-gal) expression using EphA4$^{\beta geo\text{-}PLAP}$ allele (EphA4^{PLAP}) [107]. Epha4 (β-gal) is expressed all over the spinal cord except in the dorsal horns. Dorsally located EphA4 positive cells (β-gal) are indicated by an arrow and the dorsal funiculus is indicated by a stippled line [A-C]. At E13.5, the dorsal funiculus has not yet begun to be formed. Two populations of cells strongly express EphA4 (β-gal) on either side of the midline in the dorsal spinal cord [A]. By E14.5, the dorsal funiculus begins to form. The cells that strongly express EphA4 (β-gal) in the dorsal spinal cord, line the ventral tip of the developing dorsal funiculus [B]. By E15.5, the dorsal funiculus enlarges and the EphA4 (β-gal) expressing cells maintain their position [C, C']. Scale bars: 250μm; Data in panels [B-C] were generated by Dr. S. Paixão.

4.3.3. Ablation of EphA4 hinders the extension of the dorsal funiculus and causes the cells to shift to the midline

We then asked how the DF development would be affected in the absence of EphA4. First, we crossed the two alleles of EphA4: EphA4^{PLAP} and EphA4$^{-/-}$, thus allowing us to visualize the knockout EphA4 neurons (from now EphA4$^{PLAP/-}$) using the X-gal method

described above. When we looked at the spinal cords of EphA4$^{PLAP/-}$ mice, we found that, at E13.5, the DF had still not developed similar to wildtype littermates [Figure 4.17 A]. One day later in development, at E14.5, however, the DF appeared much reduced or shallow in the knockouts compared to wildtype littermates and this effect was more pronounced in E15.5 spinal cords [Figure 4.17 B and C].

Interestingly, we noticed that, in the EphA4$^{PLAP/-}$ spinal cords, at E13.5, the darkly stained group of EphA4 (β-gal) cells were bisected by the midline similar to the EphA4$^{PLAP/+}$ controls [Figure 4.17 A]. At E14.5 and E15.5, however, we found that these cells were no longer bisected by the midline; but were mis-positioned medially and were now located at the midline [Figure 4.17 B and C].

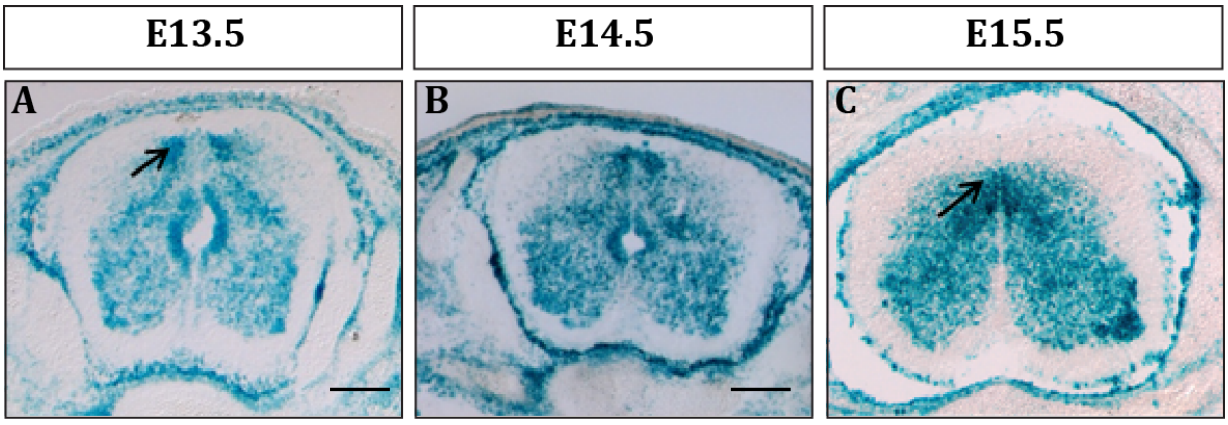

Figure 4.17: EphA4 ablation results in a shallow DF and results in a medial shift of the cells to the midline. X-gal staining in sections from E13.5 EphA4$^{PLAP/-}$ spinal cords shows a group of darkly stained cells that are bisected by the midline [A]. In E14.5 [B] and E15.5 [C] spinal cords of EphA4$^{PLAP/-}$ sections, these cells move medially to the midline thereby hindering the ventral extension of the DF. Scale bars in [A] and [B] is 250μm. Data in panel [C] were generated by Dr. S. Paixão.

4.3.4. EphA4 ablation produces a 'gap' in the dorsal spinal cord midline

What causes the cells that express EphA4 to stay bisected at the midline? From previous studies, it is already known that ephrinB3 is a repellant for EphA4 neurons of the CST and CPG at the midline [70, 99, 104]. We, therefore, examined the expression of ephrinB3 in embryonic EphA4$^{PLAP/+}$ and EphA4$^{PLAP/-}$ spinal cords via in situ hybridization. Additionally, we also performed in situ hybridization for LacZ in order to be able to visualize the EphA4 positive cells in the same sections.

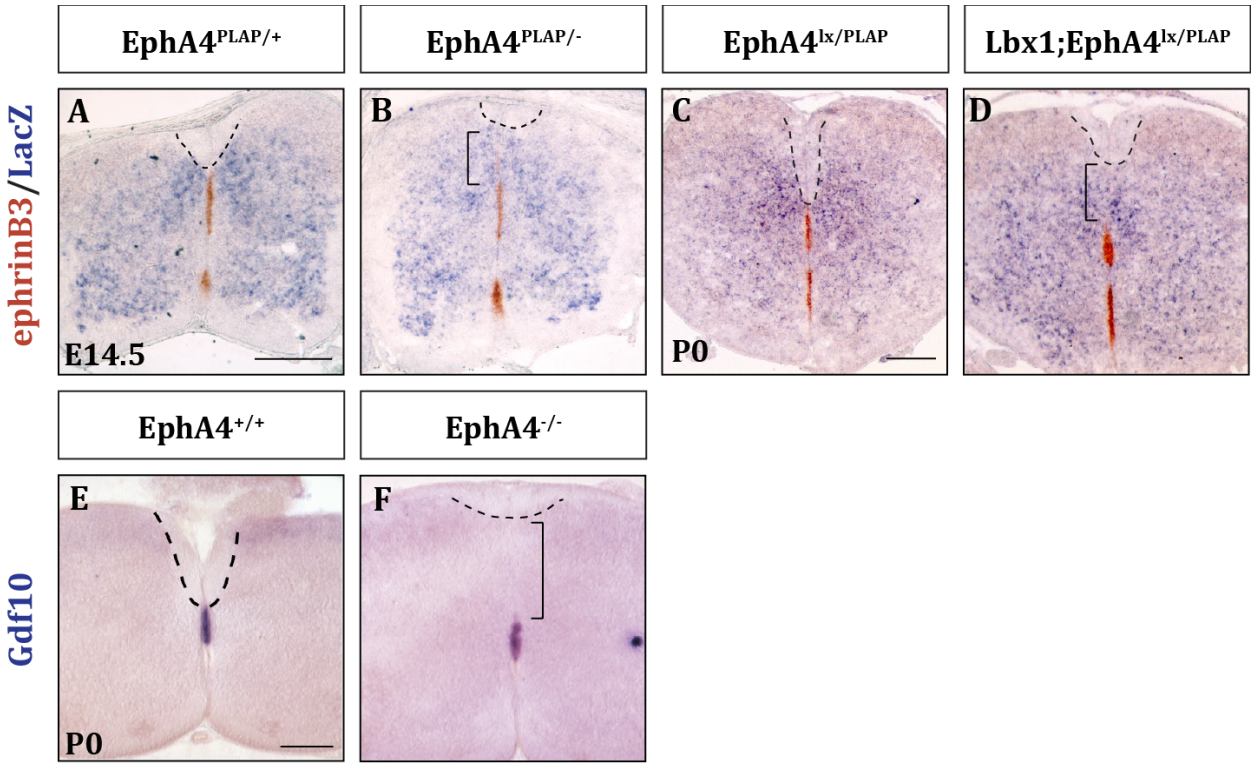

Figure 4.18: EphA4 ablation leads to a gap between the ventral tip of the DF and the expression of midline markers. Double in situ hybridization (ISH) was performed to visualize the expression of ephrinB3 (brown) and EphA4 (LacZ – blue). ephrinB3 expression was observed until the ventral tip of the DF and the EphA4 positive cells were bisected by the midline in EphA4$^{PLAP/+}$ at E14.5 and P0 [A and C] EphA4 cells (LacZ) move to the midline in an area that is devoid of ephrinB3 expression in EphA4$^{PLAP/-}$ and EphA4$^{lx/PLAP}$; Lbx1-Cre^{+} sections at E14.5 and P0 [B and D]. Another midline marker, Gdf10, shows the same midline gap in EphA4$^{-/-}$ sections [E and F]. Stippled

lines indicate the DF and brackets indicate the midline gap. Scale bars are 250μm. Data were generated by Dr. S. Paixão.

As early as E14.5, the expression of ephrinB3 mRNA could be seen at the midline and it extended from the ventral tip of the DF to the central canal. A similar expression pattern was also observed in P0 wildtype spinal cords [Figure 4.18 A and C]. However, from E14.5 onwards, EphA4$^{PLAP/-}$ sections displayed a distinct 'gap' between the dorsal tip of ephrinB3 mRNA expression at the midline and the ventral tip of the DF. Interestingly, this 'gap' was populated by the mis-positioned EphA4 (LacZ) knockout neurons that aberrantly move to the midline in the EphA4$^{PLAP/-}$ spinal cords [Figure 4.18 B and D]. Moreover, when we assessed the mRNA expression of another midline marker, Gdf10, we found the same 'gap' in knockout cords that did not exist in wildtype littermates [Figure 4.18 E and F].

Taken together, these results show that EphA4 expressed specifically in dorsal subpopulations of the spinal cord is required for the correct formation of the DF. EphA4, expressed in cells that line the DF are bisected by the midline, thus allowing the dorsal funiculus to extend ventrally. In the absence of EphA4, however, these cells move to the midline thereby hindering the ventral extension of the DF. Thus the DF phenotype observed in the knockouts is caused by the absence of EphA4 expressed in cells within the dorsal spinal cord rather than CST mis-projections as thought previously.

Additionally, the EphA4 positive cells are normally repelled by ephrinB3, a known ligand for EphA4 that is expressed at the midline. In the absence of EphA4, these cells no longer feel the repulsion from the midline and move their position medially. Indeed, this area is entirely devoid of ephrinB3. We believe that this phenotype is not due to a downregulation of ephrinB3

(since we observe a similar shift of other midline markers), but is due to a shift of the entire midline.

4.3.5. Identification of EphA4 positive cells using dorsal interneuron markers

Next we asked what the identity of the EphA4 (β-gal) cells was that lined the ventral tip of the DF. To address this question, we made use of the EphA4^{PLAP} mice. Spinal cords from E14.5 mice were dissected and cryo-protected. Since the resolution of the X-gal staining was too low to permit any quantification, we used anti-βgal antibodies to detect the presence of EphA4 (β-gal) and combined it with antibodies for dorsal interneuron markers such as Brn3a and Lbx1. Brn3a is a POU-domain transcription factor [130] that is expressed in early born dI1-3 and dI5 interneurons [31]. They ultimately give rise to glutamatergic neurons that finally migrate and settle in the deep layers of the dorsal horn. Brn3a is required for the proper specification of sensory neuron projections into the spinal cord [130]. We quantified the data by assigning x-y co-ordinates to the EphA4 (β-gal) and Brn3a double positive cells to assess their spatial distribution. X is the medial-lateral axis and 0 represents the midline, whereas Y is the dorsal-medial axis and 0 represents the central canal. When we assessed the co-localization of EphA4 (β-gal) positive and Brn3a positive neurons, we found a weak co-staining between them (~12%) [Figure 4.19 B, B', B'' and D].

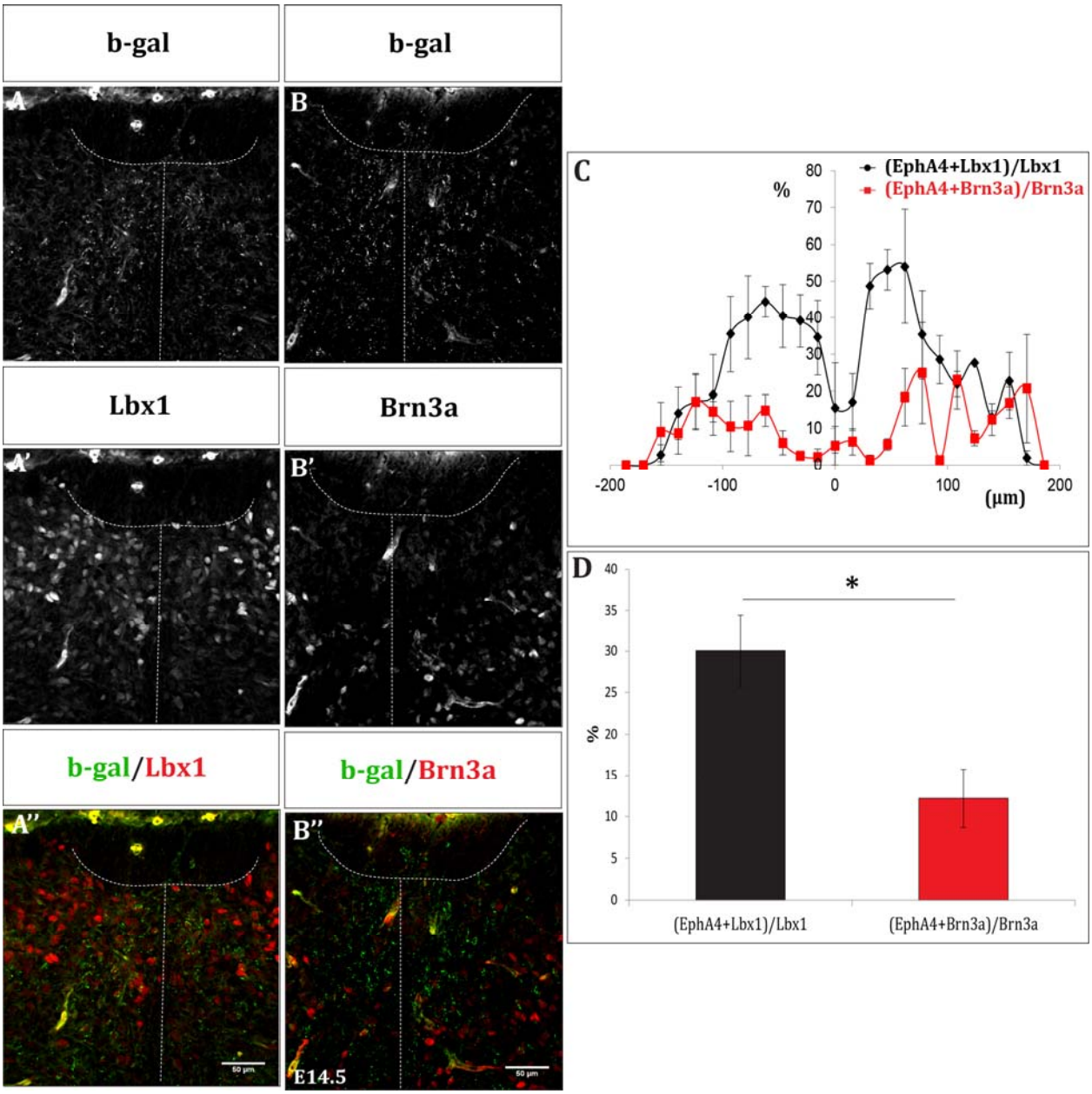

Figure 4.19: Co-localization of EphA4 (β-gal) with dorsal interneuron markers expressed in the developing spinal cord. E14.5 transverse spinal cord sections from EphA4^{PLAP} mice stained for EphA4 (β-gal) and Lbx1 to label dI4-6 interneurons, [A, A' and A''] and Brn3A to label dI1-3 interneurons [B, B' and B'']. The stippled line in the images indicates the dorsal funiculus and the midline. Mediolateral frequency distribution of the percentage of EphA4+Lbx1 (black) and EphA4 + Brn3a (red) [C]. Bar graph depicting the average percentage of EphA4+Lbx1 cells and EphA4+Brn3a cells [D]. n=3; 3 sections per embryos; *p=0.03. Scale bar is 50µm.

Additionally, we studied the co-localization of Lbx1 with EphA4 (β-gal). Lbx1 is a homeobox transcription factor [120], expressed in dI4-6 interneurons [121] and gives rise to the neurons that finally reside in the upper and superficial layers of the dorsal horn or migrate ventrally, depending on the time of their birth [121]. When we co-stained EphA4 (β-gal) with Lbx1, and quantified the data as mentioned above, we found a strong co-localization in cells that lined the ventral tip of the DF and were bisected by the midline [Figure 4.19 A, A' and A''']. On average, 30% of the Lbx1 positive cells were also positive for EphA4 (β-gal) [Figure 4.19 D].

4.3.6. EphA4 specifically co-localizes with Zic2 in cells that surround the dorsal funiculus

Recently, in a screen performed in the laboratory of Dr. Eloisa Herrera, Zic2, a transcription factor belonging to the zinc finger family of proteins [131], was shown to be a glutamatergic marker for the late born dIL_B interneurons [132]. When we co-stained Zic2 with EphA4 (β-gal) in E15.5 wildtype sections of the spinal cord, we found two populations of Zic2 positive cells: a 'dorsal' population that surrounded the DF showed strong co-localization with EphA4 (β-gal) [Figure 4.20 A and A'], and a 'central' population that was located close to the central canal and largely devoid of EphA4 (βgal) [Figure 4.20 A and A''']. Both 'dorsal' and 'central' populations were bisected by the midline [Figure 4.20 C] and cell counts to quantify the double positive cells revealed that, on average, in the 'dorsal' population, 26% of the Zic2 positive cells were also positive for EphA4 [Figure 4.20 D], whereas, in the 'central' population only 9% of the Zic2 positive cells were also positive for EphA4 (β-gal) [Figure 4.20 D]. Moreover, we found the co-localization of EphA4 (β-gal) with Zic2 to be specific to the spinal cord, since we did not detect any Zic2 expression in the motor cortex of these mice [Figure 4.20 B].

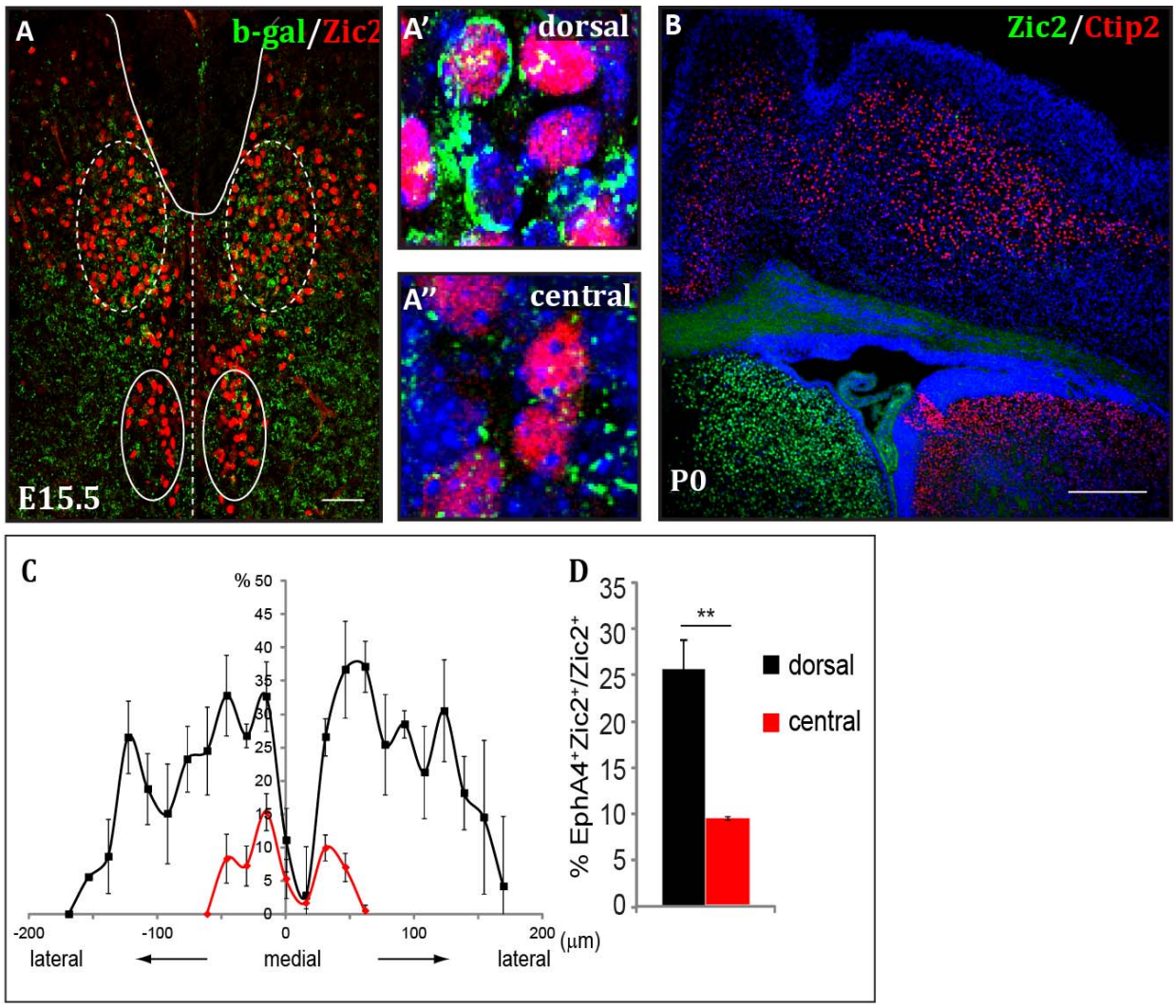

Figure 4.20: EphA4 and Zic2 specifically co-localize in cells that surround the dorsal funiculus. Immuno-staining of EphA4 (βgal) and Zic2 in transverse sections of the spinal cord from E15.5 wildtype embryos. Strong co-localization can be seen in the cell population that surrounds the dorsal funiculus [indicated by the stippled circle in A]. Zoomed in image showing co-staining of EphA4 (β-gal) and Zic2 [A']. Zic2 cells in the more ventral population that was close to the central canal were largely devoid of EphA4 (β-gal) [indicated by the solid circle in A]. Zoomed in image showing absence of EphA4 (β-gal) in the ventral Zic2 population [A'']. No co-localization between Zic2 and Ctip2 was seen in the motor cortex [B]. Medio-lateral frequency distribution of the percentage of Zic2 and EphA4 (β-gal) double positive cells in the dorsal (black line) and central (red line) populations [C]. Bar graph depicting the average cell count of EphA4 (β-gal) and Zic2 double positive cells in the dorsal and central

populations [D; n=3 embryos, 3-5 images per embryos; ** p = 0.006; t-test]. Scale bar is 50µm [A-A'’] and 250µm [D].

4.3.7. Dorsal interneurons positive for Zic2 move to the midline in EphA4 null mice

We then asked whether the EphA4 (β-gal) cells that move to the midline were also positive for Zic2. For this, we used E15.5 spinal cords from EphA4$^{PLAP/+}$ and EphA4$^{PLAP/-}$ mice and checked for co-localization of EphA4 (β-gal) and Zic2 via immunofluorescence in the 'dorsal' population. The data were quantified as mentioned previously, that is by assigning x-y co-ordinates to EphA4 (β-gal), Zic2 and EphA4 (β-gal)/Zic2 double positive cells to assess their spatial distribution [Figure 4.21 A-F and A'-F']. The medial-lateral axis was represented on the X axis with 0 representing the midline, whereas, the dorsal-lateral axis was represented on the Y axis with 0 being representative of the central canal [Figure 4.21 G-J].

We analyzed the expression of EphA4 (β-gal), Zic2 and EphA4 (β-gal) and Zic2 double positive cells in spinal cords from EphA4$^{PLAP/+}$ mice and compared it to that from EphA4$^{PLAP/-}$ mice. When we plotted the medio-lateral frequency distributions as a nonlinear regression, fitted as a sum of two Lorentizian distributions [Figure 4.21 G-I] (the corresponding raw data are also provided [Figure 4.21 G'-I']), and compared the centers of distribution, a pronounced and significant shift of EphA4 (β-gal) positive cells to the midline was observed in the knockouts. The wildtype spinal cords showed a bilateral distribution that was bisected by the midline [Figure 4.21 G-I]. In addition, for better visualization of the same phenotype, we plotted the digital coordinates of the cells [Figure 4.21 A'-F']. Moreover, we found this shift only in the medio-lateral plane; the dorso-ventral positioning of the cells seem unaltered [Figure G'' and H'']. Likewise, ephrinB3$^{-/-}$ mice phenocopy EphA4 null mutants and display similar medio-lateral shifts of Zic2 cells to the midline. The interaction of EphA4 and ephrinB3 has been shown

to important in preserving neuronal circuits in the spinal cord and is also required for the correct positioning of dorsal interneurons [100].

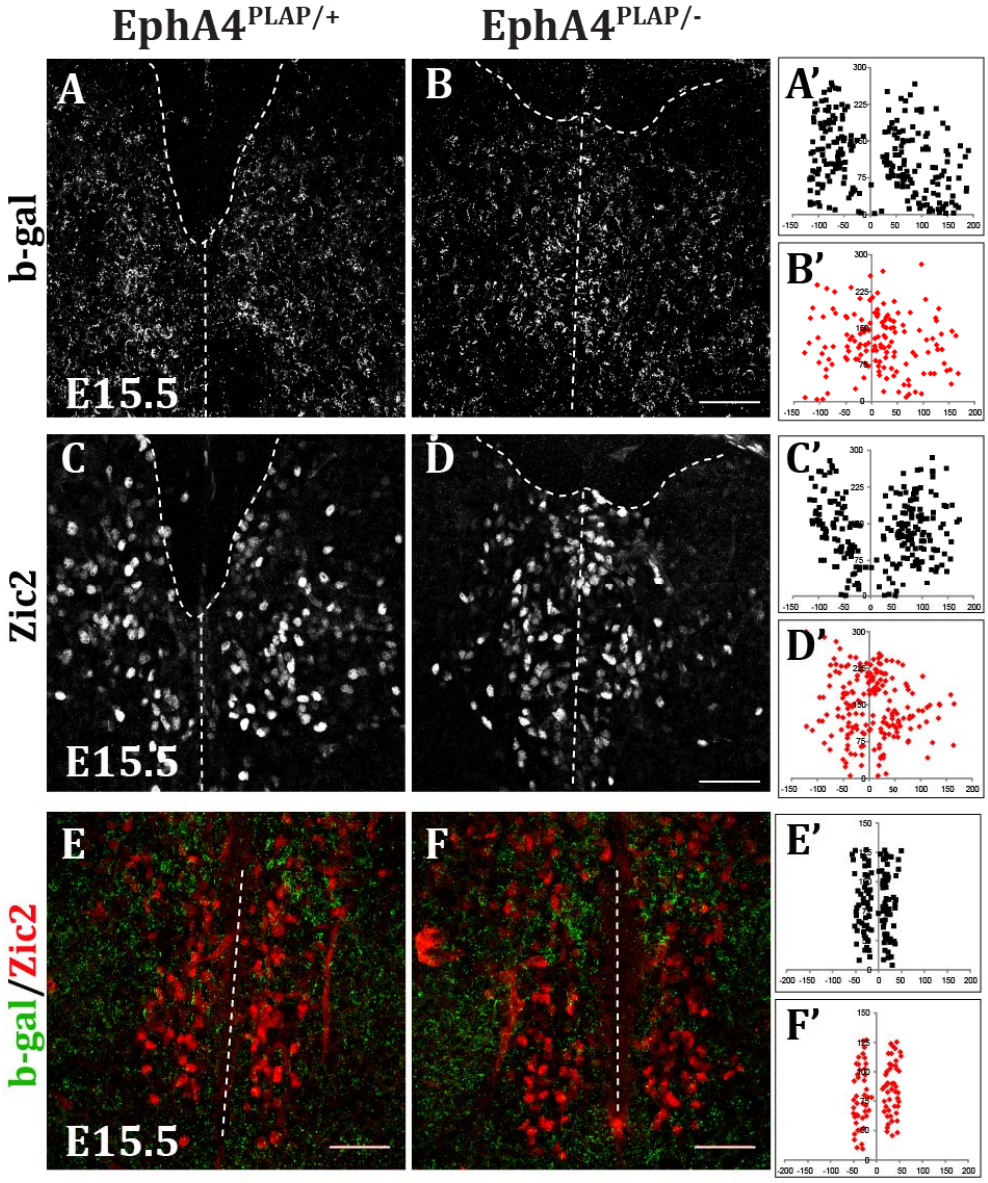

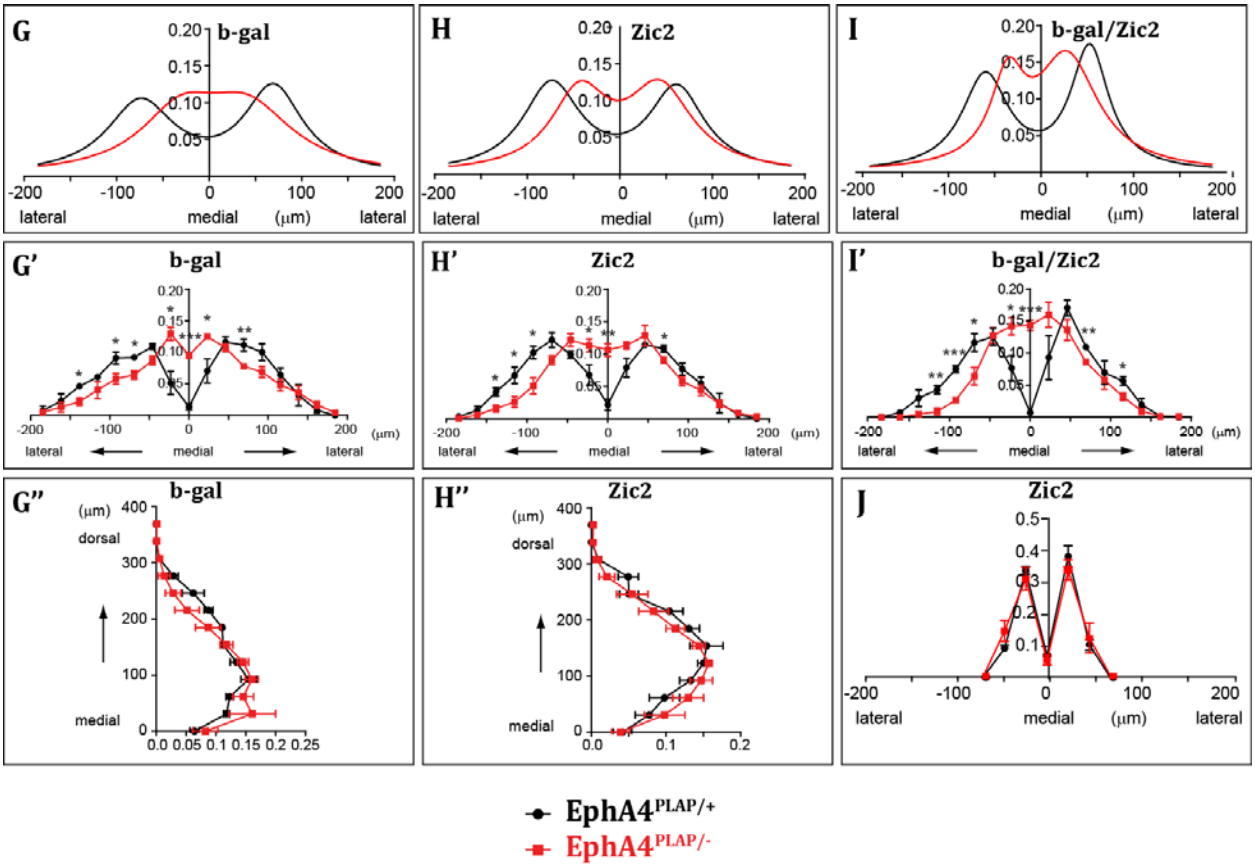

Figure 4.21: EphA4 ablation causes Zic2 positive dorsal interneurons to move to the midline. Immuno-staining of sections from E15.5 spinal cords of EphA4$^{PLAP/+}$ and EphA4$^{PLAP/-}$ mice for EphA4 (β-gal) [A and B] and Zic2 [C and D] in the dorsal population. Digital coordinates of EphA4 (β-gal) [A' and B'] and Zic2 positive cells [C' and D'] from these sections to assess the spatial distribution. X axis is medial-lateral axis and Y axis is dorso-ventral axis. Expression of EphA4 (β-gal) [E] and Zic2 [F] in the central population from these sections. Digital coordinates of Zic2 positive cells to assess their distribution [E' and F']. Medio-lateral frequency distribution of relative cells density of EphA4 (β-gal) [G], Zic2 [H] and EphA4/Zic2 double positive cells [I] in EphA4$^{PLAP/+}$ (black line) and EphA4$^{PLAP/-}$ (red line) spinal cord sections represented as a nonlinear regression (sum of two Lorentzian distributions). $p<0.0001$ extra sum-of-squares F-test, comparing distribution centers. Raw data of the corresponding fitted curves [G', H' and I']. *$p<0.05$, **$p<0.01$, ***$p<0.001$ t-test. Dorso-ventral frequency distribution of EphA4 (β-gal) [G''] and Zic2 positive cells [H''] from [A and B]. Medio-lateral frequency distribution of Zic2 [J] from EphA4$^{PLAP/+}$ (black line) and EphA4$^{PLAP/-}$ (red line) spinal cord sections. $p>0.05$. n=3-4, 2-5 images per embryo. Scale bars are 50μm.

Furthermore, we analyzed the expression of Zic2 in the 'central' population that was largely devoid of EphA4 (β-gal) and found that these cells did not shift their position in the medio-lateral plane to the midline in the knockouts [Figure 4.21 J].

Together, these results show that the EphA4 positive cells that line the DF are positive for Zic2. This co-localization is rather specific for the cells that surround the DF since very few Zic2 positive cells are also positive for EphA4 in the more ventral cell population and Zic2 is completely absent from the motor cortex of the brain. Furthermore, in the absence of EphA4, the cells that move to the midline express Zic2; however, this effect was highly specific to the cells that surround the DF, as Zic2 cells that did not express EphA4 (located close to the central canal) did not move to the midline in the absence of EphA4.

4.3.8. Cells expressing EphA4 project ipsilaterally into the dorsal funiculus

Next, we investigated the axonal projections of the EphA4 expressing cells by staining for the axonal marker, human placental alkaline phosphatase (PLAP) using the EphA4^{PLAP} mice. NBT (Nitroblue tetrazolium) and BCIP (5-bromo-4chloro-3-indolyl phosphate), substrates for the enzyme alkaline phosphatase, produce an intense insoluble blue dye upon reaction, allowing visualization of the axonal projections.

In sections from E14.5 wildtype (EphA4$^{PLAP/+}$) spinal cords, the axonal projections of the dorsally located EphA4 cells form a tight bundle on either side of the midline and project into the DF. Furthermore, these axons enter the DF ipsilaterally and do not cross the midline [Figure 4.22 A]. The same staining pattern was observed at E15.5 and in P1 spinal cords [Figure 4.22 B and C].

Additionally, since the resolution of the PLAP staining was too low to allow us to track the projection of single axons, we used an EphA4 BAC-transgenic reporter line, *Tg*(EphA4-EGFP), that was generated by GENSAT, where EGFP was placed under the regulatory elements of the EphA4 gene, thus labeling the cells bodies and axons of EphA4 expressing cells and allowing their visualization [133]. Longitudinal sections of spinal cords from post natal mice permitted us to follow to the axonal projections and indeed we were able to confirm that the axons make a rostral turn and enter the DF suggesting that this ipsilateral tract forms ascending projections [Figure 4.22 E-F].

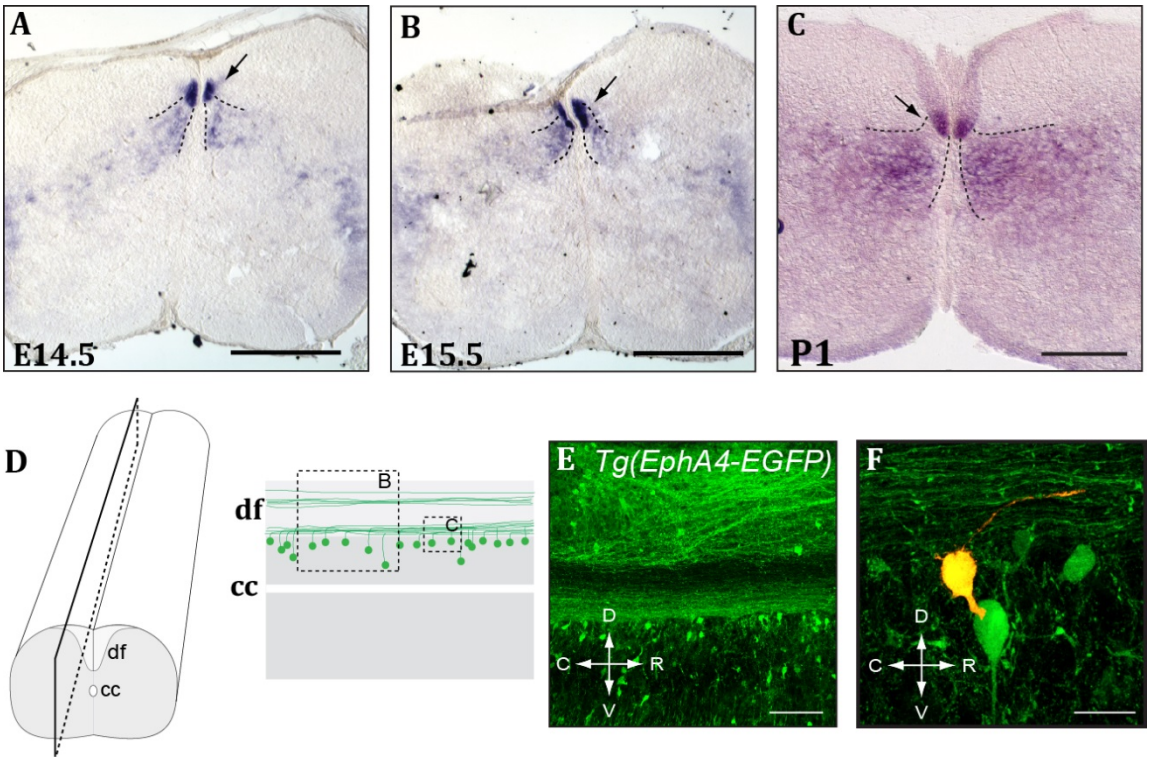

Figure 4.22: EphA4 neurons project ipsilaterally into the DF. PLAP staining to visualize axons of EphA4 positive neurons at E14.5 [A], E15.5 [B] and P1 [C]. Schematic diagram depicting the longitudinal axis along which the spinal cord was sectioned [D]. Longitudinal sections from Tg(EphA4-EGFP) mice stained with GFP show the axons projecting into the DF [E]. High magnification image of a single EphA4 positive neuron (in red) whose axon turns rostrally into the DF. The image was reconstructed and superimposed on the maximum projection of a GFP

stained longitudinal section [F]. Scale bars are 250µm in [A and B], 1mm in [C], 100µm in [E]and 20µm in [F]. Data were generated by Dr. S. Paixão.

4.3.9. EphA4 knockouts display aberrant midline mis-projections

We then asked if EphA4 in the dorsal neurons is required for the guidance of their axons. We first investigated the axonal projections of EphA4$^{PLAP/-}$ mice in comparison to their wildtype littermates using the PLAP staining in embryonic (E15.5) and postnatal (P0) spinal cords. We found that in the absence of EphA4 the axons fail to maintain their ipsilaterality and mis-project across the midline [Figure 4.23 A and B]. Also, since ephrinB3 is a known midline repellent of EphA4 [104] we investigated the axonal projections of EphA4 expressing neurons in ephrinB3$^{-/-}$ mice in early development (P0). To visualize the axons of EphA4 expressing cells, we first crossed the EphA4^{PLAP} allele into ephrinB3$^{+/+}$ (ephrinB3$^{+/+}$; EphA4$^{PLAP/+}$) and ephrinB3$^{-/-}$ (ephrinB3$^{-/-}$; EphA4$^{PLAP/+}$) mice. We found a similar phenotype as in the EphA4$^{PLAP/-}$ mice: extensive midline mis-projections of the EphA4 expressing neurons in the ephrinB3 knockouts compared to controls [Figure 4.23 C and D].

To assess the contribution of EphA4 specifically in the dorsal neurons, we first crossed the EphA4^{PLAP} allele into the EphA4^{lx} mice. We found that the axons in heterozygous controls (EphA4$^{lx/PLAP}$) behaved similar to those in EphA4$^{PLAP/+}$ mice, that is, they formed ipsilateral projections that did not cross the midline [Figure 4.23 E]. However, when EphA4 was ablated specifically in the dorsal neurons, using Pax7-Cre (Pax7-Cre; EphA4$^{lx/PLAP}$) and Lbx1-Cre (Lbx1-Cre; EphA4$^{lx/PLAP}$), aberrant mis-projections of the axons over the midline was observed [Figure 4.23 G and F]. Furthermore, when we ablated EphA4 specifically in the forebrain using the Emx1-Cre (Emx1-Cre; EphA4$^{lx/PLAP}$), we found no midline mis-projections of the dorsal neurons [Figure 4.23 H].

Collectively, these results demonstrate that the axons of EphA4 expressing cells are repelled by the midline that expresses ephrinB3, a known ligand of EphA4. This interaction allows EphA4 to guide the axons of dorsal neurons into bundles that project ipsilaterally into the DF. Ablating EphA4, specifically in the dorsal spinal cord, causes aberrant midline mis-projections.

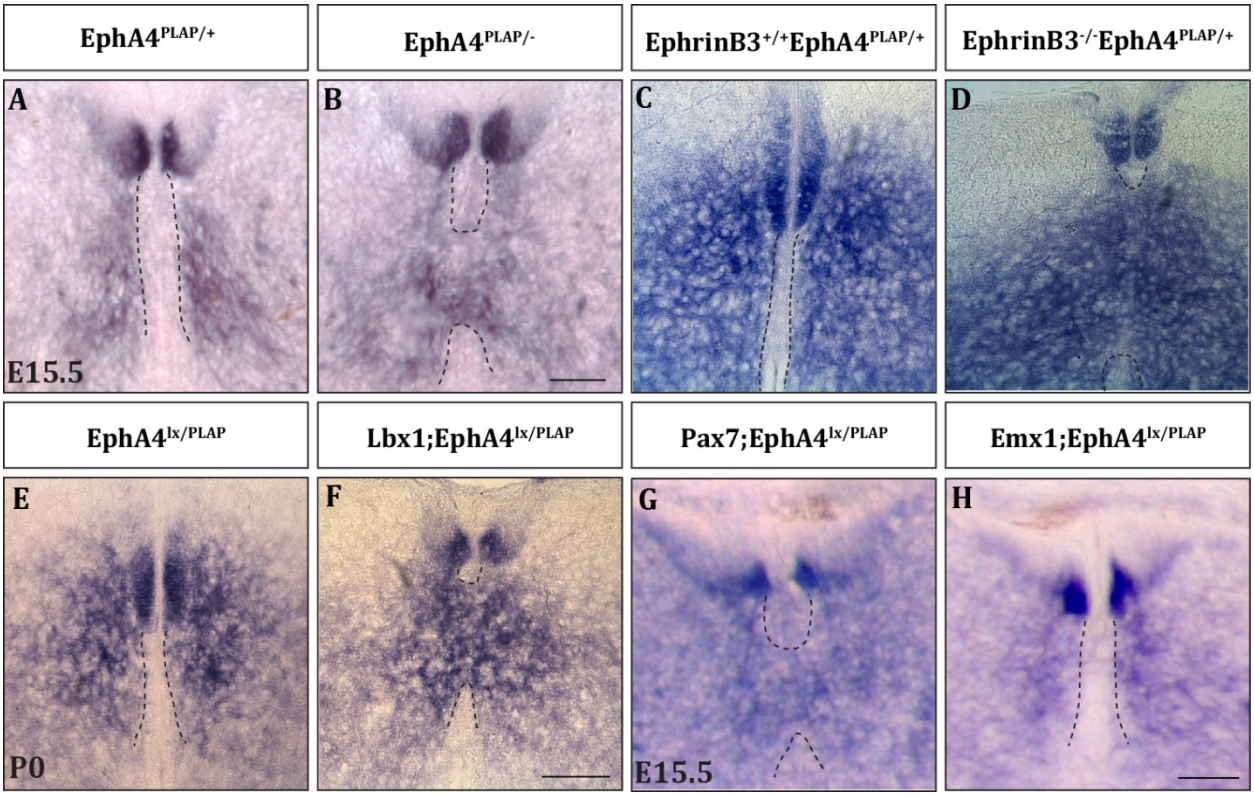

Figure 4.23: Aberrant midline misprojections in EphA4 mutant mice. PLAP staining to visualize the axons of EphA4 positive cells from the indicated genotypes of E15.5 and P0 mice. The EphA4 axons remained ipsilateral in $EphA4^{PLAP/+}$ mice [A], $ephrinB3^{+/+}$; $EphA4^{PLAP/+}$ mice [C] and forebrain specific EphA4 knockout mice [H]. Extensive mis-projections were observed in all other genotypes analyzed [D-G] n=3; scale bar = 50μm. Data in panels [A, B, E-H] were generated by Dr. S. Paixão

4.3.10. EphA4 ablation results in secondary spinal cord defects but leaves the overall laminar structure of the spinal cord intact

Sensory axon projections that arise from the dorsal root ganglia (DRG) enter the spinal cord along an ipsilateral corridor in the dorsal horn [134]. Since EphA4 is not expressed in the DRGs [135] and EphA4 knockout mice display defects in the DF morphology and dorsal midline defects, we asked if the incoming sensory axon projections are indirectly perturbed as a consequence of these phenotypes.

To address this question, we performed immunofluorescence stainings using markers of nociceptive and proprioceptive neurons. CGRP (calcitonin gene-related peptide), is a commonly accepted marker for the peptidergic subset of nociceptive sensory neurons [136, 137]. In EphA4$^{+/+}$ sections, we found that the CGRP positive axons entered the spinal cord and mostly remained ipsilateral [Figure 4.24 A]. Conversely, in EphA4$^{-/-}$ sections, we found that a large proportion of the CGRP positive axons aberrantly crossed the midline in the area just beneath the DF and thus displayed contralateral projections [Figure 4.24 B].

Furthermore, when we quantified this result by measuring the intensity of staining in an area just below the DF and normalized it to an area devoid of any staining [indicated by the solid and stippled boxes respectively in Figure 4.24 B] in sections from all genotypes, we found a significant difference in the staining intensity in sections from EphA4$^{-/-}$ mice compared to their wildtype littermates.

Additionally, since the ephrinB3$^{-/-}$ mice pheno-copy the EphA4$^{-/-}$ mice, we analyzed the CGRP positive axons in spinal cord sections from these mice. The ephrinB3$^{+/+}$ sections displayed ipsilateral CGRP axon projections as expected [Figure 4.24 C and E], however, to our surprise;

we found that the CGRP axons remained ipsilateral in the ephrinB3$^{-/-}$ mice [Figure 4.24 D and E].

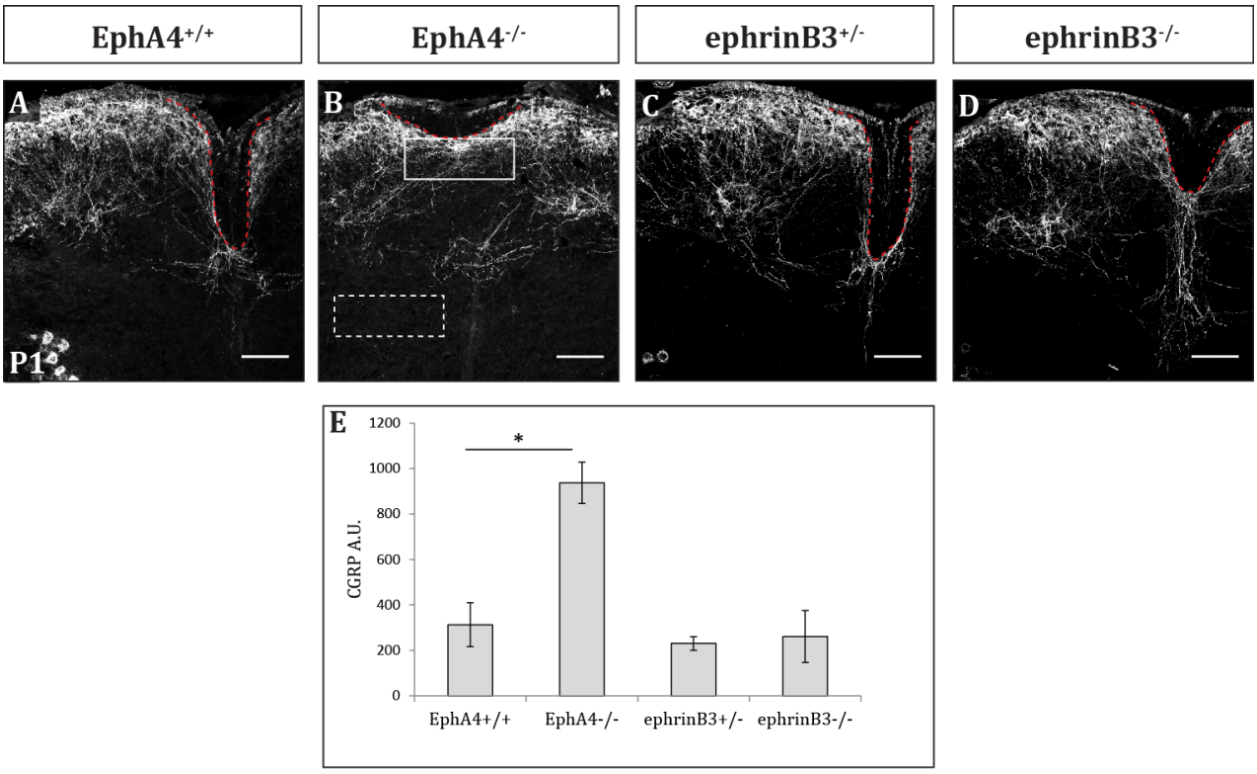

Figure 4.24: Nociceptive sensory afferents aberrantly mis-project in EphA4$^{-/-}$ mice. Immunostaining to detect CGRP positive nociceptive sensory axons in cryo-protected sections from EphA4$^{+/+}$ [A], EphA4$^{-/-}$ [B], EphrinB3$^{+/+}$ [C] and ephrinB3$^{-/-}$ [D] P1 mice. The stippled line indicates the DF. Quantification of staining intensity from the indicated genotypes [E]. *p = 0.01; t-test; n=3; 3-4 images per mouse; scale bar = 50µm. Data in panels [A] and [B] were generated by Dr. S. Paixão.

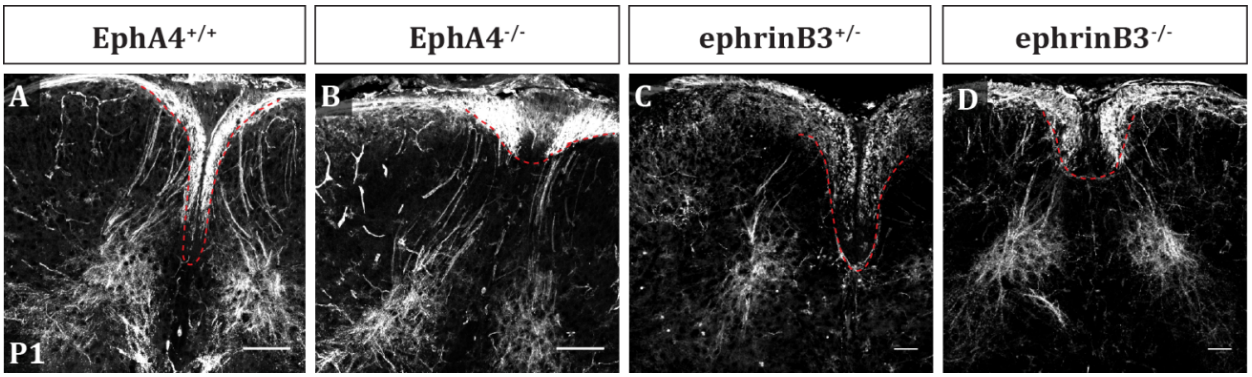

Figure 4.25: Proprioceptive sensory afferents are not affected in EphA4$^{-/-}$ mice. Immunostaining to detect parvalbumin positive proprioceptive sensory axons in cryo-protected sections from EphA4$^{+/+}$ [A], EphA4$^{-/-}$ [B], EphrinB3$^{+/+}$ [C] and ephrinB3$^{-/-}$ [D] P1 mice. The stippled line indicates the DF. n=3; scale bar = 50µm. Data in panels [A] and [B] were generated by Dr. S. Paixão.

When we used parvalbumin as a marker to label proprioceptive sensory fibers [138] and performed immunofluorescence stainings, we found that the proprioceptive sensory afferents entered the spinal cord via the DF and projected ipsilaterally in sections from both EphA4 and ephrinB3 wildtype mice [Figure 4.25 A, and C]. Similarly, we found ipsilateral projections of parvalbumin positive sensory axons in sections from both EphA4 and ephrinB3 knockout mice [Figure 4.25 B and D].

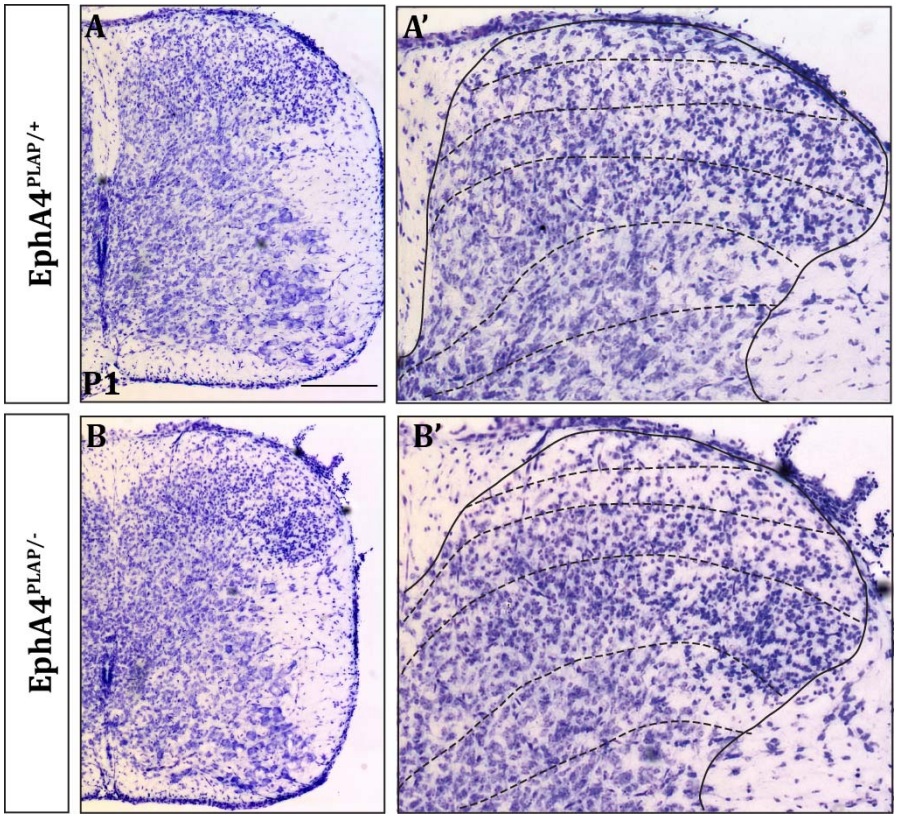

Figure 4.26: The laminar distribution of the dorsal spinal cord is preserved in EphA4 knockout mice. Nissl staining in cryo-protected sections from EphA4$^{PLAP/+}$ [A] and EphA4$^{PLAP/-}$ [B] P1 mice. High magnification images of dorsal spinal cord with stippled lines indicating the laminar distribution in both genotypes [A' and B']. n=3; scale bar = 200μm.

Finally, since we observed a shift of dorsal interneurons to the midline and aberrant midline projections of their axons, coupled with secondary defects in sensory axon misprojections, we investigated the laminar organization of the dorsal spinal cord. We performed Nissl staining to label the nuclei in cryo-protected sections from EphA4$^{PLAP/+}$ and EphA4$^{PLAP/-}$ mice and found no alterations in the laminar distribution except the shallow DF [Figure 4.26 A and B].Together, all the morphological phenotypes described above point to the critical role of EphA4 in the dorsal spinal cord in guiding dorsal interneurons to their correct positions along with maintaining their axonal projections in an ipsilateral and ascending corridor. Ablating

EphA4 leads to a shift of these dorsal interneurons to the midline, thus hindering the ventral extension of the DF. Furthermore, the axonal projections of these neurons aberrantly cross the midline and project contralaterally. Additionally, majority of the cells that shift to the midline are also positive for Zic2. Moreover, in the absence of EphA4, secondary phenotypes were observed in the guidance of nociceptive axons.

5. Discussion

5.1. The contribution of EphA4, expressed specifically in the dorsal spinal cord, to left-right coordination of locomotion

The last decade has seen a tremendous increase in the interest to understand the structure and the underlying molecular mechanisms that govern locomotory circuits of the spinal cord. Locomotory behavior entails the rhythmic and sequential stepping of the right and left limbs and is controlled by organized pools of interneuron circuits, collectively termed as the central pattern generators (CPGs), which reside in the ventral spinal cord [67, 139-141]. Therefore, in the past, a number of studies have focused their attention on this region and have shed light on the identity and role of these distinct interneuron pools in CPG function [38, 44, 142-145]. Indeed, certain studies have made use of EphA4 and ephrinB3 knockout mice, which display midline axon guidance defects and consequently, a rabbit-like hopping gait, to understand the requirement of EphA4 in the ventral spinal cord with respect to CPG function [104, 105, 146]. However, the widespread expression of EphA4 along the dorsal-ventral axis of the spinal cord raises the possibility of a dorsal contribution in locomotory behaviors. We therefore investigated the role of dorsally expressed EphA4 in left-right coordination of locomotion, by spatially restricting its expression to various regions of the brain and spinal cord, using specific Cre lines.

Like the EphA4 null mice, complete ablation of EphA4 (PGK-Cre) produces synchrony, whereas, littermate control mice display an alternating gait. Furthermore, the alternating gait is preserved when EphA4 is ablated in the forebrain alone (Emx1-Cre), however, ablating EphA4 specifically in the entire spinal cord (HoxB1-Cre) produces synchrony, reinforcing the fact that EphA4, expressed in the spinal cord, is involved in left-right coordination of locomotion.

Specifically ablating EphA4 in the dorsal interneurons produces an interesting partial hopping phenotype. The mice display 3 distinct gaits within the same experiment – synchrony, alternation and intermediate. Indeed, ablating EphA4 from the entire dorsal spinal cord (dI1-6), using Pax7-Cre, or from a more restricted subpopulation of dorsal interneurons (dI-4-6), using Lbx1-Cre, produces the same phenotype. Furthermore, experiments conducted by Dr. S. Paixão, using the ventral midline tracing technique [104], to label commissural interneurons, substantiate these results as they reveal aberrant midline misprojections specifically in dorsal spinal cord EphA4 mutants (using Lbx1-Cre), in addition to ventral midline crossings observed in control spinal cords [100]. Hence, it is compelling to conclude that the dorsal contribution of EphA4 to left-right coordination of locomotion must arise from this subpopulation of interneurons (dI4-6).

However, it is necessary to draw attention to the findings of experiments conducted in the laboratory of Prof. Ole Kiehn, since they are in disagreement with the observations presented here [105]. This study utilized isolated spinal cord preparations from EphA4 knockout mice to test drug-induced fictive locomotion. To determine the dorsal versus ventral contribution of EphA4 to left-right coordination of locomotion, localized lesions were made to sever the dorsal and/or the ventral commissure prior to inducing fictive locomotion. The authors found that a lesion of the ventral commissure alone rescued the synchronous firing pattern, whereas, the synchronous firing pattern was preserved upon the lesion of the dorsal commissure. Hence, they conclude that EphA4 expressed in the dorsal spinal cord is dispensable for left-right coordination of locomotion [105].

This disparity could be explained by the different methods employed in both studies to assess the contribution of dorsally expressed EphA4. So far, fictive locomotion has been elicited successfully in spinal cords isolated from P0-P2 mice [45, 55, 67, 103, 105, 147, 148].

Preparations from older mice have been attempted in the past [149-153], however, eliciting fictive locomotion from these preparations are challenging as they pose problems, such as hypoxia, owing to the increased generation of myelin that hinders adequate oxygenation of the spinal cord [151]. Conversely, the experiments conducted in our study utilized adult intact mice in treadmill locomotion. It is possible that the circuits controlling locomotion undergo 'hard-wired' changes during the development of the animal. If this is true, it is probable that dorsally expressed EphA4 interneurons become functionally mature at a time point later than that investigated using fictive locomotion, thus explaining the difference in results.

How does dorsally expressed EphA4 contribute to left-right coordination of locomotion? Extensive research on the locomotor circuitry of the spinal cord has revealed that alternating movements are orchestrated by the balanced interplay of inhibitory commissural interneurons that promote left-right alternation [154-158], and excitatory commissural interneurons that promote synchrony [46]. Based on the transcription factors they express, five classes of interneurons have been described in the ventral spinal cord [Table 5.01] that participate in left-right coordination of locomotion [38, 44, 46, 142, 144, 145, 155, 156, 159].

Inhibitory	V0D; dI6	Contralateral	Left-right pathway
Excitatory	V2a	Ipsilateral	Speed dependent changes of gait/ project to iCINs
	V0V; V3	Contralateral	Synchrony pathway/Rhythmicity of motor neurons

Table 5.01: Summary of ventral interneuron classes that participate in CPG function [140]

In order to understand how dorsally expressed EphA4 might contribute to left-right coordination of locomotion, it might be beneficial to consider the potential projection of EphA4

positive dorsal interneurons, to each of these classes in isolation, as depicted in the simplified models below:

1. EphA4 positive dorsal interneurons project to iCINs (inhibitory commissural interneurons):

$V0_D$ and dI6 neurons, present in lamina VIII of the ventral spinal cord [58], are two classes of CINs that have been shown to participate in generating left-right limb movements. These neurons project to the contralateral motor neurons and inhibit their function. Together with excitatory commissural interneurons, which promote synchrony of the motor neurons, they lead to alternating limb movements [Figure 5.01 A]. Indeed, ablating the $V0_D$ population using Dbx1 mutants and the dI6 population using Dmrt3 mutants, leads to a loss of inhibition to the motor neurons and results in synchronous limb movements in these mice [Figure 5.01 B] [35, 55].

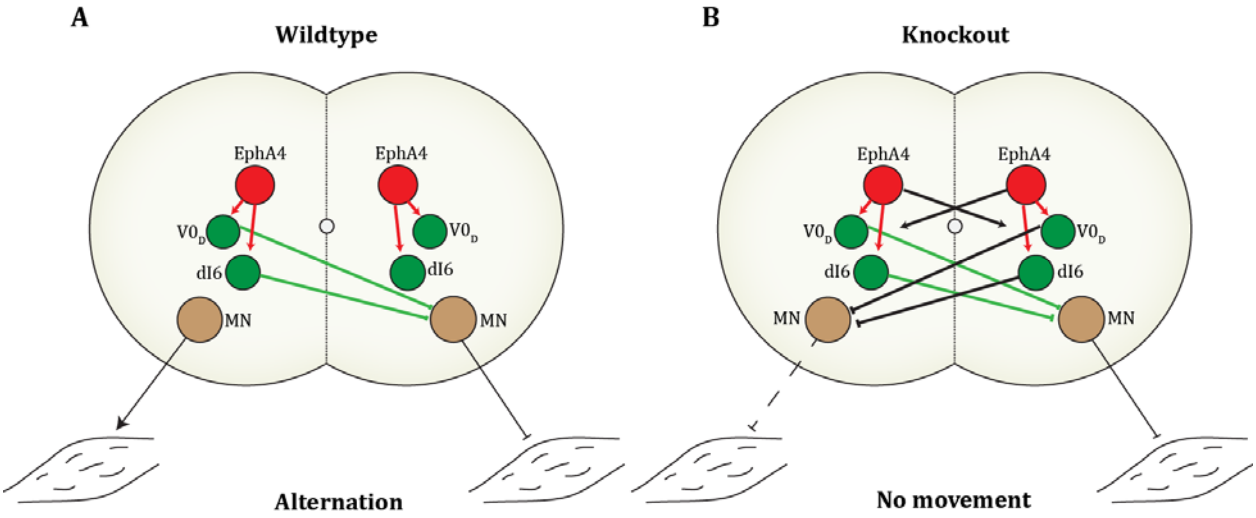

Figure 5.01: Simplified scheme depicting the hypothetical outcome of dorsal EphA4 projections to iCINs in the ventral spinal cord. [A] Ipsilateral projection of dorsally expressed EphA4 to the iCINs ($V0_D$ and dI6) leads to alternation of limbs in wildtype mice. [B] Contralateral misprojection of dorsally expressed EphA4 to iCINs leads to no limb movement rather than hopping in EphA4 knockout mice.

The majority of the EphA4 expressing neurons have been shown to be excitatory in nature [104, 105]. Therefore, if EphA4 positive dorsal interneurons project to iCINs, they would activate them, leading to the inhibition of the contralateral motor neurons, as depicted in Figure 5.01 A. However, abrogating dorsally expressed EphA4 leads to aberrant projections over the midline, resulting in the activation of the iCINs and inhibition of motor neuron function in both halves of the spinal cord simultaneously [Figure 5.01 B]. The increased inhibition would result in no limb movements rather than the synchronous gait that is observed in the EphA4 knockout mice. Additionally, this hypothesis is in contradiction with other studies, which have shown that the hopping phenotype in EphA4 mutants is a result of increased excitation and decreased inhibition of circuits impinging on motor neurons [105]. Hence, the projection of EphA4 positive dorsal interneurons to iCINs is highly unlikely.

2. EphA4 positive dorsal interneurons project to eCINs (excitatory commissural interneurons):

$V0_V$ and V3 interneurons are excitatory commissural interneurons [46, 55]. $V0_V$ interneurons, marked by the transcription factor Evx1, participate in the synchrony pathway of limb movements. However, alternating limb movements are achieved together with iCINs [55, 140]. V3 interneurons, marked by the transcription factor Sim1, are thought to be dispensable for left-right coordination of locomotion, but required for maintaining stable rhythmicity of motor neurons [46].

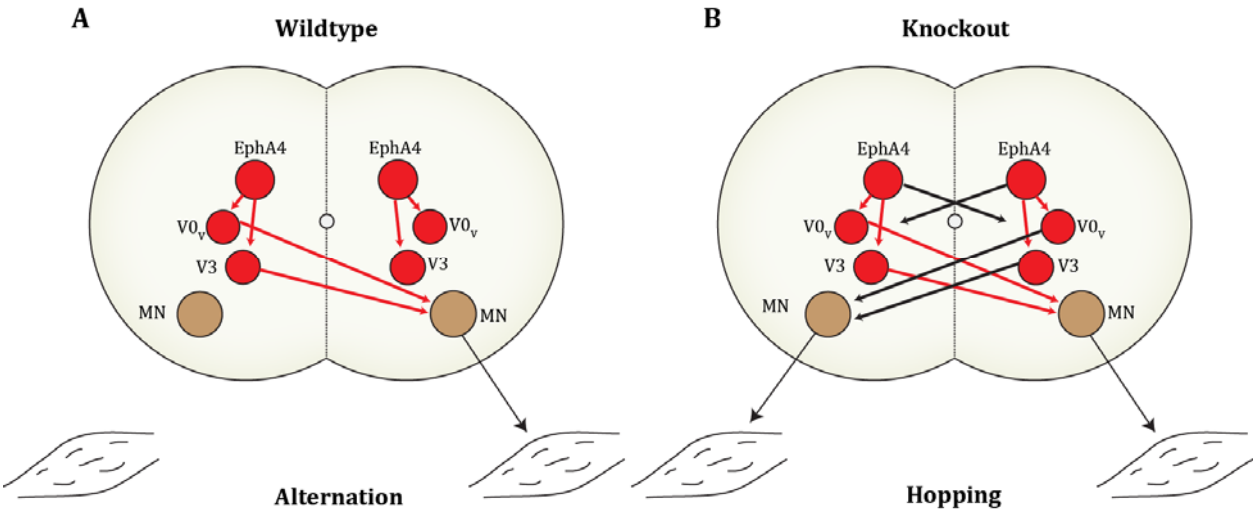

Figure 5.02: Simplified scheme depicting the hypothetical outcome of dorsal EphA4 projections to eCINs in the ventral spinal cord. (A) Ipsilateral projection of dorsally expressed EphA4 to the eCINs ($V0_V$ and V3) leads to alternation of limbs in wildtype mice. (B) Contralateral misprojection of dorsally expressed EphA4 to eCINs leads to hopping in EphA4 knockout mice.

The axonal projections of EphA4 positive excitatory dorsal interneurons impinging upon eCINs could lead to the activation of contralateral motor neurons, and together with functionally active iCINs, produce asynchronous limb movements that are typical of wildtype mice [Figure 5.02 A]. However, the misprojecting axons of dorsal EphA4 mutants could activate eCINs in both halves of the spinal cord leading to strengthening of the synchronous pathway that could override the inhibition of iCINs. Thus, the resultant increased excitatory drive of the synchronous pathway could be the underlying reason for synchronous limb movements observed in these mice. Indeed, previous studies have demonstrated that ablation of EphA4 produces the hopping phenotype as a result of an imbalance between the excitation and inhibition across the midline [Figure 5.02 B][105]. Taken together, it is possible that EphA4 expressing dorsal interneurons project to eCINs and integrate into the synchronous pathway to maintain left-right coordination of locomotion.

3. EphA4 positive dorsal interneurons project to eIINs (excitatory ipsilateral interneurons):

V2a interneurons have been described as an excitatory and ipsilaterally projecting class of ventral spinal cord neurons that are indirectly required for maintaining left-right coordination of locomotion [61, 62]. These interneurons, marked by the transcription factor, Chx10 [45, 61], are known to impinge upon inhibitory commissural V0 interneurons [61].

The potential projection of EphA4 positive dorsal interneurons to V2a interneurons, would activate them, leading to the activation of V0 iCINs. Together with eCINs, they may be able to produce alternating limb movements [Figure 5.03 A]. However, the aberrant midline misprojections in dorsal EphA4 mutants would lead to activation of V0 iCINs and subsequent inhibition of motor neurons, bilaterally, which would result in no limb movements, rather than the hopping gait observed [Figure 5.03 B]. Hence, the projection of dorsally expressed EphA4 to V2a interneurons is unlikely.

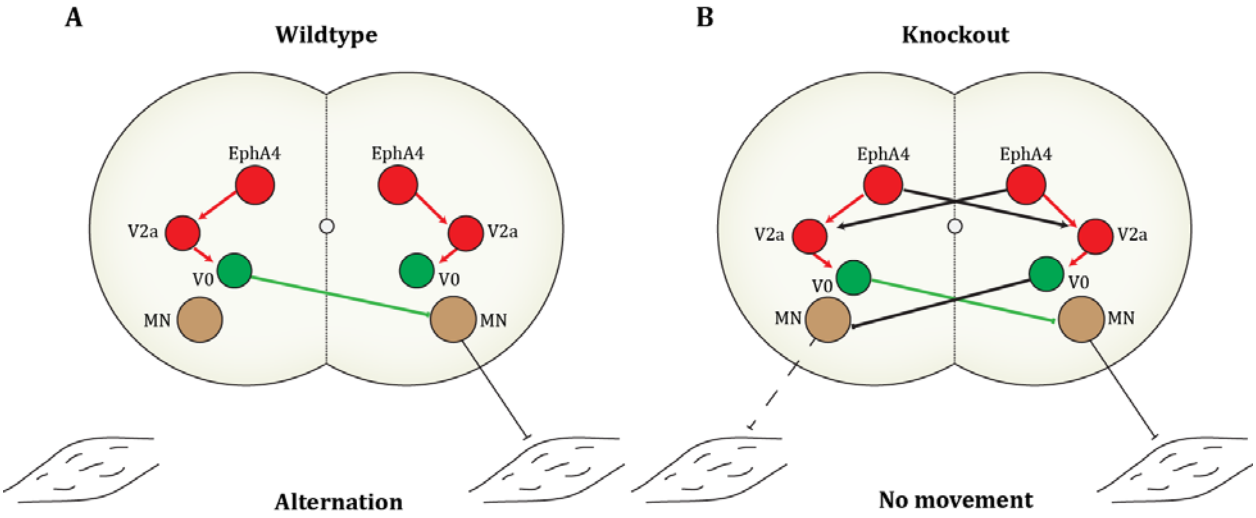

Figure 5.03: Simplified scheme depicting the hypothetical outcome of dorsal EphA4 projections to eIINs in the ventral spinal cord. (A) Ipsilateral projection of dorsally expressed EphA4 to the eIINs (V2a) leads to alternation of limbs in wildtype mice. (B) Contralateral misprojection of dorsally expressed EphA4 to eIINs leads to no limb movement rather than hopping in EphA4 knockout mice.

Furthermore, V2a interneurons are recruited by iCINs and integrate information of speed-dependent changes in gait [45, 60]. Indeed, these interneurons were shown to be required at very high speeds during treadmill locomotion. Ablating these neurons led to limb synchronization during shift in gait, that is, from trotting to galloping at high speeds, but preserved left-right coordination at low speeds [45]. However, dorsal EphA4 mutants do not display any changes in gait with an increase of treadmill speed, thereby, indicating that they do not project to V2a interneurons.

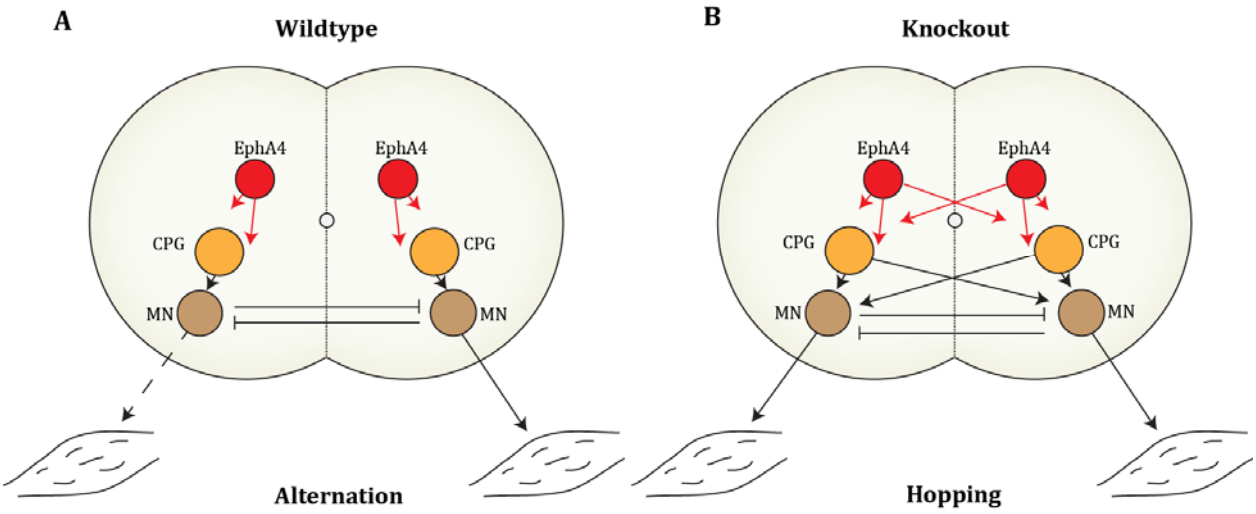

Figure 5.04: Simplified model to depict the projection of dorsal interneurons expressing EphA4 to CPG interneurons in the ventral spinal cord. (A) Ipsilateral projection of dorsally expressed EphA4 to the CPGs leads to alternation of limbs in wildtype mice. (B) Contralateral misprojection of dorsally expressed EphA4 to the CPGs leads to hopping in EphA4 knockout mice.

Taken together, the results presented here implicate dorsally expressed EphA4 in CPG function [Figure 5.04A and B]. The loss of dorsal EphA4 leads to aberrant projections over the midline which may cause bilateral activation of motor circuits and, as a consequence, synchronous limb movements. However, since the loss of dorsal EphA4 produces a partial hopping phenotype, it is possible, that these interneurons impinge on ventral interneurons that

are known to participate in left-right coordination, eCINs being the most likely candidates. Further studies are required to map the connectivity of dorsal interneurons expressing EphA4 to specifically describe their function in locomotory behaviors.

5.2. EphA4-dependent cortical control of voluntary stepping behavior

Stereotypic and repetitive stepping movements are controlled by the spinal interneurons of the CPG network [[140] and references within]. However, supraspinal input from different regions of the brain, such as the motor cortex, brainstem and cerebellum are required to allow the animal to adjust its limb trajectory on demand [160, 161]. The role of the motor cortex and CST have been well studied in generating these movements, and are often termed as adaptive [73], voluntary [160] or goal oriented [72]. They are distinct from those generated by spinal locomotor circuits, as they are neither stereotypic nor repetitive [72]. However, the precise interplay between CPG and CST neurons is essential to allow the animal to respond appropriately to various environmental cues.

The results presented here demonstrate the requirement of EphA4 in generating precise voluntary movements. Wildtype mice subjected to voluntary stepping over obstacles in a treadmill paradigm display alternating limb movements over the hurdles, whereas, EphA4 full knockouts display synchronous movements. We ablated EphA4 specifically in the forebrain (using Emx1-Cre), thereby preserving the spinal cord circuitry, and tested the cortical requirement of EphA4 in voluntary locomotion. We found that these mice present robust bilateral limb movements over the obstacles, while exhibiting alternating movements when subjected to normal treadmill locomotion (that is, in the absence of obstacles). Additionally, CST tracing experiments performed by Dr. S. Paixão provides anatomical evidence to support the

observed voluntary stepping behavior in these mice. Usually, the CST innervates the contralateral half of the spinal cord. As EphA4 is a repulsive guidance cue [75, 86, 100], its interaction with ephrinB3, expressed at the spinal cord midline, promotes repulsion of the incoming CST axons in wildtype mice [70], thus confining them to the contralateral half of the spinal cord. However, forebrain specific and EphA4 full knockouts display aberrant midline projections, thus innervating the spinal cord bilaterally.

Furthermore, experiments conducted in the laboratory of Prof. John Martin [72, 100] provide physiological evidence of a bilateral motor phenotype in these mice. Electrical stimulation of the motor cortex in wildtype mice evoked contralateral forelimb muscle activity, whereas, both contralateral and ipsilateral muscle activity was recorded in forebrain specific EphA4 mutants at the same threshold currents [72, 100]. These results provide strong evidence for the requirement of cortical EphA4 in a cell-autonomous manner in generating voluntary movements.

To our surprise, voluntary stepping experiments using dorsal spinal cord specific EphA4 mutants (with Pax7-Cre), where EphA4 in the CST is spared, also display a similar bilateral response. Additionally, CST tracings demonstrate bilateral innervation of the spinal cord [100] and motor cortex stimulation leads to bilateral muscle activity [100] in these mice. Furthermore, as these mutants also display a shallow DF and display defects in patterning of premotor dorsal interneurons. Therefore, the defect in voluntary stepping could arise due an accumulation of all these phenotypes and hence, it is imperative to conclude that, EphA4 also acts in a non-cell autonomous manner in contributing to voluntary stepping behavior. The rodent CST is known to participate in motor function, indirectly, via projections to premotor spinal interneurons, rather than direct projection to motor neurons [162]. Thus, all together, the voluntary stepping behavior

observed in forebrain and dorsal EphA4 mutants, points to the importance of EphA4/ephrinB3 signaling in guiding the contralateral innervation of the CST and the likelihood of its projections to CPG neurons.

5.3. EphA4-dependent development of the dorsal funiculus and guidance of descending and ascending tracts

The dorsal funiculus (DF) is an area in the spinal cord that is populated by a multitude of ascending and descending tracts that serve to link the brain and spinal cord and establish communication between them [68]. These tracts extend longitudinally and typically traverse long distances along the anterior-posterior axis of the body to reach their final destinations. A classic example of such a tract is the CST, one of the longest axon tracts in the CNS, which arises in the motor cortex, decussates at the level of the hindbrain [68, 96] and innervates the spinal cord at the cervical and lumbar level [96]. A number of short and long-range guidance systems participate in guiding the CST through the brain [68], including EphA4/ephrinB3 signaling, which prevents the recrossing of the CST once it enters the spinal cord [70, 72, 100, 104, 163].

The bilateral CST phenotype observed in the EphA4 mutants, led us to perform further anatomical investigations in the spinal cord. Ablating EphA4 leads to the development of a shallow dorsal funiculus. Indeed, ablating EphA4 in the dorsal spinal cord alone is sufficient to produce this phenotype. Previous studies have implicated the bilateral innervation of the CST to be the underlying cause of the shallow DF [104]. However, examination of spinal cords from forebrain specific EphA4 mutants did not reveal defects in the DF anatomy, thereby proving that the correct development of the DF is intrinsic to the spinal cord rather than due to the innervating

CST axons. Indeed, the defect in the development of the DF arises during embryogenesis itself, that is, before the arrival of the CST in the spinal cord.

Upon closer examination of the developing spinal cord, we found that, EphA4 expressed in cells surrounding the DF are critical in directing the dorsal-ventral extension of the DF. EphA4 full knockouts display a medial shift of dorsal interneurons and aberrant projections of their axons over the midline, along with a shallow DF. Ablating EphA4 only in the dorsal spinal cord, using Lbx1-Cre is sufficient to produce the DF defect [100]. We, therefore, conclude that EphA4, specifically expressed in cells lining the DF, is crucial in preserving the anatomy of the dorsal spinal cord.

A screen performed to identify the EphA4 positive neurons that surround the DF revealed Zic2, a transcription factor, to be abundantly expressed in these neurons. This result is coherent with chromatin immunoprecipitation (ChIP) assays, performed in the laboratory of Dr. Eloisa Herrera, from wildtype spinal cords, demonstrating the binding of Zic2 to the region immediately upstream of the EphA4 transcription start site, and thus regulating its expression [132]. Indeed, the cells that move to the midline, upon EphA4 ablation, are also positive for Zic2. The regulation of EphA4 expression by Zic2 is specific to the cells that surround the DF, since Zic2 positive cells, located close to the central canal are largely devoid of EphA4 and do not shift to the midline in EphA4 knockouts.

What causes the medial shift of EphA4 expressing cells to the midline? The interaction of Eph receptors with its ligands, ephrins, promotes growth cone collapse via modulation of Rho GTPases [164, 165], which are key downstream targets of Ephs and regulators of the cytoskeleton, thus promoting repulsion [102]. To test if EphA4 positive dorsal spinal cord neurons are also repelled by ephrinB3, Dr. S. Paixão performed *in vitro* growth cone collapse

assays using cultures of dissociated dorsal spinal cord neurons from Zic2-GFP transgenic mice [100] and stimulated them with ephrinB3-Fc or Fc alone. Indeed, stimulation with ephrinB3-Fc produced a two-fold increase in growth cone collapse compared to stimulation with Fc alone, indicating that these neurons are repelled by interaction with ephrinB3. Furthermore, spinal cords from mice with impaired downstream EphA4 signaling (using EphA4-GFP mice, where the intracellular domain of EphA4 is replaced with GFP, thus blocking EphA4-mediated forward signaling [106]), and ephrinB3 knockout mice [70], showed a similar shift of EphA4+;Zic2+ cells to the midline and aberrant projections by their axons [100]. Additionally, the position of ephrinB3 positive cells, that reside at the midline, is shifted ventrally, exposing a 'gap' that is devoid of the ephrinB3 expression, in the midline. This 'gap' is occupied by cells that are positive for Zic2 and their aberrantly projecting axons in EphA4 knockout spinal cords.

Moreover, upon close examination of the axonal projections of EphA4 positive cells, we found that they bundle into fascicles and project ipsilaterally into the ventral tip of the DF in wildtype spinal cords. Indeed, longitudinal spinal cord sections from the transgenic reporter line, EphA4-EGFP, demonstrate the rostral turn that axons from EphA4 positive cells make as they enter the DF. Furthermore, the descending CST axons exit the DF via the same area in the DF (ventral tip) and thus enter and innervate the spinal cord [100].

Taken together, these data underline the importance of the interaction of EphA4 with ephrinB3 in the correct development of the dorsal spinal cord. Our hypothesis is that ablation of EphA4 renders the axons of dorsal interneurons incapable of sensing the midline repellent, ephrinB3, and thus leads to aberrant axonal projections across the midline. Furthermore, this causes the cells bodies to shift their position to the midline, thereby, hindering the ventral extension of the DF and producing a shift in the expression of the EphA4 midline repellent,

ephrinB3 [Figure 5.05 A and B]. Since it is known that axons usually explore the surrounding environment and influence the location of the cell body [166, 167], this hypothesis is highly plausible, however, further experimentation, using live-cell imaging is required to confirm its validity.

The axons of EphA4 positive cells usually form ascending ipsilateral projections into the DF. The ipsilaterality of these axons is maintained by EphA4/ephrinB3 signaling. Similarly, the descending CST axons also utilize EphA4/ephrinB3 signaling to prevent them from recrossing at the level of the spinal cord. The fact that both the ascending and descending tracts utilize the same signaling pathway to confine their axons to the appropriate side of the spinal cord indicates that the ascending tract may serve as pioneering axons that the descending tracts use to enter the spinal cord. It may also be possible that the axons of the two tracts interact; however, investigating this requires the identification of distinct markers belonging to these tracts and the development of tools that would aid in the visualization of these tracts.

Although we provide evidence that the axonal projections of EphA4+Zic2+ cells form ascending ipsilateral tracts, we are far from understanding their nature and function. A number of studies have revealed the existence of ipsilateral ascending tracts that arise in the spinal cord [68]. The dorsal spinal gray matter can be divided into 7 distinct laminae that convey somatosensory information from the spinal cord to higher brain centers [168]. The dorsal spinal cord predominantly receives sensory information from the dorsal root ganglia (DRG). Sensory projections enter the spinal cord by extending their axons to the dorsal root entry zone (DREZ) and innervate the dorsal spinal cord at various locations of the dorsal horn [169]. Upon entry into the spinal cord, they project extensively to spinal interneurons in different laminae, which then

form ascending projections that relay information related to different modalities such as touch, proprioception, pain and temperature to appropriate brain regions [170-175]

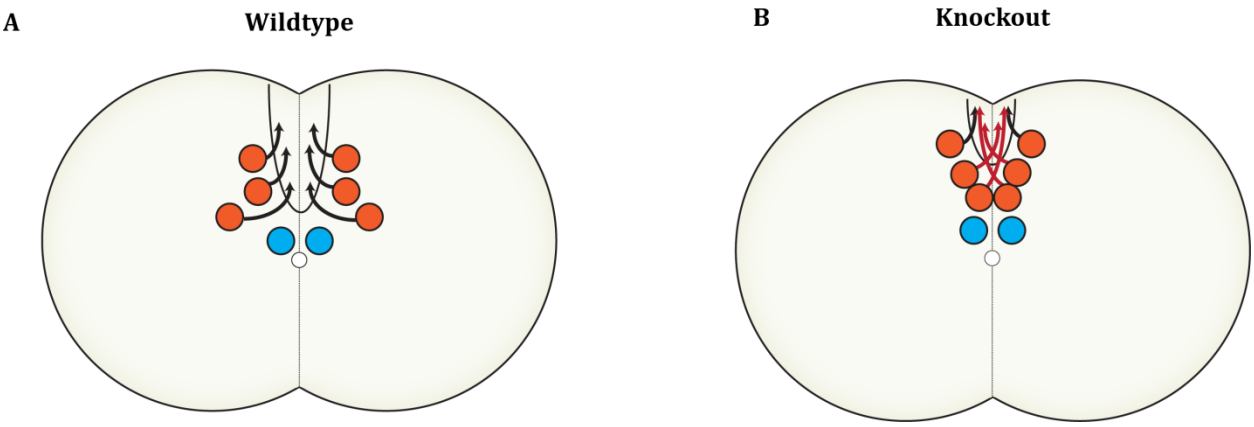

Figure 5.05: Simplified model to depict the formation of the DF and guidance of ascending tracts in the dorsal spinal cord. (A) Wildtype: The DF extends almost until the central canal. EphA4+Zic2+ cells (orange) surround the DF and are bisected by the midline. The projections of these cells ascend and enter the DF via an ipsilateral corridor (black). Zic2+ cells close to the central canal (blue) are devoid of EphA4 and are bisected by the midline. (B) EphA4 knockout: The DF is shallow. Absence of EphA4 causes these cells (orange) to move to the midline. The projections of these cells ascend and enter the DF contralaterally due to aberrant crossing of the midline (red). Zic2+ cells close to the central canal (blue) are devoid of EphA4 and are bisected by the midline.

5.4. Functions of EphA4+Zic2+cells

Information on touch and proprioception is transmitted to the brain via ipsilaterally projecting tracts of the dorsal column-lemniscal pathway. They project to the gracile and cuneate nuclei of the medulla, after which they decussate and finally target the thalamus [172]. Neurons transmitting information on touch typically terminate in laminae III and IV or the dorsal horn, whereas, those mediating proprioception terminate in lamina VII which forms the Clarke's column [176]. These projections show an extensive overlap with those of EphA4+Zic2+ neurons. However, since the projections of the Clarke's column form ipsilateral ascending tracts

via the dorsolateral funiculus [68], they are distinct from the EphA4+Zic2+ population described here.

Noxious information, such as pain and temperature, are thought to be transmitted to the thalamus via the anterolateral pathway which essentially ascends contralaterally [177, 178]. Another pathway, the postsynaptic dorsal column (PSDC), consists of a heterogeneous population of neurons that relay information on touch and pain. This tract is poorly characterized in comparison to the other ascending pathways mediating somatosensory information [179-181]; however, a recent study has shown that some projections of the PSDC pathway terminate in the gracile and cuneate nuclei of the medulla [182]. Furthermore, this tract ascends ipsilaterally in the ventral DF and shows a great degree of overlap with the Zic2+EphA4+ population we describe.

To further characterize the EphA4+Zic2+ cells, we performed immunofluorescence stainings in collaboration with Dr. Sonia Paixão and Dr. Wenqin Luo. Staining with the vesicular glutamate transporter, VGlut1, a synaptic marker of sensory axons, showed great colocalization with EphA4+Zic2+ cells. Markers of proprioceptive and nociceptive axons (stained with antibodies against parvalbumin and CGRP) did not colocalize with Zic2 positive cells. The innervation by low-threshold mechanosensory afferents was tested using the Ret-Cre mice crossed to the Tomato-reporter line and further co-stained with VGlut1 and Zic2. The majority of the Zic2+ cells were found to be positive for VGlut1 and Ret, indicating that the EphA4+Zic2+ cells receive mechanosensory input [183, 184]. Therefore, it is likely that this population is involved in mediating tactile information.

We also investigated the innervation of the spinal cord by nociceptive afferents, using the marker, CGRP [136, 137]. We found that in wildtype spinal cords, these axons innervate the

spinal cord via the dorsal horn and remain mainly ipsilateral. However, spinal cords from EphA4 knockout spinal cords reveal an interesting phenotype as they show extensive midline misprojections [Figure 5.06 A and B]. Initially, this led us to conclude that the lack of EphA4 in these neurons, results in impaired EphA4/ephrinB3 forward signaling due to the absence of ephrinB3 in the midline 'gap.' If this was true, then ephrinB3 knockout spinal cords must display similar midline misprojections of nociceptive axons. Much to our surprise, we found that the nociceptive projections in ephrinB3 knockout spinal cords remained ipsilateral and did not show extensive midline misprojections. Therefore, it is imperative to conclude that other signaling mechanisms may participate in guiding nociceptive axons. Indeed, it is now known that EphA4 expression is absent in DRG neurons [185]. However, since spinal cord derived EphA4 is necessary in guiding nociceptive axons, it may be possible that other ephrin ligands interact with EphA4 and EphA4/ephrin reverse signaling is required for the proper guidance of these neurons. It may also be possible that EphA4, expressed on spinal interneurons, acts non-cell autonomously in guiding nociceptive axons correctly. Indeed, it has been demonstrated that sensory axons expressing ephrinAs interact with EphA3/4 expressed on motor neurons and track alongside motor projections to reach their final targets [186]. Since the nociceptive axon misprojections and spinal interneuron misprojections occur around the same time (E14.5 spinal cords) in EphA4 knockout spinal cords, new tools are required to allow the visualization of these projections in real time.

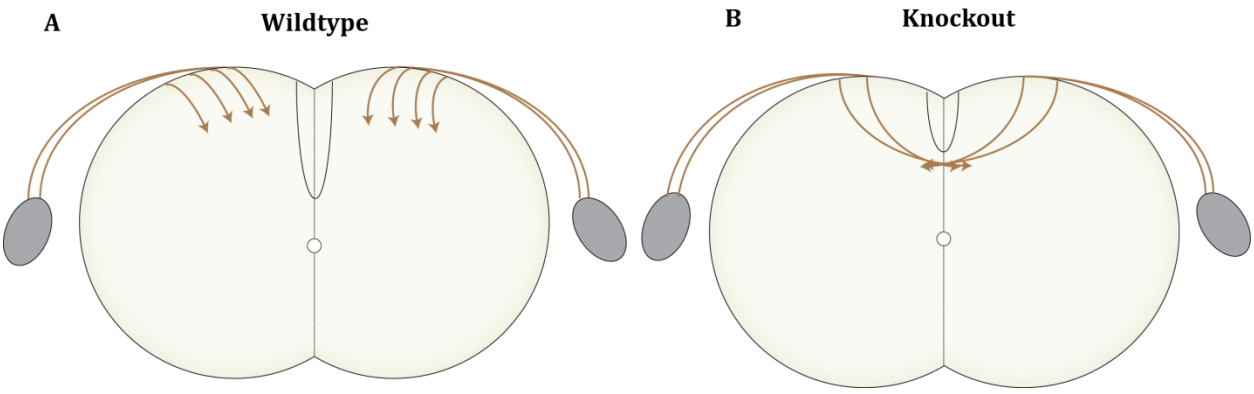

Figure 5.06: Simplified model to depict the guidance of sensory afferents in the dorsal spinal cord. (A) Wildtype: CGRP+ axons enter the spinal cord via the dorsal horn and remain ipsilateral. (B) EphA4 knockout: CGRP+ axons display aberrant midline misprojections in the absence of EphA4.

5.5. Concluding remarks

The results presented in this thesis delineate novel roles for EphA4 in defining circuits involved in locomotion advance our understanding of the principles of ascending and descending tract guidance. This study demonstrates the requirement of EphA4/ephrinB3 signaling in maintaining spinal circuits that control left-right coordination of locomotion and bring to light the contribution of a previously unknown population of dorsal interneurons in preserving these circuits. Furthermore, it also highlights the importance of the same signaling pathway in more complex behaviors that require input from higher brain centers. Furthermore, EphA4/ephrinB3 signaling is required to guide ipsilateral ascending projections into the DF and these projections serve as guideposts for descending CST tracts. Disruption of EphA4/ephrinB3 signaling leads to behavioral consequences such as in voluntary stepping and stereotyped and repetitive locomotion. Additionally, ablating this pathway also amounts to morphological defects in the development of the DF and guidance of ipsilateral axon tracts along with indirect secondary guidance defects of nociceptive axon projections.

Our advancement in understanding the underlying neural circuitry of the dorsal spinal cord leaves us with many unanswered and interesting questions, some of which are mentioned here:

- What are the downstream targets of the CST projections? Do they project to spinal interneurons of the dorsal cord; perhaps EphA4+Zic2+ population?
- Where do the dorsal interneurons that participate in left-right coordination of locomotion project to; perhaps CPG neurons or motor neurons?
- What is the rostral extent of the ipsilateral ascending EphA4+Zic2+ axonal projections?

Answering these questions by additional characterization of the circuits investigated in this study, using a plethora of new emerging tools, will improve our understanding of the spinal cord circuitry in the future.

6. References

1. Chitnis, A.B., Control of neurogenesis--lessons from frogs, fish and flies. Curr Opin Neurobiol, 1999. 9(1): p. 18-25.
2. Lewis, J., Neurogenic genes and vertebrate neurogenesis. Curr Opin Neurobiol, 1996. 6(1): p. 3-10.
3. Godsave, S.F. and J.M. Slack, Clonal analysis of mesoderm induction in Xenopus laevis. Dev Biol, 1989. 134(2): p. 486-90.
4. Grunz, H. and L. Tacke, Neural differentiation of Xenopus laevis ectoderm takes place after disaggregation and delayed reaggregation without inducer. Cell Differ Dev, 1989. 28(3): p. 211-7.
5. Sato, S.M. and T.D. Sargent, Development of neural inducing capacity in dissociated Xenopus embryos. Dev Biol, 1989. 134(1): p. 263-6.
6. Bier, E., Anti-neural-inhibition: a conserved mechanism for neural induction. Cell, 1997. 89(5): p. 681-4.
7. Cox, W.G. and A. Hemmati-Brivanlou, Caudalization of neural fate by tissue recombination and bFGF. Development, 1995. 121(12): p. 4349-58.
8. Dessaud, E., A.P. McMahon, and J. Briscoe, Pattern formation in the vertebrate neural tube: a sonic hedgehog morphogen-regulated transcriptional network. Development, 2008. 135(15): p. 2489-503.
9. Hemmati-Brivanlou, A., O.G. Kelly, and D.A. Melton, Follistatin, an antagonist of activin, is expressed in the Spemann organizer and displays direct neuralizing activity. Cell, 1994. 77(2): p. 283-95.

10. Lamb, T.M., et al., Neural induction by the secreted polypeptide noggin. Science, 1993. 262(5134): p. 713-8.

11. Sasai, Y., et al., Xenopus chordin: a novel dorsalizing factor activated by organizer-specific homeobox genes. Cell, 1994. 79(5): p. 779-90.

12. Wilson, S.W. and C. Houart, Early steps in the development of the forebrain. Dev Cell, 2004. 6(2): p. 167-81.

13. Pombero, A. and S. Martinez, Telencephalic morphogenesis during the process of neurulation: an experimental study using quail-chick chimeras. J Comp Neurol, 2009. 512(6): p. 784-97.

14. Rubenstein, J.L., et al., Regionalization of the prosencephalic neural plate. Annu Rev Neurosci, 1998. 21: p. 445-77.

15. McGrew, L.L., C.J. Lai, and R.T. Moon, Specification of the anteroposterior neural axis through synergistic interaction of the Wnt signaling cascade with noggin and follistatin. Dev Biol, 1995. 172(1): p. 337-42.

16. Sharpe, C.R., Retinoic Acid Can Mimic Endogenous Signals Involved in Transformation of the Xenopus Nervous-System. Neuron, 1991. 7(2): p. 239-247.

17. Lamb, T.M. and R.M. Harland, Fibroblast Growth-Factor Is a Direct Neural Inducer, Which Combined with Noggin Generates Anterior-Posterior Neural Pattern. Development, 1995. 121(11): p. 3627-3636.

18. Diez del Corral, R. and K.G. Storey, Opposing FGF and retinoid pathways: a signalling switch that controls differentiation and patterning onset in the extending vertebrate body axis. Bioessays, 2004. 26(8): p. 857-869.

19. Chizhikov, V.V. and K.J. Millen, Control of roof plate formation by Lmx1a in the developing spinal cord. Development, 2004. 131(11): p. 2693-705.

20. Millonig, J.H., K.J. Millen, and M.E. Hatten, The mouse Dreher gene Lmx1a controls formation of the roof plate in the vertebrate CNS. Nature, 2000. 403(6771): p. 764-9.

21. Le Dreau, G. and E. Marti, Dorsal-ventral patterning of the neural tube: a tale of three signals. Dev Neurobiol, 2012. 72(12): p. 1471-81.

22. Echelard, Y., et al., Sonic-Hedgehog, a Member of a Family of Putative Signaling Molecules, Is Implicated in the Regulation of Cns Polarity. Cell, 1993. 75(7): p. 1417-1430.

23. Muller, T., et al., The homeodomain factor lbx1 distinguishes two major programs of neuronal differentiation in the dorsal spinal cord. Neuron, 2002. 34(4): p. 551-62.

24. Gross, M.K., M. Dottori, and M. Goulding, Lbx1 specifies somatosensory association interneurons in the dorsal spinal cord. Neuron, 2002. 34(4): p. 535-49.

25. Lee, K.J., P. Dietrich, and T.M. Jessell, Genetic ablation reveals that the roof plate is essential for dorsal interneuron specification. Nature, 2000. 403(6771): p. 734-740.

26. Muller, T., et al., The bHLH factor Olig3 coordinates the specification of dorsal neurons in the spinal cord. Genes Dev, 2005. 19(6): p. 733-43.

27. Wildner, H., et al., dILA neurons in the dorsal spinal cord are the product of terminal and non-terminal asymmetric progenitor cell divisions, and require Mash1 for their development. Development, 2006. 133(11): p. 2105-2113.

28. Bermingham, N.A., et al., Proprioceptor pathway development is dependent on MATH1. Neuron, 2001. 30(2): p. 411-422.

29. Ding, Q., et al., BARHL2 transcription factor regulates the ipsilateral/contralateral subtype divergence in postmitotic dI1 neurons of the developing spinal cord. Proc Natl Acad Sci U S A, 2012. 109(5): p. 1566-1571.

30. Avraham, O., et al., Transcriptional control of axonal guidance and sorting in dorsal interneurons by the Lim-HD proteins Lhx9 and Lhx1. Neural Dev, 2009. 4.

31. Alaynick, W.A., T.M. Jessell, and S.L. Pfaff, SnapShot: spinal cord development. Cell, 2011. 146(1): p. 178-178 e1.

32. Bui, T.V., et al., Circuits for Grasping: Spinal dI3 Interneurons Mediate Cutaneous Control of Motor Behavior. Neuron, 2013. 78(1): p. 191-204.

33. Glasgow, S.M., et al., Ptf1a determines GABAergic over glutamatergic neuronal cell fate in the spinal cord dorsal horn. Development, 2005. 132(24): p. 5461-9.

34. Ding, Y.Q., et al., Lmx1b controls the differentiation and migration of the superficial dorsal horn neurons of the spinal cord. Development, 2004. 131(15): p. 3693-3703.

35. Andersson, L.S., et al., Mutations in DMRT3 affect locomotion in horses and spinal circuit function in mice. Nature, 2012. 488(7413): p. 642-6.

36. Dyck, J., G.M. Lanuza, and S. Gosgnach, Functional characterization of dI6 interneurons in the neonatal mouse spinal cord. J Neurophysiol, 2012. 107(12): p. 3256-3266.

37. Caspary, T. and K.V. Anderson, Patterning cell types in the dorsal spinal cord: What the mouse mutants say. Nature Reviews Neuroscience, 2003. 4(4): p. 289-297.

38. Pierani, A., et al., Control of interneuron fate in the developing spinal cord by the progenitor homeodomain protein Dbx1. Neuron, 2001. 29(2): p. 367-84.

39. Zagoraiou, L., et al., A Cluster of Cholinergic Premotor Interneurons Modulates Mouse Locomotor Activity. Neuron, 2009. 64(5): p. 645-662.

40. Gosgnach, S., The Role of Genetically-Defined Interneurons in Generating the Mammalian Locomotor Rhythm. Integr Comp Biol, 2011. 51(6): p. 903-912.

41. Zhang, J.M., et al., V1 and V2b Interneurons Secure the Alternating Flexor-Extensor Motor Activity Mice Require for Limbed Locomotion. Neuron, 2014. 82(1): p. 138-150.

42. Alvarez, F.J., et al., Postnatal phenotype and localization of spinal cord V1 derived interneurons. Journal of Comparative Neurology, 2005. 493(2): p. 177-192.

43. Gosgnach, S., et al., V1 spinal neurons regulate the speed of vertebrate locomotor outputs. Nature, 2006. 440(7081): p. 215-9.

44. Lundfald, L., et al., Phenotype of V2-derived interneurons and their relationship to the axon guidance molecule EphA4 in the developing mouse spinal cord. Eur J Neurosci, 2007. 26(11): p. 2989-3002.

45. Crone, S.A., et al., In mice lacking V2a interneurons, gait depends on speed of locomotion. J Neurosci, 2009. 29(21): p. 7098-109.

46. Zhang, Y., et al., V3 spinal neurons establish a robust and balanced locomotor rhythm during walking. Neuron, 2008. 60(1): p. 84-96.

47. Grillner, S., et al., Neural bases of goal-directed locomotion in vertebrates--an overview. Brain Res Rev, 2008. 57(1): p. 2-12.

48. Grillner, S. and P. Zangger, On the central generation of locomotion in the low spinal cat. Exp Brain Res, 1979. 34(2): p. 241-61.

49. Kiehn, O., Locomotor circuits in the mammalian spinal cord. Annu Rev Neurosci, 2006. 29: p. 279-306.

50. Kudo, N. and T. Yamada, N-methyl-D,L-aspartate-induced locomotor activity in a spinal cord-hindlimb muscles preparation of the newborn rat studied in vitro. Neurosci Lett, 1987. 75(1): p. 43-8.

51. Smith, J.C. and J.L. Feldman, In vitro brainstem-spinal cord preparations for study of motor systems for mammalian respiration and locomotion. J Neurosci Methods, 1987. 21(2-4): p. 321-33.

52. Cowley, K.C. and B.J. Schmidt, A comparison of motor patterns induced by N-methyl-D-aspartate, acetylcholine and serotonin in the in vitro neonatal rat spinal cord. Neurosci Lett, 1994. 171(1-2): p. 147-50.

53. Kiehn, O. and O. Kjaerulff, Spatiotemporal characteristics of 5-HT and dopamine-induced rhythmic hindlimb activity in the in vitro neonatal rat. J Neurophysiol, 1996. 75(4): p. 1472-82.

54. Nishimaru, H., C.E. Restrepo, and O. Kiehn, Activity of Renshaw cells during locomotor-like rhythmic activity in the isolated spinal cord of neonatal mice. J Neurosci, 2006. 26(20): p. 5320-8.

55. Talpalar, A.E., et al., Dual-mode operation of neuronal networks involved in left-right alternation. Nature, 2013. 500(7460): p. 85-8.

56. Quinlan, K.A. and O. Kiehn, Segmental, synaptic actions of commissural interneurons in the mouse spinal cord. J Neurosci, 2007. 27(24): p. 6521-30.

57. Restrepo, C.E., et al., Transmitter-phenotypes of commissural interneurons in the lumbar spinal cord of newborn mice. J Comp Neurol, 2009. 517(2): p. 177-92.

58. Lanuza, G.M., et al., Genetic identification of spinal interneurons that coordinate left-right locomotor activity necessary for walking movements. Neuron, 2004. 42(3): p. 375-86.

59. Kiehn, O., et al., Probing spinal circuits controlling walking in mammals. Biochem Biophys Res Commun, 2010. 396(1): p. 11-8.

60. Zhong, G., K. Sharma, and R.M. Harris-Warrick, Frequency-dependent recruitment of V2a interneurons during fictive locomotion in the mouse spinal cord. Nat Commun, 2011. 2: p. 274.

61. Crone, S.A., et al., Genetic ablation of V2a ipsilateral interneurons disrupts left-right locomotor coordination in mammalian spinal cord. Neuron, 2008. 60(1): p. 70-83.

62. Zhong, G., et al., Electrophysiological characterization of V2a interneurons and their locomotor-related activity in the neonatal mouse spinal cord. J Neurosci, 2010. 30(1): p. 170-82.

63. Brownstone, R.M. and J.M. Wilson, Strategies for delineating spinal locomotor rhythm-generating networks and the possible role of Hb9 interneurones in rhythmogenesis. Brain Res Rev, 2008. 57(1): p. 64-76.

64. Hinckley, C.A., et al., Locomotor-like rhythms in a genetically distinct cluster of interneurons in the mammalian spinal cord. J Neurophysiol, 2005. 93(3): p. 1439-49.

65. Wilson, J.M., et al., Conditional rhythmicity of ventral spinal interneurons defined by expression of the Hb9 homeodomain protein. J Neurosci, 2005. 25(24): p. 5710-9.

66. Kwan, A.C., et al., Activity of Hb9 interneurons during fictive locomotion in mouse spinal cord. J Neurosci, 2009. 29(37): p. 11601-13.

67. Dougherty, K.J., et al., Locomotor rhythm generation linked to the output of spinal shox2 excitatory interneurons. Neuron, 2013. 80(4): p. 920-33.

68. Sakai, N. and Z. Kaprielian, Guidance of longitudinally projecting axons in the developing central nervous system. Front Mol Neurosci, 2012. 5: p. 59.

69. Harel, N.Y. and S.M. Strittmatter, Can regenerating axons recapitulate developmental guidance during recovery from spinal cord injury? Nature Reviews Neuroscience, 2006. 7(8): p. 603-616.

70. Kullander, K., et al., Ephrin-B3 is the midline barrier that prevents corticospinal tract axons from recrossing, allowing for unilateral motor control. Genes Dev, 2001. 15(7): p. 877-88.

71. Drew, T., Motor Cortical Cell Discharge during Voluntary Gait Modification. Brain Res, 1988. 457(1): p. 181-187.

72. Serradj, N., et al., EphA4-Mediated Ipsilateral Corticospinal Tract Misprojections Are Necessary for Bilateral Voluntary Movements But Not Bilateral Stereotypic Locomotion. J Neurosci, 2014. 34(15): p. 5211-21.

73. Asante, C.O., et al., Cortical control of adaptive locomotion in wild-type mice and mutant mice lacking the ephrin-Eph effector protein alpha2-chimaerin. J Neurophysiol, 2010. 104(6): p. 3189-202.

74. Egea, J. and R. Klein, Bidirectional Eph-ephrin signaling during axon guidance. Trends Cell Biol, 2007. 17(5): p. 230-8.

75. Kullander, K. and R. Klein, Mechanisms and functions of Eph and ephrin signalling. Nat Rev Mol Cell Biol, 2002. 3(7): p. 475-86.

76. Himanen, J.P., et al., Repelling class discrimination: ephrin-A5 binds to and activates EphB2 receptor signaling. Nat Neurosci, 2004. 7(5): p. 501-9.

77. Qin, H., et al., Structural characterization of the EphA4-Ephrin-B2 complex reveals new features enabling Eph-ephrin binding promiscuity. J Biol Chem, 2010. 285(1): p. 644-54.

78. Davis, S., et al., Ligands for Eph-Related Receptor Tyrosine Kinases That Require Membrane Attachment or Clustering for Activity. Science, 1994. 266(5186): p. 816-819.

79. Stein, E., et al., Eph receptors discriminate specific ligand oligomers to determine alternative signaling complexes, attachment, and assembly responses. Genes Dev, 1998. 12(5): p. 667-78.

80. Binns, K.L., et al., Phosphorylation of tyrosine residues in the kinase domain and juxtamembrane region regulates the biological and catalytic activities of Eph receptors. Mol Cell Biol, 2000. 20(13): p. 4791-805.

81. Heasman, S.J. and A.J. Ridley, Mammalian Rho GTPases: new insights into their functions from in vivo studies. Nature Reviews Molecular Cell Biology, 2008. 9(9): p. 690-701.

82. Murai, K.K. and E.B. Pasquale, 'Eph'ective signaling: forward, reverse and crosstalk. J Cell Sci, 2003. 116(Pt 14): p. 2823-32.

83. Shamah, S.M., et al., EphA receptors regulate growth cone dynamics through the novel guanine nucleotide exchange factor ephexin. Cell, 2001. 105(2): p. 233-244.

84. Cowan, C.W., et al., Vav family GEFs link activated Ephs to endocytosis and axon guidance. Neuron, 2005. 46(2): p. 205-17.

85. Hunter, S.G., et al., Essential role of Vav family guanine nucleotide exchange factors in EphA receptor-mediated angiogenesis. Mol Cell Biol, 2006. 26(13): p. 4830-42.

86. Wegmeyer, H., et al., EphA4-dependent axon guidance is mediated by the RacGAP alpha2-chimaerin. Neuron, 2007. 55(5): p. 756-67.

87. Fawcett, J.P., et al., Nck adaptor proteins control the organization of neuronal circuits important for walking. Proc Natl Acad Sci U S A, 2007. 104(52): p. 20973-8.

88. Lim, Y.S., et al., p75(NTR) mediates ephrin-A reverse signaling required for axon repulsion and mapping. Neuron, 2008. 59(5): p. 746-58.

89. Marler, K.J., et al., A TrkB/EphrinA interaction controls retinal axon branching and synaptogenesis. J Neurosci, 2008. 28(48): p. 12700-12.

90. Palmer, A., et al., EphrinB phosphorylation and reverse signaling: regulation by Src kinases and PTP-BL phosphatase. Mol Cell, 2002. 9(4): p. 725-37.

91. Xu, N.J. and M. Henkemeyer, Ephrin-B3 reverse signaling through Grb4 and cytoskeletal regulators mediates axon pruning. Nat Neurosci, 2009. 12(3): p. 268-276.

92. Cowan, C.A. and M. Henkemeyer, The SH2/SH3 adaptor Grb4 transduces B-ephrin reverse signals. Nature, 2001. 413(6852): p. 174-9.

93. Segura, I., et al., Grb4 and GIT1 transduce ephrinB reverse signals modulating spine morphogenesis and synapse formation. Nat Neurosci, 2007. 10(3): p. 301-10.

94. Bruckner, K., et al., EphrinB ligands recruit GRIP family PDZ adaptor proteins into raft membrane microdomains. Neuron, 1999. 22(3): p. 511-524.

95. Lu, Q., et al., Ephrin-B reverse signaling is mediated by a novel PDZ-RGS protein and selectively inhibits G protein-coupled chemoattraction. Cell, 2001. 105(1): p. 69-79.

96. Stanfield, B.B., The development of the corticospinal projection. Prog Neurobiol, 1992. 38(2): p. 169-202.

97. Kullander, K., et al., Kinase-dependent and kinase-independent functions of EphA4 receptors in major axon tract formation in vivo. Neuron, 2001. 29(1): p. 73-84.

98. Egea, J., et al., Regulation of EphA4 kinase activity is required for a subset of axon guidance decisions suggesting a key role for receptor clustering in Eph function. Neuron, 2005. 47(4): p. 515-528.

99. Yokoyama, N., et al., Forward signaling mediated by ephrin-B3 prevents contralateral corticospinal axons from recrossing the spinal cord midline. Neuron, 2001. 29(1): p. 85-97.

100. Paixao, S., et al., EphrinB3/EphA4-mediated guidance of ascending and descending spinal tracts. Neuron, 2013. 80(6): p. 1407-20.

101. Beg, A.A., et al., alpha 2-chimaerin is an essential EphA4 effector in the assembly of neuronal locomotor circuits. Neuron, 2007. 55(5): p. 768-778.

102. Mulherkar, S., et al., The small GTPase RhoA is required for proper locomotor circuit assembly. PLoS One, 2013. 8(6): p. e67015.

103. Borgius, L., et al., Spinal Glutamatergic Neurons Defined by EphA4 Signaling Are Essential Components of Normal Locomotor Circuits. J Neurosci, 2014. 34(11): p. 3841-53.

104. Kullander, K., et al., Role of EphA4 and EphrinB3 in local neuronal circuits that control walking. Science, 2003. 299(5614): p. 1889-92.

105. Restrepo, C.E., et al., Change in the balance of excitatory and inhibitory midline fiber crossing as an explanation for the hopping phenotype in EphA4 knockout mice. Eur J Neurosci, 2011. 34(7): p. 1102-12.

106. Grunwald, I.C., et al., Hippocampal plasticity requires postsynaptic ephrinBs. Nat Neurosci, 2004. 7(1): p. 33-40.

107. Leighton, P.A., et al., Defining brain wiring patterns and mechanisms through gene trapping in mice. Nature, 2001. 410(6825): p. 174-9.

108. Herrmann, J.E., et al., Generation of an EphA4 conditional allele in mice. Genesis, 2010. 48(2): p. 101-5.

109. Lallemand, Y., et al., Maternally expressed PGK-Cre transgene as a tool for early and uniform activation of the Cre site-specific recombinase. Transgenic Res, 1998. 7(2): p. 105-12.

110. Gorski, J.A., et al., Cortical excitatory neurons and glia, but not GABAergic neurons, are produced in the Emx1-expressing lineage. J Neurosci, 2002. 22(15): p. 6309-14.

111. Arenkiel, B.R., et al., Hoxb1 functions in both motoneurons and in tissues of the periphery to establish and maintain the proper neuronal circuitry. Genes Dev, 2004. 18(13): p. 1539-52.

112. Keller, C., et al., Pax3:Fkhr interferes with embryonic Pax3 and Pax7 function: implications for alveolar rhabdomyosarcoma cell of origin. Genes Dev, 2004. 18(21): p. 2608-13.

113. Sieber, M.A., et al., Lbx1 acts as a selector gene in the fate determination of somatosensory and viscerosensory relay neurons in the hindbrain. J Neurosci, 2007. 27(18): p. 4902-9.

114. Brault, V., et al., Inactivation of the beta-catenin gene by Wnt1-Cre-mediated deletion results in dramatic brain malformation and failure of craniofacial development. Development, 2001. 128(8): p. 1253-64.

115. Kawaguchi, Y., et al., The role of the transcriptional regulator Ptf1a in converting intestinal to pancreatic progenitors. Nat Genet, 2002. 32(1): p. 128-34.

116. Soriano, P., Generalized lacZ expression with the ROSA26 Cre reporter strain. Nat Genet, 1999. 21(1): p. 70-1.

117. Madisen, L., et al., A toolbox of Cre-dependent optogenetic transgenic mice for light-induced activation and silencing. Nat Neurosci, 2012. 15(5): p. 793-802.

118. Mansouri, A., et al., Dysgenesis of cephalic neural crest derivatives in Pax7-/- mutant mice. Development, 1996. 122(3): p. 831-8.

119. Huang, X., Y. Litingtung, and C. Chiang, Region-specific requirement for cholesterol modification of sonic hedgehog in patterning the telencephalon and spinal cord. Development, 2007. 134(11): p. 2095-105.

120. Kruger, M., K. Schafer, and T. Braun, The homeobox containing gene Lbx1 is required for correct dorsal-ventral patterning of the neural tube. J Neurochem, 2002. 82(4): p. 774-82.

121. Matise, M., A dorsal elaboration in the spinal cord. Neuron, 2002. 34(4): p. 491-3.

122. Pyott, S.M., et al., WNT1 mutations in families affected by moderately severe and progressive recessive osteogenesis imperfecta. Am J Hum Genet, 2013. 92(4): p. 590-7.

123. Alexandre, C., A. Baena-Lopez, and J.P. Vincent, Patterning and growth control by membrane-tethered Wingless. Nature, 2014. 505(7482): p. 180-5.

124. Galli, L.M., et al., Frizzled10 mediates WNT1 and WNT3a signaling in the dorsal spinal cord of the developing chick embryo. Dev Dyn, 2014.

125. Dai, X., et al., Localization of spinal neurons activated during locomotion using the c-fos immunohistochemical method. J Neurophysiol, 2005. 93(6): p. 3442-52.

126. Blaszczyk, J.W. and C. Dobrzecka, Speed control in quadrupedal locomotion: principles of limb coordination in the dog. Acta Neurobiol Exp (Wars), 1989. 49(2-3): p. 105-24.

127. Schmidt, M., Quadrupedal locomotion in squirrel monkeys (Cebidae: Saimiri sciureus): a cineradiographic study of limb kinematics and related substrate reaction forces. Am J Phys Anthropol, 2005. 128(2): p. 359-70.

128. Maes, L. and A. Abourachid, Gait transitions and modular organization of mammal locomotion. J Exp Biol, 2013. 216(Pt 12): p. 2257-65.

129. Forssberg, H., et al., The locomotion of the low spinal cat. II. Interlimb coordination. Acta Physiol Scand, 1980. 108(3): p. 283-95.

130. Eng, S.R., et al., Coordinated regulation of gene expression by Brn3a in developing sensory ganglia. Development, 2004. 131(16): p. 3859-70.

131. Aruga, J., The role of Zic genes in neural development. Mol Cell Neurosci, 2004. 26(2): p. 205-21.

132. Escalante, A., et al., Zic2-dependent axon midline avoidance controls the formation of major ipsilateral tracts in the CNS. Neuron, 2013. 80(6): p. 1392-406.

133. Gong, S., et al., A gene expression atlas of the central nervous system based on bacterial artificial chromosomes. Nature, 2003. 425(6961): p. 917-25.

134. Holder, N., J.D. Clarke, and D. Tonge, Pathfinding by dorsal column axons in the spinal cord of the frog tadpole. Development, 1987. 99(4): p. 577-87.

135. Eberhart, J., et al., Expression of EphA4, ephrin-A2 and ephrin-A5 during axon outgrowth to the hindlimb indicates potential roles in pathfinding. Dev Neurosci, 2000. 22(3): p. 237-50.

136. McCoy, E.S., et al., Peptidergic CGRPalpha primary sensory neurons encode heat and itch and tonically suppress sensitivity to cold. Neuron, 2013. 78(1): p. 138-51.

137. McCoy, E.S., B. Taylor-Blake, and M.J. Zylka, CGRPalpha-expressing sensory neurons respond to stimuli that evoke sensations of pain and itch. PLoS One, 2012. 7(5): p. e36355.

138. Inoue, K., et al., Runx3 controls the axonal projection of proprioceptive dorsal root ganglion neurons. Nat Neurosci, 2002. 5(10): p. 946-54.

139. Kiehn, O. and S.J. Butt, Physiological, anatomical and genetic identification of CPG neurons in the developing mammalian spinal cord. Prog Neurobiol, 2003. 70(4): p. 347-61.

140. Goulding, M., Circuits controlling vertebrate locomotion: moving in a new direction. Nat Rev Neurosci, 2009. 10(7): p. 507-18.

141. Kjaerulff, O. and O. Kiehn, Distribution of networks generating and coordinating locomotor activity in the neonatal rat spinal cord in vitro: a lesion study. J Neurosci, 1996. 16(18): p. 5777-94.

142. Al-Mosawie, A., J.M. Wilson, and R.M. Brownstone, Heterogeneity of V2-derived interneurons in the adult mouse spinal cord. Eur J Neurosci, 2007. 26(11): p. 3003-15.

143. Moran-Rivard, L., et al., Evx1 is a postmitotic determinant of v0 interneuron identity in the spinal cord. Neuron, 2001. 29(2): p. 385-99.

144. Saueressig, H., J. Burrill, and M. Goulding, Engrailed-1 and netrin-1 regulate axon pathfinding by association interneurons that project to motor neurons. Development, 1999. 126(19): p. 4201-12.

145. Matise, M.P. and A.L. Joyner, Expression patterns of developmental control genes in normal and Engrailed-1 mutant mouse spinal cord reveal early diversity in developing interneurons. J Neurosci, 1997. 17(20): p. 7805-16.

146. Butt, S.J., L. Lundfald, and O. Kiehn, EphA4 defines a class of excitatory locomotor-related interneurons. Proc Natl Acad Sci U S A, 2005. 102(39): p. 14098-103.

147. Rybak, I.A., N.A. Shevtsova, and O. Kiehn, Modelling genetic reorganization in the mouse spinal cord affecting left-right coordination during locomotion. J Physiol, 2013. 591(Pt 22): p. 5491-508.

148. Talpalar, A.E., et al., Identification of minimal neuronal networks involved in flexor-extensor alternation in the mammalian spinal cord. Neuron, 2011. 71(6): p. 1071-84.

149. Meehan, C.F., et al., Fictive locomotion in the adult decerebrate and spinal mouse in vivo. J Physiol, 2012. 590(Pt 2): p. 289-300.

150. Nakanishi, S.T. and P.J. Whelan, A decerebrate adult mouse model for examining the sensorimotor control of locomotion. J Neurophysiol, 2012. 107(1): p. 500-15.

151. Jiang, Z., K.P. Carlin, and R.M. Brownstone, An in vitro functionally mature mouse spinal cord preparation for the study of spinal motor networks. Brain Res, 1999. 816(2): p. 493-9.

152. Biscoe, T.J. and M.R. Duchen, Synaptic physiology of spinal motoneurones of normal and spastic mice: an in vitro study. J Physiol, 1986. 379: p. 275-92.

153. Fulton, B.P., Motoneurone activity in an isolated spinal cord preparation from the adult mouse. Neurosci Lett, 1986. 71(2): p. 175-80.

154. Grillner, S., Biological pattern generation: the cellular and computational logic of networks in motion. Neuron, 2006. 52(5): p. 751-66.

155. Goulding, M., et al., The formation of sensorimotor circuits. Curr Opin Neurobiol, 2002. 12(5): p. 508-15.

156. Shirasaki, R. and S.L. Pfaff, Transcriptional codes and the control of neuronal identity. Annu Rev Neurosci, 2002. 25: p. 251-81.

157. Soffe, S.R., J.D. Clarke, and A. Roberts, Activity of commissural interneurons in spinal cord of Xenopus embryos. J Neurophysiol, 1984. 51(6): p. 1257-67.

158. Dale, N., Reciprocal inhibitory interneurones in the Xenopus embryo spinal cord. J Physiol, 1985. 363: p. 61-70.

159. Jessell, T.M., Neuronal specification in the spinal cord: inductive signals and transcriptional codes. Nat Rev Genet, 2000. 1(1): p. 20-9.

160. Alstermark, B. and J. Ogawa, In vivo recordings of bulbospinal excitation in adult mouse forelimb motoneurons. J Neurophysiol, 2004. 92(3): p. 1958-62.

161. Ghez, C., W. Hening, and J. Gordon, Organization of voluntary movement. Curr Opin Neurobiol, 1991. 1(4): p. 664-71.

162. Courtine, G., et al., Can experiments in nonhuman primates expedite the translation of treatments for spinal cord injury in humans? Nat Med, 2007. 13(5): p. 561-6.

163. Dottori, M., et al., EphA4 (Sek1) receptor tyrosine kinase is required for the development of the corticospinal tract. Proc Natl Acad Sci U S A, 1998. 95(22): p. 13248-53.

164. Etienne-Manneville, S. and A. Hall, Rho GTPases in cell biology. Nature, 2002. 420(6916): p. 629-35.

165. Luo, L., Rho GTPases in neuronal morphogenesis. Nat Rev Neurosci, 2000. 1(3): p. 173-80.

166. Marin, O., et al., Guiding neuronal cell migrations. Cold Spring Harb Perspect Biol, 2010. 2(2): p. a001834.

167. CJ, O.L. and K.W. McDermott, Spinal cord neuroepithelial progenitor cells display developmental plasticity when co-cultured with embryonic spinal cord slices at different stages of development. Dev Dyn, 2011. 240(4): p. 785-95.

168. Sengul, G., R.B. Puchalski, and C. Watson, Cytoarchitecture of the spinal cord of the postnatal (P4) mouse. Anat Rec (Hoboken), 2012. 295(5): p. 837-45.

169. Schmidt, H., et al., The receptor guanylyl cyclase Npr2 is essential for sensory axon bifurcation within the spinal cord. J Cell Biol, 2007. 179(2): p. 331-40.

170. Abraira, V.E. and D.D. Ginty, The sensory neurons of touch. Neuron, 2013. 79(4): p. 618-39.

171. Johnson, K.O. and S.S. Hsiao, Neural mechanisms of tactual form and texture perception. Annu Rev Neurosci, 1992. 15: p. 227-50.

172. Niu, J., et al., Modality-based organization of ascending somatosensory axons in the direct dorsal column pathway. J Neurosci, 2013. 33(45): p. 17691-709.

173. Pomeranz, B., Specific nociceptive fibers projecting from spinal cord neurons to the brain: a possible pathway for pain. Brain Res, 1973. 50(2): p. 447-51.

174. Zylka, M.J., F.L. Rice, and D.J. Anderson, Topographically distinct epidermal nociceptive circuits revealed by axonal tracers targeted to Mrgprd. Neuron, 2005. 45(1): p. 17-25.

175. Morrison, S.F., K. Nakamura, and C.J. Madden, Central control of thermogenesis in mammals. Exp Physiol, 2008. 93(7): p. 773-97.

176. Hantman, A.W. and T.M. Jessell, Clarke's column neurons as the focus of a corticospinal corollary circuit. Nat Neurosci, 2010. 13(10): p. 1233-9.

177. Luz, L.L., et al., Monosynaptic excitatory inputs to spinal lamina I anterolateral-tract-projecting neurons from neighbouring lamina I neurons. J Physiol, 2010. 588(Pt 22): p. 4489-505.

178. Szucs, P., et al., Local axon collaterals of lamina I projection neurons in the spinal cord of young rats. J Comp Neurol, 2010. 518(14): p. 2645-65.

179. Giesler, G.J., Jr., R.L. Nahin, and A.M. Madsen, Postsynaptic dorsal column pathway of the rat. I. Anatomical studies. J Neurophysiol, 1984. 51(2): p. 260-75.

180. Giesler, G.J., Jr. and K.D. Cliffer, Postsynaptic dorsal column pathway of the rat. II. Evidence against an important role in nociception. Brain Res, 1985. 326(2): p. 347-56.

181. Cliffer, K.D. and G.J. Giesler, Jr., Postsynaptic dorsal column pathway of the rat. III. Distribution of ascending afferent fibers. J Neurosci, 1989. 9(9): p. 3146-68.

182. Watson, C. and M. Harrison, The location of the major ascending and descending spinal cord tracts in all spinal cord segments in the mouse: actual and extrapolated. Anat Rec (Hoboken), 2012. 295(10): p. 1692-7.

183. Honma, Y., et al., Axonal projections of mechanoreceptive dorsal root ganglion neurons depend on Ret. Development, 2010. 137(14): p. 2319-28.

184. Luo, W., et al., Molecular identification of rapidly adapting mechanoreceptors and their developmental dependence on ret signaling. Neuron, 2009. 64(6): p. 841-56.

185. Gallarda, B.W., et al., Segregation of axial motor and sensory pathways via heterotypic trans-axonal signaling. Science, 2008. 320(5873): p. 233-6.

186. Wang, L., et al., Anatomical coupling of sensory and motor nerve trajectory via axon tracking. Neuron, 2011. 71(2): p. 263-77.

Eidesstattliche Versicherung/Affidavit

Hiermit versichere ich an Eides statt, dass ich die vorliegende Dissertation **'Role of EphA4 in spinal circuits controlling locomotion'** selbstständig angefertigt habe, mich außer der angegebenen keiner weiteren Hilfsmittel bedient und alle Erkenntnisse, die aus dem Schrifttum ganz oder annähernd übernommen sind, als solche kenntlich gemacht und nach ihrer Herkunft unter Bezeichnung der Fundstelle einzeln nachgewiesen habe.

I hereby confirm that the dissertation **'Role of EphA4 in spinal circuits controlling locomotion'** is the result of my own work and that I have only used sources or materials listed and specified in the dissertation.

München, den /Munich, Date Unterschrift/ Signature

List of author contributions

Figures contributed by Aarathi Balijepalli	4.03, 4.04, 4.05, 4.06, 4.09, 4.10, 4.11, 4.13, 4.14. 4.17, 4.19, 4.20, 4.21, 4.26
Figures contributed by Dr. Sónia Paixão	4.02, 4.07, 4.18, 4.22
Figures contributed by both Aarathi Balijepalli and Dr. Sónia Paixão	4.08, 4.12, 4.15, 4.16, 4.23, 4.24, 4.25

Signature of Lab head……..

List of Abbreviations

˚C	Degrees centigrade
5-HT	5- Hydroxytrytamine
BCIP	5-Bromo-4-chloro-3-indolyl phosphate
BMP	Bone morphogenetic protein
Chx10	Ceh-10 homeodomain containing- homolog
CIN	Commissural interneuron
CNS	Central nervous system
CST	Corticospinal tract
Dbx1	Developing brain homeobox 1
DF	Dorsal funiculus
dNTP	Deoxyribonucleotide
DREZ	Dorsal root entry zone
DRG	Dorsal root ganglion
eCIN	Excitatory CIN
ECL	Enhanced chemiluminiscence
EDTA	Ethylenediaminetetraacetic acid

eIIN	Excitatory IIN
En1	Engrailed 1
ERK	Extracellular signal regulated kinase
Exv1	Even-skipped homeobox 1
FAK	Focal adhesion kinase
FGF	Fibroblast growth factor
GABA	Gamma-Aminobutyric acid
GAP	GTPase activating protein
GDP	Guanosine diphosphate
GEF	Guanine nucleotide exchange factor
GFP	Green fluorescent protein
GPI	Glycophosphatidylinositol
GTP	Guanosine – 5’ – triphosphate
Hox	Homeobox
iCIN	Inhibitory CIN
Ig	Immunoglobulin
iIIN	Inhibitory IIN

IIN	Ipsilateral interneuron
Isl1	Islet 1
KO	Knockout
Lbx	Ladybird homeobox
Lhx	LIM homeodomain
MAPK	Mitogen activated protein kinase
MN	Motor neuron
NBT	Nitroblue tetrazolium
NMDA	N-Methyl-D-Aspartate
PAGE	Polyacrylamide gel electrophoresis
Pax	Paired box protein
PBS	Phosphate buffered saline
PI3K	Phosphoinositide 3 kinase
Pitx2	Pituitary homeobox 2
RA	Retinoic acid
RC	Renshaw cell
RGC	Retinal ganglion cell

SEM	Standard error of mean
SH2	Src homology 2
Shh	Sonic hedgehog
Sim1	Single minded homolog 1
TGF- β	Transforming growth factor β
Wnt	Wingless related integration site
WT	Wildtype
µ	Micro

List of Figures

List of Tables

List of Publications

EphrinB3/EphA4-Mediated Guidance of Ascending and Descending Spinal Tracts

Sónia Paixão, **Aarathi Balijepalli**, Najet Serradj, Jingwen Niu, Wenqin Luo, John H. Martin, Rüdiger Klein

Neuron. 2013 Dec 18;80(6):1407-20.

doi: 10.1016/j.neuron.2013.10.006.

Permissions

Figure 2.02

Opposing FGF and retinoid pathways: a signalling switch that controls differentiation and patterning onset in the extending vertebrate body axis

Ruth Diez del Corral, Kate G. Storey

BioEssays August 2004 Volume 26, Issue 8, pages 857–869

License number: 3385790142269

Figure 2.04

Patterning cell types in the dorsal spinal cord: what the mouse mutants say

Tamara Caspary and Kathryn V. Anderson

Nature Reviews Neuroscience 4, 289-297 (April 2003)

License number: 500876209

Figure 4.02, 4.04, 4.15, 4.16, 4.18, 4.20, 4.21, 4.22, 4.23, 4.26

EphrinB3/EphA4-Mediated Guidance of Ascending and Descending Spinal Tracts

Sónia Paixão, **Aarathi Balijepalli**, Najet Serradj, Jingwen Niu, Wenqin Luo, John H. Martin, Rüdiger Klein

Neuron. 2013 Dec 18; 80(6):1407-20.

License number: 3363690602373

Acknowledgements

I owe sincere thanks and gratitude to my PhD supervisor, Rüdiger Klein, for his exceptional support in guiding me throughout my PhD studies. He has provided encouragement and critical insights during our discussions and most importantly, he has given me the freedom to explore my ideas. I am appreciative to have the opportunity to work with him.

I am immensely thankful to Sonia Paixão, my supervising post doc and collaborator, for the constant guidance and trust she has shown in me. I have learned a lot from her and she has been very patient in teaching me most of the techniques I have used in my thesis. She has also been supportive and understanding during testing times and I am grateful to her for that.

I would also like to thank Ilona Kadow, for agreeing to be on my thesis committee and for all the discussions and advice she has given me on the project and otherwise. I specially want to thank Daniel del Toro for his never-ending enthusiasm and encouragement during our discussions and his willingness to help me whenever I asked. I thank Pilar Alcala for not only always sparing some time for me from her busy schedule, but also, for the warm hand of friendship she has extended towards me. I sincerely thank Alessandro Filosa for helping me throughout my PhD and introducing me to Ephs and ephrins.

I am greatly thankful to my wonderful friends Marion Ponserre, Archana Mishra, Annelies Van Hoecke and Katharina Schulz-Trieglaff for the amazing friendship and support they have given me. Tom Gaitanos, Daniel Nagel and Graziana Gatto, your friendly banter made the atmosphere in the lab thoroughly enjoyable; thank you. To all the members of the Klein lab, thank you for your support and scientific and non-scientific discussions. I specially thank Nagarjuna Nagaraj, Krishna Sreenivasan and Priyanka Sahasrabuddhe for being such wonderful and supportive friends.

Finally, this dissertation would not be possible without the support of my loving family. I thank my parents and my brothers, Arvind and Arun for their constant encouragement and motivation. I am also thankful to Kartik for all the support and guidance in the past months. I am lucky to have them in my life and am indebted to them forever.